StEER-EERI: 2023 Mw 7.8 Kahramanmaras, Türkiye Earthquake Sequence Joint Preliminary Virtual Reconnaissance Report (PVRR)

Report

Author(s):
Dilsiz, Abdullah; Günay, Selim; Mosalam, Khalid M.; Miranda, Eduardo; Arteta, Carlos; Sezen, Halil; Fischer, Erica; Hakhamaneshi, Manny; Hassan, Wael M.; Alhawamdeh, Bilal; Andrus, Samuel; Archbold, Jorge; Arslantürkoglu, Safak (iD); Bektas, Nurullah; Ceferino, Luis; Cohen, Jade; Duran, Burak; Erazo, Kalil; Faraone, Gloria; Feinstein, Tal; Marinković, Marko; Amory, Martin; Merino, Yvonne; Mivehchi, Maziar; Moya, Luis; Pájaro, César; Quintero, Nicolas; Gautam, Rajendra; Gupta, Abhineet; Haj Ismail, Salah; Jana, Amalesh; Javadinasab Hormozabad, Sajad; Kasalanati, Amarnath; Kenawy, Maha; Khalil, Zeyad; Liou, Irene; Rivera, Juliana; Romão, Xavier; Ruiz, Maria Camila Lopez; Sorosh, Shokrullah; Vargas, Laura; Velani, Pulkit; Wibowo, Hartanto; Xu, Susu; Yılmaz, Taner; Alam, Mohammed; Holtzer, Gabor; Kijewski-Correa, Tracy; Robertson, Ian; Roueche, David; Safiey, Amir

2023 Türkiye Earthquake Sequence
Initiated 6 February 2023
Released: March 29, 2023
NHERI DesignSafe Project ID: PRJ-3824

EARTHQUAKE ENGINEERING RESEARCH INSTITUTE EERI

JOINT PRELIMINARY VIRTUAL RECONNAISSANCE REPORT (PVRR)

Joint Report Leads:
Abdullah Dilsiz, Ankara Yildirim Beyazit University, Türkiye Selim Günay, University of California, Berkeley Khalid M. Mosalam, University of California, Berkeley

Joint Report Section Leads:	
Eduardo Miranda, Stanford University Carlos Arteta, Universidad del Norte Halil Sezen, Ohio State University Erica Fischer, Oregon State University	Manny Hakhamaneshi, California High-speed Rail Authority Wael M. Hassan, University of Alaska

Joint Report Authors: (in alphabetical order)	
Bilal Alhawamdeh, Western Michigan University Samuel Andrus, Chapman University Jorge Archbold, Universidad del Norte Safak Arslantürkoglu, ETH Zurich Nurullah Bektaş, Széchenyi István University Luis Ceferino, New York University Jade Cohen, Exponent Burak Duran, University of New Hampshire Kalil Erazo, Rice University Gloria Faraone, San Diego State University Tal Feinstein, Exponent	Marko Marinković, University of Belgrade, Serbia Amory Martin, Exponent Yvonne Merino, Pontificia Universidad Católica de Chile, Chile Maziar Mivehchi, University of California, Davis Luis Moya, Pontificia Universidad Católica del Perú, Peru César Pájaro, Universidad del Norte Nicolas Quintero, Universidad del Norte

Joint PVRR: 2023 Türkiye Earthquake Sequence
PRJ-3824 | Released: 3/29/2023
Building Resilience through Reconnaissance

1

Rajendra Gautam, Tribhuvan University
Abhineet Gupta, Marqeta
Salah Haj Ismail, Ankara Yildirim Beyazit University, Türkiye
Amalesh Jana, Oregon State University
Sajad Javadinasab Hormozabad, McNamara Salvia
Amarnath Kasalanati, University of California, Berkeley
Maha Kenawy, Exponent
Zeyad Khalil, Imperial College London, United Kingdom
Irene Liou, University of California, Davis

Juliana Rivera, Universidad del Norte
Xavier Romão, University of Porto, Portugal
Maria Camila Lopez Ruiz, University of California, Berkeley
Shokrullah Sorosh, University of California, San Diego
Laura Vargas, Pontificia Universidad Católica de Chile, Chile
Pulkit Velani, IIIT Hyderabad, India
Hartanto Wibowo, Iowa State University
Susu Xu, Stony Brook University
Taner Yılmaz, Ozyegin University, Türkiye

Joint Report Editors:
(in alphabetical order)

Mohammad Alam, University of Notre Dame
Gabor Holtzer, University of Notre Dame
Tracy Kijewski-Correa, University of Notre Dame
Ian Robertson, University of Hawaii

David Roueche, Auburn University
Amir Safiey, Auburn University

Joint PVRR: 2023 Türkiye Earthquake Sequence
PRJ-3824 | Released: 3/29/2023
Building Resilience through Reconnaissance

2

DEDICATION

This report is dedicated to the memory of all those who lost their lives in the February 2023 sequence of earthquakes in Türkiye and in solidarity with those who were injured or displaced by these events. We also wish to honor those who labored tirelessly to rescue as many as possible under extremely challenging conditions. This report is the first symbol of our ongoing commitment to learn from this disaster and work with colleagues in the region to build more resilient communities in the future.

Joint PVRR: 2023 Türkiye Earthquake Sequence
PRJ-3824 | Released: 3/29/2023
Building Resilience through Reconnaissance

3

PREFACE

This report is a collaboration between the Structural Extreme Events Reconnaissance (StEER) Network and Learning From Earthquakes (LFE) Program of the Earthquake Engineering Research Institute (EERI).

The National Science Foundation (NSF) awarded an EAGER grant (CMMI 1841667) to a consortium of universities to form the Structural Extreme Events Reconnaissance (StEER) Network (see https://www.steer.network for more details). StEER was renewed through a second award (CMMI 2103550) to further enhance its operational model and develop new capabilities for more efficient and impactful post-event reconnaissance. StEER builds societal resilience by generating new knowledge on the performance of the built environment through impactful post-disaster reconnaissance disseminated to affected communities. StEER achieves this vision by: (1) deepening structural engineers' capacity for post-event reconnaissance by promoting community-driven standards, best practices, and training, as well as their understanding of the effect of natural hazards on society; (2) coordination leveraging its distributed network of members and partners for early, efficient and impactful responses to disasters; and (3) collaboration that broadly engages communities of research, practice and policy to accelerate learning from disasters. Visit www.steer.network to learn more.

Under the banner of the Natural Hazards Engineering Research Infrastructure (NHERI) CONVERGE node, StEER works closely with the wider Extreme Events Reconnaissance consortium to promote interdisciplinary disaster reconnaissance and research. The consortium includes the Geotechnical Extreme Events Reconnaissance (GEER) Association and the networks for Interdisciplinary Science and Engineering Extreme Events Research (ISEEER), Nearshore Extreme Event Reconnaissance (NEER), Operations and Systems Engineering Extreme Events Research (OSEEER), Social Science Extreme Events Research (SSEER), and Sustainable Material Management Extreme Events Reconnaissance (SUMMEER), as well as the NHERI RAPID equipment facility, the NHERI Network Coordination Office (NCO), and NHERI DesignSafe CI, curation site for all StEER products.

The **Earthquake Engineering Research Institute (EERI)** is the leading non-profit membership organization that connects those dedicated to reducing earthquake risk. Its multidisciplinary members include engineers, geoscientists, social scientists, architects, planners, emergency managers, academics, students, and other like-minded professionals. EERI has been bringing people and disciplines together since 1948. The objective of the Earthquake Engineering Research Institute is to reduce earthquake risk by (1) advancing the science and practice of earthquake engineering, (2) improving understanding of the impact of earthquakes on the physical, social, economic, political, and cultural environment, and (3) advocating comprehensive and realistic measures for reducing the harmful effects of earthquakes. For more information about EERI, please visit: https://www.eeri.org/

Joint PVRR: 2023 Türkiye Earthquake Sequence
PRJ-3824 | Released: 3/29/2023
Building Resilience through Reconnaissance

4

COPYRIGHT DISCLAIMER

This report was developed to contribute to the efforts of the international research community with the ultimate goal of understanding certain scientific aspects of the earthquake sequence in Türkiye and Syria. No resources included in this report are used for commercial purposes and none of the authors receive remuneration directly related to the publication of this research document.

All external resources in this report were utilized in line with the Berne Convention for the Protection of Literary and Artistic Works, Section 107 of the Copyright Act of 1976, and the practice of the courts in the United States.

All external resources in this report were used in good faith and in consideration of the possibility of 'fair use' which allows otherwise infringing resource usage to be exempted based on the criteria established by the aforementioned regulations and the practice of the courts.

Fair use is a doctrine in United States copyright law that allows limited use of copyrighted material without requiring licensing and permission from the rights holders, such as commentary, criticism, news reporting, research, teaching or scholarship. It provides for the legal, non-licensed citation or incorporation of copyrighted material in another author's work under a four-factor balancing test.

Joint PVRR: 2023 Türkiye Earthquake Sequence
PRJ-3824 | Released: 3/29/2023
Building Resilience through Reconnaissance

5

ATTRIBUTION GUIDANCE

Reference to PVRR Analyses, Discussions or Recommendations

Reference to the analyses, discussions or recommendations within this report should be cited using the full citation information and DOI from DesignSafe (see callout box).

Citing Images from this PVRR

Images in this report are taken from public sources. Each figure caption specifies the source; re-use of the image should cite that original source directly. Note that these original sources hold image copyright and thus must comply with fair use practices. Depending on the use case, the user may need to secure additional permissions/rights from the original copyright owner.

ACCESS THIS AND OTHER PRODUCTS

For a full listing of this report and all other StEER products (briefings, reports and datasets) with full citation information and DOIs, please visit the StEER website: https://www.steer.network/products

For a full listing of over 300 different earthquakes occurring in more than 50 countries during the last 70 years that the EERI's Learning From Earthquakes program, including this and other Virtual Earthquake Reconnaissance Team (VERT) reports, datasets, and publications, please visit the EERI LFE website:

http://www.learningfromearthquakes.org/

Joint PVRR: 2023 Türkiye Earthquake Sequence
PRJ-3824 | Released: 3/29/2023
Building Resilience through Reconnaissance

6

ACKNOWLEDGMENTS

Joint PVRR: 2023 Türkiye Earthquake Sequence
PRJ-3824 | Released: 3/29/2023
Building Resilience through Reconnaissance

7

Common Terms & Acronyms

Acronym	General Terms	Brief Description
--	DesignSafe	Data Repository
--	DesignSafe-CI	Academic Organization within NHERI
ASCE	American Society of Civil Engineers	Professional Organization
ASTM	American Society for Testing and Materials (now ASTM International)	Standards Body
ATC	Applied Technology Council	Professional Organization
BOCA	Building Officials and Code Administrators	Code Body
CC-BY	Creative Commons Attribution License	Code/Standard
CESMD	Center for Engineering Strong Motion Data	Governmental Agency
CI	Cyberinfrastructure	Research Asset
CLPE	Critical Load Path Elements	StEER Term
CMU	Concrete Masonry Unit	Building Material
DBE	Design Basis Earthquake	Design Terminology
DEQC	Data Enrichment and Quality Control	StEER Term
DOI	Digital Object Identifier	Common Term
EARR	Early Access Reconnaissance Report	StEER Term
EERI	Earthquake Engineering Research Institute	Professional Organization
EEFIT	Earthquake Engineering Field Investigation Team	Professional Organization
EF	Enhanced Fujita Scale	Hazard Intensity Scale
EF	Equipment Facility	Academic Organization within NHERI
EIFS	Exterior Insulation Finish System	Building Component
FAA	Federal Aviation Administration	Governmental Agency
FAQ	Frequently Asked Questions	Common Term
FAST	Field Assessment Structural Team	StEER Term
FEMA	Federal Emergency Management Agency	Governmental Agency

Joint PVRR: 2023 Türkiye Earthquake Sequence
PRJ-3824 | Released: 3/29/2023
Building Resilience through Reconnaissance

8

GEER	Geotechnical Extreme Events Reconnaissance	Academic Organization within NHERI
GPS	Global Positioning System	Measurement Technology
GSA	Government Services Administration	Governmental Agency
HVAC	Heating, ventilation and air conditioning	Building System
HWM	High Water Mark	Intensity Measure
IBC	International Building Code	Code/Standard
ICC	International Code Council	Code Body
IRC	International Residential Code	Code/Standard
ISEEER	Interdisciplinary Science and Engineering Extreme Events Research	Academic Organization within NHERI
LiDAR	Light Detection and Ranging	Measurement Technology
MCE	Maximum Considered Earthquake	Design Terminology
ME&P	Mechanical, electrical and plumbing	Building System
MMI	Modified Mercalli Intensity	Hazard Intensity Scale
NBC	National Building Code	Code/Standard
NEER	Nearshore Extreme Event Reconnaissance	Academic Organization within NHERI
NFIP	National Flood Insurance Program	Government Program
NHERI	Natural Hazards Engineering Research Infrastructure	Academic Organization within NHERI
NIST	National Institute of Standards and Technology	Governmental Agency
NOAA	National Oceanic and Atmospheric Administration	Governmental Agency
NSF	National Science Foundation	Governmental Agency
NWS	National Weather Service	Governmental Agency
OSB	Oriented strand board	Construction Material
OSEEER	Operations and Systems Engineering Extreme Events Research	Academic Organization within NHERI
PEER	Pacific Earthquake Engineering Research center	Academic Organization (Earthquakes)
PGA	Peak Ground Acceleration	Intensity Measure

Joint PVRR: 2023 Türkiye Earthquake Sequence
PRJ-3824 | Released: 3/29/2023
Building Resilience through Reconnaissance

9

PHEER	Public Health Extreme Events Research	Academic Organization within NHERI
PVRR	Preliminary Virtual Reconnaissance Report	StEER Term
QC	Quality Control	Oversight process
RAPID	RAPID Grant	Funding Mechanism
RAPID-EF	RAPID Experimental Facility	Academic Organization within NHERI
RC	Reinforced Concrete	Building Material
SAR	Search and Rescue	Standard Hazards Terminology
SGI	Special Government Interest	FAA Process
SLP	Surface-Level Panoramas	Measurement Technology
SMS	Short Message Service	Communication Modality
SPC	Storm Prediction Center	Governmental Agency
SSEER	Social Science Extreme Events Research	Academic Organization within NHERI
StEER	Structural Extreme Events Reconnaissance network	Academic Organization within NHERI
SUMMEER	SUstainable Material Management Extreme Events Reconnaissance	Academic Organization within NHERI
TAS	Testing Application Standard	Technical Standard
UAS/V	Unmanned Aerial Survey/System/Vehicle	Measurement Technology
USD	US Dollar	Standard Currency
USGS	United States Geological Survey	Governmental Agency
VAST	Virtual Assessment Structural Team	StEER Term
WS	Windshield Survey	Measurement Technology

Joint PVRR: 2023 Türkiye Earthquake Sequence
PRJ-3824 | Released: 3/29/2023
Building Resilience through Reconnaissance

10

TABLE OF CONTENTS

Joint PVRR: 2023 Türkiye Earthquake Sequence
PRJ-3824 | Released: 3/29/2023
Building Resilience through Reconnaissance

11

Joint PVRR: 2023 Türkiye Earthquake Sequence
PRJ-3824 | Released: 3/29/2023
Building Resilience through Reconnaissance

12

EXECUTIVE SUMMARY

An Mw 7.8 earthquake occurred at a depth of 17.9 km and with epicenter coordinates 37.174°N 37.032°E near the city of Nurdağı in the Gaziantep province of Türkiye at about 4:17 am local time on February 6, 2023. Due to the shallow depth of the earthquake and a bilateral rupture towards the southwest and the northeast with an area of approximately 100 km × 75 km, the earthquake impacted 10 provinces in Türkiye and several others in Syria, resulting in significant casualties due to the collapse of many buildings. Because of a combination of forward directivity, basin effects, and site amplification, very large ground shaking (up to 1.3g Peak Ground Acceleration (PGA) and 170 cm/s Peak Ground Velocity (PGV)) was recorded in Hatay. The response spectra of several of the recorded ground motions considerably exceeded the Maximum Considered Earthquake (MCE) levels for certain period ranges. This earthquake was followed by many aftershocks, including several larger than magnitude 6 (one with Mw 6.6). Approximately 9 hours later, a Mw 7.5 induced earthquake occurred on the Sürgü Cardak fault at a depth of 10 km, with epicenter coordinates 38.024°N 37.203°E near the town of Ekinözü in the Kahramanmaraş province at about 1:24 pm local time. This second major earthquake resulted in very large shaking at a few locations (Kahramanmaras PGA: 0.63g, PGV: 170 cm/s; Malatya PGA: 0.47g, and Adana PGA: 0.4g).

As a result of this sequence of earthquakes and aftershocks, around 28,500 buildings partially or completely collapsed, while another 66,000 buildings were severely damaged in Türkiye. In Syria, more than 22,000 buildings were affected by the earthquakes, with 2,850 of them partially/completely collapsed or severely damaged. As of March 8, the total official death toll due to these earthquakes was reported to be 45,968 confirmed deaths in Türkiye and 7,259 deaths in Syria. In Türkiye alone, more than 100,000 people were reported as injured. The province of Hatay in Türkiye was severely impacted by this sequence of ground shaking including a Mw 6.4 earthquake that occurred on February 20, two weeks after the main event.

Around half of the buildings in the affected regions of Türkiye were constructed before 2000, i.e., before modern principles of earthquake design were implemented in the Turkish Seismic Code. Fragility functions developed for the building stock in the area showed that collapse under large shaking was possible for these relatively older buildings. However, several collapses of buildings constructed after 2000 were also observed. There are several reasons for the collapse of these relatively newer buildings, including: (a) ground motions exceeding MCE levels, (b) impact of a sequence of large ground motions with compounding effects, (c) possibility of buildings not designed according to seismic code provisions, and (d) possibility of construction that did not comply with the design and specifications in the structural drawings. Compared to the response of buildings, other infrastructure performance was generally acceptable, with most of the bridges, roads and tunnels remaining operational, and no major issues with the power grid and water supply infrastructure.

In terms of good performance, the 12 seismically isolated hospitals in the earthquake-impacted region were operational after the earthquakes, and more importantly, allowed these healthcare facilities to serve their emergency response functions in the aftermath of the extraordinary destruction. Seismic isolation was employed in these hospitals, as required by law for hospitals with 100+ beds in seismic zones I and II after 2013. Their operational performance was in major contrast with the observed collapses of some of the hospitals that were not seismically isolated.

The objectives of this joint Preliminary Virtual Reconnaissance Report (PVRR) issued by the Structural Extreme Events Reconnaissance (StEER) network and Earthquake Engineering Research Institute (EERI) Learning From Earthquakes (LFE) Program are: 1) to provide details of the February 6 Mw 7.8 and Mw 7.5 earthquakes, 2) to describe local seismic codes and building construction practices, 3) to compare the recorded ground shaking with the parameters used for design, 4) to summarize the preliminary reports of damage to buildings and other infrastructure, including the disruption to the community in terms of fatalities, downtime, and economic losses, and 5) to highlight key lessons learned, with recommendations to inform continued study of this event by the engineering community.

Joint PVRR: 2023 Türkiye Earthquake Sequence
PRJ-3824 | Released: 3/29/2023
Building Resilience through Reconnaissance

14

1.   Introduction

The Republic of Türkiye is located in one of the most seismically active regions in the world. It lies mostly on the Anatolian plate and is surrounded by three main tectonic plates, namely the Arabian plate, the African plate, and the Eurasian plate. Consequently, many devastating earthquakes have occurred in this region. Some notable earthquakes in the last century include the 1939 Great Erzincan earthquake (surface wave magnitude Ms 7.9), which caused 33,000 casualties and the collapse or severe damage of more than 115,000 dwellings (Akkar et al. 2018), the 1976 Çaldıran earthquake (moment magnitude Mw 7.0), the 1999 Kocaeli earthquake (Mw 7.6), the 1999 Duzce earthquake (Mw 7.2), the 2003 Bingöl earthquake (duration magnitude Md 6.1), the 2011 Van earthquake (local "Richter" magnitude ML 6.7), the 2020 Elazığ earthquake (Mw 6.8), the 2020 Izmir, Seferihisar earthquake (also referred to as Samos Island earthquake) (Mw 6.6), and the 2022 Düzce earthquake (Mw 6.1).

This report focuses on the Mw 7.8 earthquake that occurred on the Eastern Anatolian fault and the induced Mw 7.5 earthquake that occurred on the Sürgü Cardak fault. The first earthquake initiated at a depth of 17.9 km with epicenter coordinates 37.174°N 37.032°E near the city of Nurdağı in the Gaziantep province of Türkiye at about 4:17 am local time on February 6, 2023 (USGS 2023a), while the second was at a depth of 10 km and epicenter coordinates 38.024°N 37.203°E near the town of Ekinözü in the Kahramanmaraş province at about 1:24 pm local time on February 6, 2023 (USGS 2023b), approximately 9 hours after the first event. The epicenter of the Mw 7.5 earthquake was approximately 95 km north-northeast of the epicenter of the Mw 7.8 earthquake. The Mw 7.8 earthquake affected a very large region of Türkiye including 10 provinces (i.e., Kahramanmaraş, Gaziantep, Şanlıurfa, Diyarbakır, Adana, Adıyaman, Osmaniye, Hatay, Kilis, and Malatya), and northwestern regions of Syria (AFAD 2023a). The combined population of the 10 provinces in Türkiye is approximately 13.5 million, and the impacted area of these provinces is approximately 100,000 km^2.

The epicenter and magnitude of the earthquakes reported by AFAD (the Disaster and Emergency Management Authority of Türkiye) are slightly different from those provided by the United States Geological Survey (USGS). According to AFAD, the first earthquake had an Mw 7.7 magnitude with hypocenter at a depth of 8.6 km, and with epicenter coordinates 37.288°N 37.043°E near the city of Pazarcık in the Kahramanmaraş province. Meanwhile, the second earthquake was reported as a Mw 7.6 earthquake with a hypocenter depth of 7 km and with epicenter coordinates 38.089°N 37.239°E that struck near the city of Elbistan, also in the Kahramanmaraş province (AFAD 2023b). These small differences with respect to the epicenters' coordinates and earthquake magnitudes reported by USGS are common, as they are based on considerations of different recording stations and different algorithms for determining the focus and magnitude of seismic events.

Joint PVRR: 2023 Türkiye Earthquake Sequence
PRJ-3824 | Released: 3/29/2023
Building Resilience through Reconnaissance

15

1.1.   Casualties and Injuries

The earthquake sequence resulted in a very large number of fatalities and injuries. As of March 9, 2023, the total death toll was reported to be 45,968 people in Türkiye and around 6,000 in Syria (ECHO 2023). In Türkiye alone, more than 100,000 people were reported as injured (AFAD 2023a).

The USGS PAGER (Prompt Assessment of Global Earthquakes for Response) tool provides estimates of the population exposed to different levels of ground motion intensity. This information is summarized in Figure 1.1, which shows curves of equal Modified Mercalli Intensity (MMI) (USGS 2023c). From this information, it was estimated that approximately 12.74 million people felt the main event was weak, 240.89 million as *light*, 22.86 million as *moderate*, 12.84 million as *strong*, 7.57 million as *very strong*, 1.19 million as *severe*, and 0.657 million as *violent*.

MMI	Shaking	Population
I	Not Felt	0 k*
II-III	Weak	12744 k*
IV	Light	240897 k
V	Moderate	22861 k
VI	Strong	12841 k
VII	Very Strong	7574 k
VIII	Severe	1191 k
IX	Violent	657 k
X	Extreme	0 k

*Estimated exposure only includes population within map area (k = x1,000)
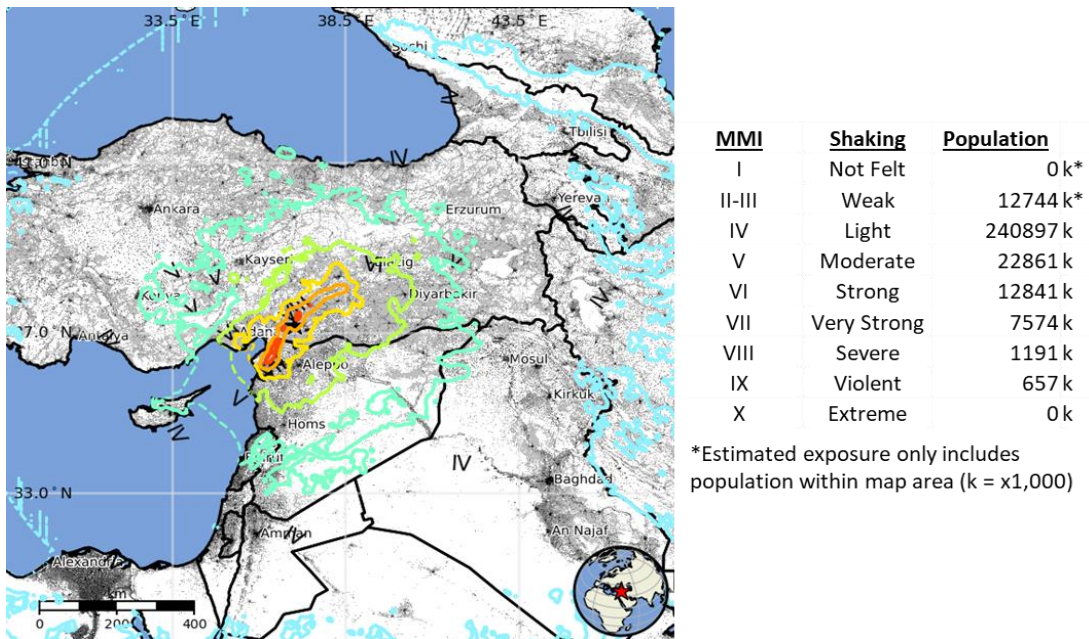
Figure 1.1. Isoseismals (curves of equal MMI) estimated for Mw 7.8 earthquake (USGS 2023a).

The number of fatalities estimated by PAGER for the Mw 7.8 event is shown in Figure 1.2. The number of fatalities were estimated to be from 100 to 1,000, 1,000 to 10,000, 10,000 to 100,000 and more than 100,000, with probabilities of 10%, 28%, 36%, and 25%, respectively.

Joint PVRR: 2023 Türkiye Earthquake Sequence
PRJ-3824 | Released: 3/29/2023
Building Resilience through Reconnaissance

16
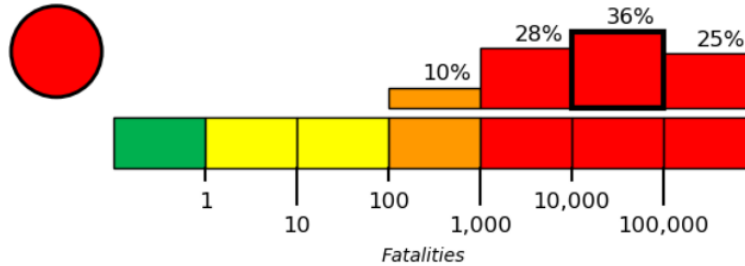
Figure 1.2. Number of fatalities estimated by PAGER for the Mw 7.8 earthquake (USGS 2023c).

After the earthquakes, Iskenderun State Hospital, the main training, and research hospital in the city of Iskenderun, stopped functioning due to a partial collapse. On February 7, the Ministry of Health reported that injured people from Iskenderun were transferred to Mersin City Hospital in ambulances and by the Iskenderun ship of the Ministry of National Defense. Ninety-eight wounded patients were transferred the day of the earthquake. As of February 7, Mersin City Hospital was assisting 590 injured, with 170 in intensive care units. In general, patients from the affected province of Hatay were transferred to Adana City Hospital and other hospitals in the region. As of February 7, the Adana City Hospital was treating 600 injured patients, including 220 in intensive care units. Furthermore, critically injured patients were transferred by plane to city hospitals in Ankara and Istanbul (Ministry of Health 2023).

1.2. Economic Losses

For the Mw 7.8 earthquake, PAGER estimated economic losses in USD from $100 to $1,000 million, $1,000 to $10,000 million, $10,000 to $100,000 million, and greater than 100,000 million with probabilities of 7%, 23%, 35%, and 34%, respectively, as shown in Figure 1.3 (USGS 2023c). PAGER estimated economic losses for the Mw 7.5 earthquake are shown in Figure 1.4, and they are smaller than those of the Mw 7.8 earthquake. Note that this does not include the cascading effects of the two earthquakes, i.e., the first event could have induced damages that made some structures more vulnerable to the second event than if they were subjected solely to the second event. Extreme Event Solutions at Verisk predicted that the economic losses and industry-insured losses due to the earthquake sequence in Türkiye will likely exceed $20 billion (USD) and $1 billion (USD), respectively (Verisk 2023).
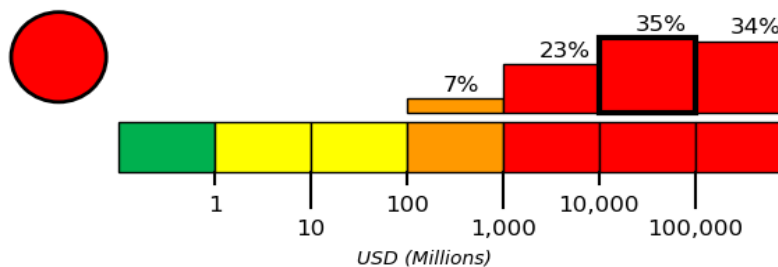
Figure 1.3. Economic losses estimated by PAGER for the Mw 7.8 earthquake (USGS 2023c).

Joint PVRR: 2023 Türkiye Earthquake Sequence
PRJ-3824 | Released: 3/29/2023
Building Resilience through Reconnaissance

17
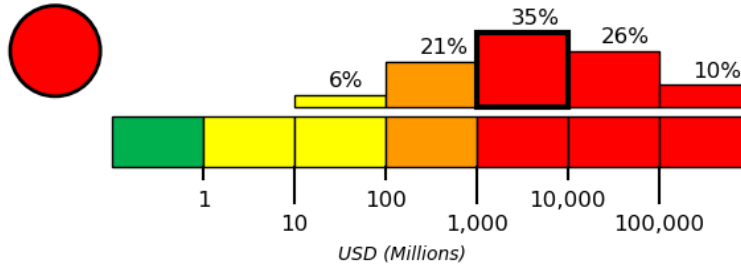
Figure 1.4. Economic losses estimated by PAGER for the Mw 7.5 earthquake (USGS 2023b).

1.2.1. Direct Losses Due to Structural Damage

Damage to personal property is expected to be significant, particularly given the number of complete collapses that result in not only significant threats to life safety, but also total loss of contents (Figure 1.5). Unfortunately, insured losses may be only around $1 billion (USD) due to low insurance coverage in the affected regions (Fitch 2023). The Turkish Catastrophe Insurance Pool (TCIP) was created after the 1999 Izmit earthquake to cover damage to residential buildings, but it does not cover human loss, liability claims, or business interruptions.

Figure 1.5. Collapsed multi-family residential building in Kahramanmaras. The photograph illustrates how observed collapse scenarios lead to complete loss of contents and the inability to recover personal possessions (Source: Reuters via CNN).

1.2.2. Losses Due to Impacts on Supply Chains

Iskenderun is home to heavy industries, e.g., steel production, and two major container hubs on Türkiye's Southeastern coast. A fire occurred at one of these ports, Türkiye's southern international shipping port, after the earthquake sequence (Figure 1.6) (Daily Sabah 2023a). The fire began at 1400 GMT on February 6 and was eventually extinguished via military helicopters and planes two days later. Reportedly, hundreds of shipping containers were ablaze. A leading global container shipping group, AP Moller Maersk, said that there had been significant damage

Joint PVRR: 2023 Türkiye Earthquake Sequence
PRJ-3824 | Released: 3/29/2023
Building Resilience through Reconnaissance

18

to logistics and transport infrastructure specifically around the Port of Iskenderun, requiring that company and other shipping lines to divert containers to nearby ports and hubs.

Figure 1.6. While gantry cranes appear unaffected by the earthquake, primary and secondary effects from fire after the earthquake compounded losses and downtime at the Iskenderun Port (Source: Odessa Journal).

The earthquakes also caused damage to gas transmission lines and disrupted the energy supply. In particular, gas supply was halted in Kahramanmaraş, Gaziantep, and Hatay provinces and some other districts. In terms of economic loss, the ramifications could include the spoiling of food items requiring refrigeration (Daily Sabah 2023), but also disruptions to key industries. For example, the earthquake sequence has affected several provinces in the country's southeast, which is home to around 30% of Türkiye's steel-producing Electric-Arc Furnace (EAF) capacity, equivalent to approximately 11.7 million tons per year of steel production. Iskenderun is an important port in Türkiye for steel imports and exports, as well as for raw material, mostly steel scrap. Thus the port's closure, as well as disruptions in power and gas supply, caused steel production to be disrupted. Roughly 80% of these mills are long steel producers (wire, rod, rail, bars, structural sections), which could lead to shortages of a commodity vital for reconstruction.

In Southern Türkiye, members of commerce chambers, exchanges, and industrial zones have opted to halt their production to provide aid to survivors. Members of the Turkish business sector have promised to dispatch hundreds of trucks loaded with supplies and equipment including cranes and excavators. Diyarbakır Commerce and Industry Chamber Chair Mehmet Kaya stated that industrialists in the region paused their production for at least a week after the earthquakes and have chosen to allocate their factories to the housing and food needs of survivors. In terms of structural integrity of these facilities, Kaya confirmed there were cracks in some of the factories but no severe damage (Daily Sabah 2023).

Due to the earthquake sequence affecting 10 provinces, on February 8, 2023, the Capital Markets

Joint PVRR: 2023 Türkiye Earthquake Sequence
PRJ-3824 | Released: 3/29/2023
Building Resilience through Reconnaissance

19

Board (SPK) announced that the Turkish Electronic Fund Trading Platform (TEFAS) and Private Pension Fund Trading Platform (BEFAS) transactions were suspended (Haber7 2023). Borsa İstanbul, the sole Turkish stock exchange, announced on February 8, 2023, that all transactions would be halted for at least five business days and any exchanges made on that date were canceled (Haber7 2023).

1.3.   Other Societal Impacts

Since the Mw 7.8 earthquake occurred at 4:17 am local time, its large impact was not apparent until dawn. The TAMP (Disaster Response Plan of Türkiye) was activated immediately following the earthquake. Soon after, a level 4 disaster level was announced, which is the highest level in the Türkiye emergency response plan.

As of February 19, 2023, the number of reported completely and partially collapsed buildings was 28,362 according to the Turkish Ministry of Environment, Urbanization and Climate Change, EUCC. Additionally, according to preliminary damage assessments, it was announced by the Minister of Environment, Urbanization and Climate Change, Mr. Murat Kurum, that 75,717 buildings and 306,563 dwellings were either collapsed or severely damaged (NTV 2023a). These numbers continued to evolve in the weeks that followed the earthquake, with damage encompassing residential, governmental, and commercial buildings. Since these numbers are provided by the official reports of EUCC, they only reflect losses in Türkiye.

In addition to the official response activities, Türkiye's citizens were mobilized to help the victims of the disaster and those in need. Civil society, non-governmental organizations, and private companies activated their full capacity and resources. These campaigns have been focused on the needs of the people, especially for food, accommodation, and clothing.

Turkish Airlines (THY) announced that they would be offering free flights from Adana, Adıyaman, Gaziantep, Kayseri, Diyarbakır, Şanlıurfa, Malatya, Elazığ, and Kahramanmaraş provinces on February 7, 2023, as part of their relief efforts. Thousands of volunteers were flown by THY to the cities impacted by the earthquakes to assist in rescue efforts and offer support. Bilal Ekşi, the CEO of THY announced that about 11,780 citizen volunteers, who went to airports to go to the earthquake zone following an invitation from AFAD, were taken to Adana, Gaziantep, Adiyaman, and Urfa in 80 flights (Daily Sabah 2023b).

Many individual and local initiatives were launched to respond to the earthquakes and mobilize shelters in the regions affected. Syrians have circulated many posts via social media of various restaurant owners announcing they would feed people displaced by the earthquakes. Several hotels have also stated their readiness to house survivors free of charge, some even offering further aid. Volunteer teams also launched initiatives to identify buildings vulnerable to further collapse (Enab Baladi 2023).

1.4.   Official Response

The earthquake sequence was announced to be a 4th level (the highest) disaster according to the National Disaster Response Plan of Türkiye. Therefore, the total resources of the country have been deployed to the earthquake region, according to the Response Plan.

On February 7, 2023, President Erdoğan issued a "State of Emergency" declaration for the ten

most affected provinces for a duration of three months. This decision follows Article #119 of the Turkish Constitution and facilitates the response and recovery activities in the region.

According to the National Response Plan, the official response details can be summarized as follows: The Search And Rescue (SAR) teams of the Disaster and Emergency Management Presidency (AFAD) of the Interior Ministry of Türkiye were sent to the affected region immediately after the earthquake. As of 10:55 am on February 13, 2023, there were a total of 35,495 SAR personnel, where 9,793 of them were from different countries. The total number of personnel serving in the area from different organizations reached up to 238,459 (AFAD 2023a).

1.5. Report Scope

StEER activated a Level 1 response with a Virtual Assessment Structural Team (VAST) formed on February 7, 2023 to evaluate this event, based on the event having the strong potential to generate new knowledge (evidenced by achieving more than 50% of the activation criteria in Table 1.1). The Earthquake Engineering Research Institute (EERI) Learning from Earthquakes (LFE) program Virtual Earthquake Reconnaissance Team (VERT) joined the VAST shortly thereafter to collaborate on the production of the primary product of StEER's Level 1 response to this earthquake sequence: this joint **Preliminary Virtual Reconnaissance Report (PVRR).** The joint PVRR is intended to:

1. Provide an overview of the 2023 Türkiye earthquake sequence and its impact on the built environment;
2. Summarize the codes and regulations and construction practices in the affected area;
3. Synthesize preliminary reports of damage to buildings, roads, bridges, and other infrastructure;
4. Provide recommendations for continued study of this event by StEER, EERI LFE, and the broader natural hazards engineering community.

While offering some evidence from Syria, the PVRR focuses heavily on the evidence and impacts in Türkiye. This is not intended to diminish the effects in Syria but is reflective of the limited amount of information and reporting from Syria and the Türkiye-Syria border region due to ongoing security concerns in that area.

Joint PVRR: 2023 Türkiye Earthquake Sequence
PRJ-3824 | Released: 3/29/2023
Building Resilience through Reconnaissance

21

Table 1.1. Summary of Level 1 Activation Criteria.

Hazard	Exposure	Feasibility
- Major intensity event - Succession of events - Joint/compounding hazards	- Sufficiently populated areas to create measurable impact - Communities with a history of recovery - Noteworthy code or construction practices - Critical infrastructure - Under-documented structure classes - Instrumented structures	- Availability/interest of members - Sufficient media/social media coverage of the event, including the potential to automate the mining of information - Sufficient bandwidth for multiple concurrent responses

Joint PVRR: 2023 Türkiye Earthquake Sequence
PRJ-3824 | Released: 3/29/2023
Building Resilience through Reconnaissance

22

2. Seismic Hazard and Recorded Ground Motions

On February 6, 2023, at 4:17 am local time (01:17 UTC), AFAD reported that an Mw 7.7 (USGS Mw 7.8) earthquake struck Pazarcık, Kahramanmaraş. A second Mw 7.6 (USGS Mw 7.5) earthquake hit Elbistan at 1:24 pm local time (10:24 UTC). The focus of the Mw 7.7 event was located at 37.288°N, 37.043°E with a depth of 8.6 km (AFAD 2023b, c). The Mw 7.6 earthquake occurred at 38.089°N and 37.239°E at a depth of 7 km (AFAD 2023b, c). Over 300 aftershocks occurred in the region within the first 48 hours of these two events. As of the afternoon of February 9, 2023, approximately 1,300 aftershocks were reported with magnitudes up to Mw 6.6, as shown in Figure 2.1 (AFAD 2023b).
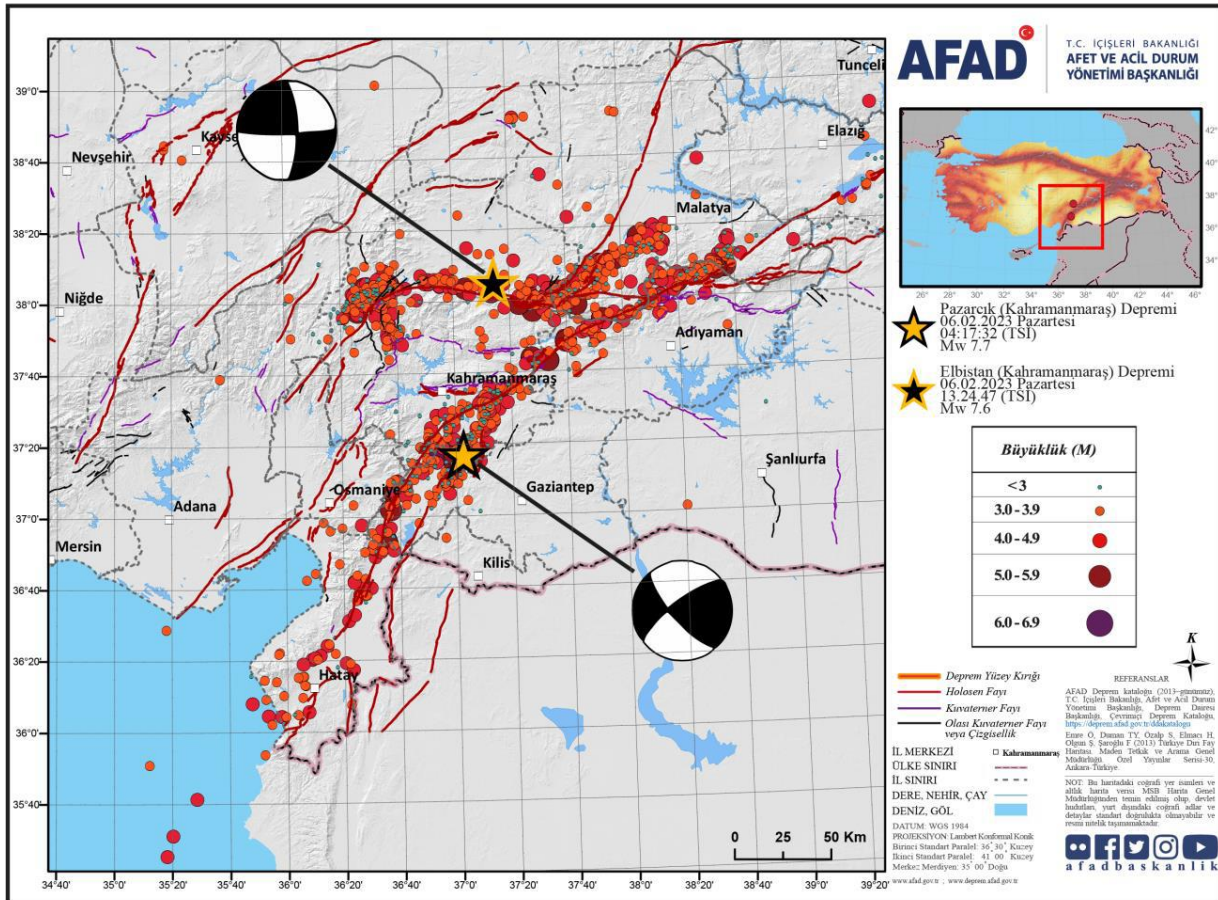
Figure 2.1. February 6, 2023, Pazarcık (Kahramanmaraş) Mw 7.7 and Elbistan (Kahramanmaraş) Mw 7.6 Earthquakes and corresponding aftershock activity (AFAD 2023b).

2.1. Tectonic Setting of Türkiye

Türkiye is situated in a complex tectonic setting, where the interaction of several tectonic plates results in a high level of seismic activity. The tectonic setting of Türkiye is mainly defined by the convergence of the Arabian, African, and Eurasian plates with the Anatolian plate that lies

Joint PVRR: 2023 Türkiye Earthquake Sequence
PRJ-3824 | Released: 3/29/2023
Building Resilience through Reconnaissance

23

between the Aegean Sea and the Iranian Plateau (Figure 2.2). The tectonic deformation of Türkiye is largely accommodated by a series of active faults, including the East Anatolian Fault (EAF), the North Anatolian Fault (NAF), the Sungurlu Fault (SF), the Ovacık Fault (OF), and the Dead Sea Fault (DSF) (Figure 2.3). These active faults, along with others in the region, pose a significant seismic hazard to the population and the built environment of Türkiye.
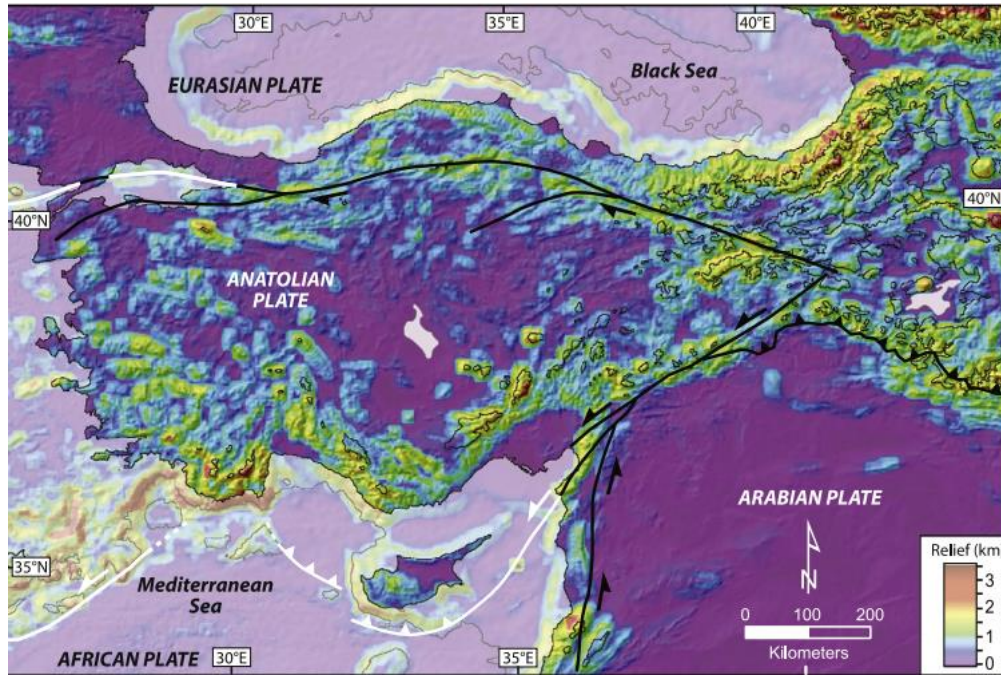
Figure 2.2. Convergence of the African, Arabian, and Eurasian plates with the Anatolian plate (Schildgen et al. 2014).

Joint PVRR: 2023 Türkiye Earthquake Sequence
PRJ-3824 | Released: 3/29/2023
Building Resilience through Reconnaissance

24
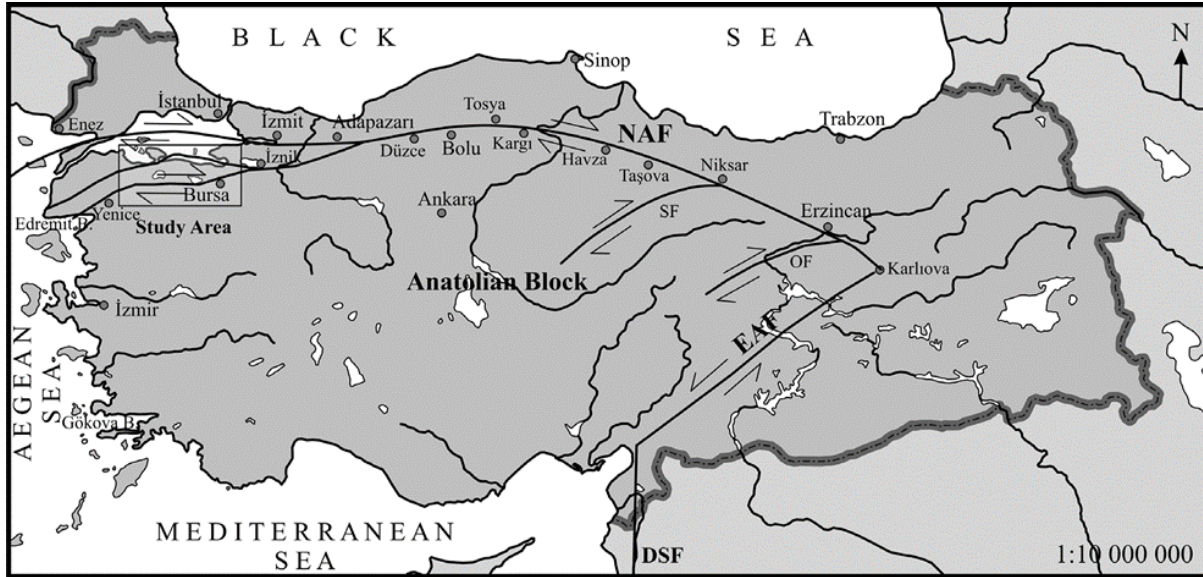
Figure 2.3. Simplified Neotectonic map of Türkiye (Selim & Tüysüz 2013).

The North Anatolian Fault (NAF) accommodates the westward motion of the Anatolian block with respect to the Eurasian plate, primarily through right-lateral strike-slip motion. Between 1939 and 1999, a series of devastating M7.0+ strike-slip earthquakes propagated westwards along the NAF system. The NAF has produced several devastating earthquakes in the past century, including the 1999 M7.6 İzmit earthquake. The East Anatolian Fault (EAF) is another major active fault in Türkiye. It extends for over 1200 km and accommodates the eastward motion of the Anatolian block with respect to the Arabian plate. The EAF has been responsible for several large earthquakes, including the 1983 M6.9 Erzurum earthquake. The Dead Sea Fault (DSF) is a major transform fault that extends from the Red Sea to Türkiye and intersects with the EAF in southeast Türkiye. The northern termination of the DSF occurs within a complex tectonic region of southeast Türkiye where the interaction of the African and Arabian plates and the Anatolian block occurs. This involves translational motion of the Anatolian Block westwards, with a speed of approximately 25 mm/yr with respect to the Eurasia plate to accommodate closure of the Mediterranean basin.

According to the USGS, the region where the earthquake sequence occurred is seismically active. Three earthquakes of magnitude 6 or larger have occurred within 250 km of the focus of the Feb. 6, 2023 Mw 7.7 earthquake since 1970. The largest of these, the Mw 6.8, Elazığ earthquake, occurred northeast of the Mw 7.7 earthquake on January 24, 2020. All these earthquakes occurred along or in the vicinity of the EAF. Despite the relative seismic quiescence of the epicentral area of this earthquake, southern Türkiye and northern Syria have experienced significant and damaging earthquakes in the past. Aleppo, in Syria, was devastated several times historically by large earthquakes. However, the precise locations and magnitudes of these earthquakes can only be estimated. Aleppo was struck by earthquakes of estimated magnitudes of 7.1 and 7.0 in 1138 and 1822, respectively. Fatality estimates of the 1822 earthquake are in the range 20,000 to 60,000 deaths.

Joint PVRR: 2023 Türkiye Earthquake Sequence
PRJ-3824 | Released: 3/29/2023
Building Resilience through Reconnaissance

25

2.2. 2023 Mw 7.7 and Mw 7.6 Earthquakes Features

2.2.1. Mw 7.7 Event

According to the current finite fault model, the Mw 7.7 earthquake resulted from strike-slip faulting at shallow depth (Figures 2.4 and 2.5) (USGS 2023a). The event ruptured over three fault segments within the vicinity of a triple-junction between the Anatolian, Arabian, and African plates (refer to Figure 2.2). The mechanism and location of the earthquake are consistent with the EAF and DSF systems (Figure 2.3). Preliminary finite-fault model estimates suggest the main slips asperity extends about 150 km long and 20 km wide in Segment 2, parallel to the EAF, and about 120 km long and 10 km wide in Segment 3, parallel to the DSF (Figures 2.4 and 2.5).

2.2.2. Mw 7.6 Event

According to USGS (2023b), the Mw 7.6 earthquake occurred 95 km to the northeast of the Mw 7.7 event, approximately nine hours later. The event ruptured over three fault segments (Figures 2.6 and 2.7), within the vicinity of the triple-junction between the Anatolia, Arabia, and Africa plates (refer to Figure 2.2). The mechanism and location of the earthquake are consistent with the EAF (Figure 2.3). The event ruptured either a near-vertical left-lateral fault striking east-west or a right-lateral fault striking north-south. The location and mechanism of the earthquake, along with aftershocks that have occurred since the Mw 7.7 earthquake, are consistent with the February 6 earthquake sequence having occurred within the broad EAF zone, though not necessarily all on the same fault strands. Preliminary finite-fault model estimates suggest main slip asperity measuring about 80 km long and 20 km wide (Figure 2.6). Figure 2.8 provides an example of relative ground displacement (fault slip) observed after the February 6, 2023 Mw 7.6 event. The ground displacement matches that expected from a shallow strike-slip mechanism.

Joint PVRR: 2023 Türkiye Earthquake Sequence
PRJ-3824 | Released: 3/29/2023
Building Resilience through Reconnaissance

26
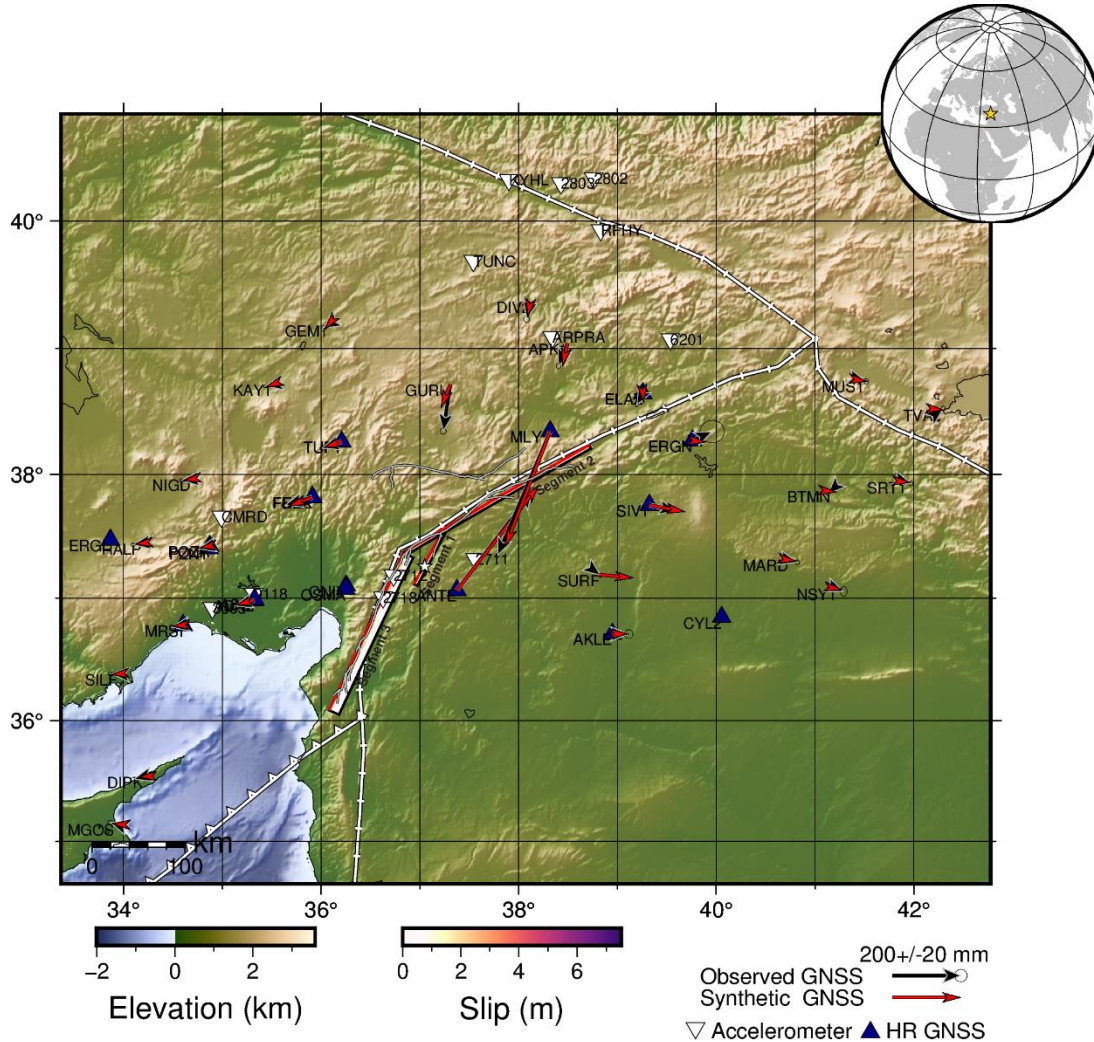
Figure 2.4. Surface projection of the slip distribution for the February 6, 2023, Mw 7.7 Kahramanmaraş, Türkiye (USGS 2023a, last accessed 2-20-2023).

Joint PVRR: 2023 Türkiye Earthquake Sequence
PRJ-3824 | Released: 3/29/2023
Building Resilience through Reconnaissance

27
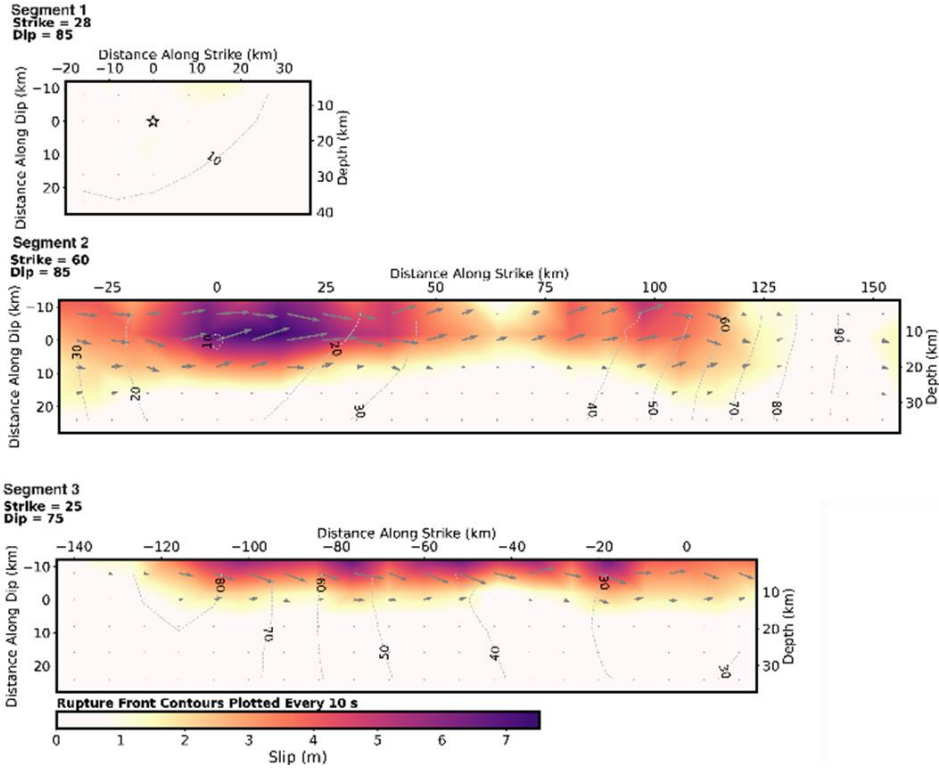
Figure 2.5. Cross-section of slip distribution for February 6, 2023, Mw 7.7 Kahramanmaraş, Türkiye (USGS 2023a, last accessed 2-20-2023).
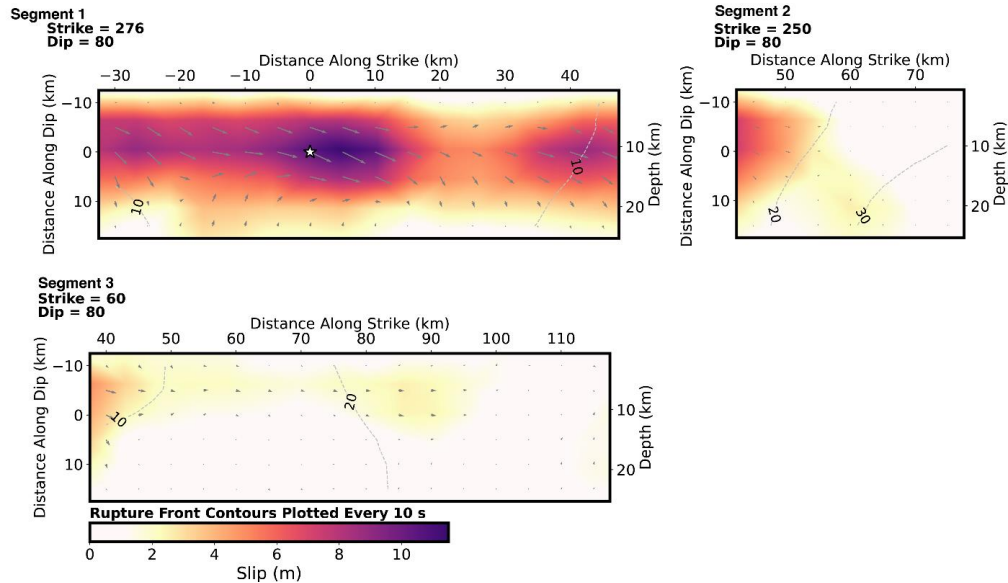
Figure 2.6. Cross-section of slip distribution for February 6, 2023, Mw 7.6, Türkiye (USGS 2023b, last accessed 2-20-2023).

Joint PVRR: 2023 Türkiye Earthquake Sequence
PRJ-3824 | Released: 3/29/2023
Building Resilience through Reconnaissance

28
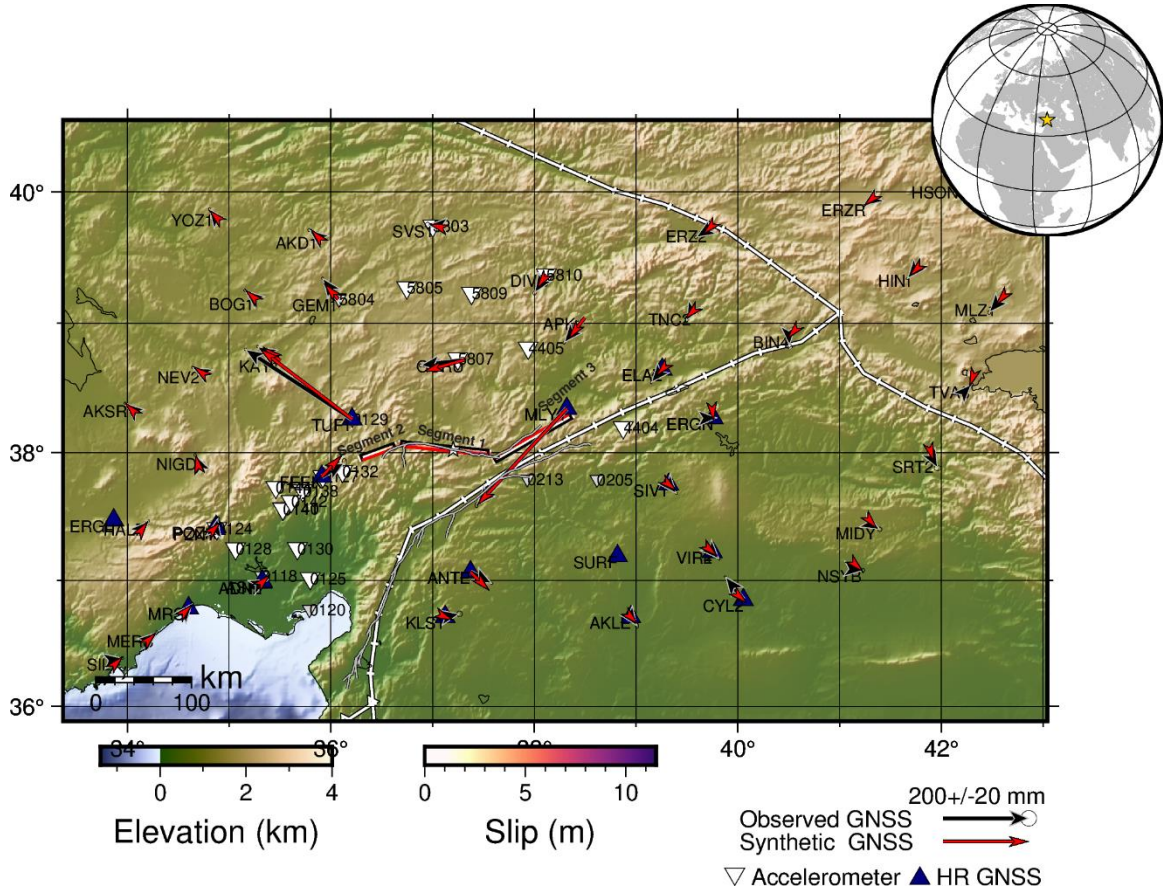
Figure 2.7. Surface projection of the slip distribution for the February 6, 2023, Mw 7.6, Türkiye (USGS 2023b, last accessed 2-20-2023).

Figure 2.8. Fault slip of 3.0 to 3.5 m at the Anatolian plate from the February 6, 2023 earthquake sequence (adapted from reddit post by u/kebabG 2023a, last accessed 2-20-2023).

Joint PVRR: 2023 Türkiye Earthquake Sequence
PRJ-3824 | Released: 3/29/2023
Building Resilience through Reconnaissance

29

2.3.   Evolution of Seismic Zonation and Current Seismic Hazard Maps

2.3.1. Türkiye

Between 1985 and 2018, at least eight national and international studies were used to update the seismic hazard estimates in Türkiye (Akkar et al. 2018). The 2018 model (Akkar et al. 2018) referred to as T-SHM (*The revised national probabilistic seismic hazard maps*) was initiated in 2013 with the leadership of AFAD, under the National Earthquake Strategy and Action Plan-2023. The T-SHM incorporated several new features and improvements that led to a more comprehensive assessment of the seismic hazard in Türkiye. For example, the updated model includes smooth contour maps of seismic hazard in rock developed for intensity measures such as PGA, PGV (peak ground velocity), and spectral acceleration at natural periods of T=0.2 and 1.0 seconds. The return periods considered in the hazard maps of the 2018 model are 43, 72, 475, and 2,475 years. The 2018 model contrasts with the typical zonation maps that were previously used in the country, which assumed constant values of the plausible seismic demands (intended as upper values) within five zones with no consideration of distance from the fault.

Before 1996, the zonation maps in Türkiye were based on building damage or macroseismic intensity, and hence were more related to the observed seismic risk than to the hazard. These maps had no smooth transitions between known seismically active regions and "non-seismic" regions. In contrast, the 1996 map considered PGA as the ground motion intensity parameter to define the seismic zonation within the country. Figure 2.9 shows examples of seismic zonation maps in Türkiye developed in 1945, 1963, and 1996. Note the increase in areas considered with high active seismicity over the years.

For the updated seismic hazard model (T-SHM), the researchers incorporated several important features for seismic source and ground motion characterization. In terms of source characterization, the model includes a comprehensive earthquake catalog that incorporates historical and instrumental data. The source model considers both areal and fault sources, complemented by background seismicity. For spectral acceleration-based intensity measures, these classified and ranked available Ground Motion Models (GMMs) and defined logic trees for active shallow crustal and subduction tectonic settings, to account for epistemic uncertainty.

The seismic hazard map of Türkiye (2018) for reference rock (Vs30=760 m/s) is shown in Figure 2.10 for PGA and the Design Basis Earthquake (DBE), i.e., an event with a 475-year return period. In contrast to the zonation results, the smooth contours offer a meaningful interpretation of the seismic hazard, which is consistent with the location of the seismic sources and the relative location of sites of interest. Based on the hazard map from AFAD, Figure 2.11 shows that the region near Kahramanmaras in Türkiye has a high seismicity with a PGA larger than 0.5g throughout the zone for a 475-year return period.

Joint PVRR: 2023 Türkiye Earthquake Sequence
PRJ-3824 | Released: 3/29/2023
Building Resilience through Reconnaissance

30

(a) High seismicity in dark red, less seismicity in light red, no seismicity in blank areas.
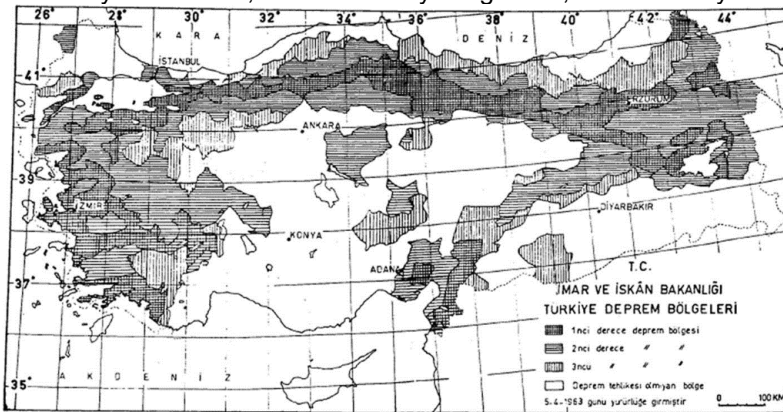
(b) Zone 1 of height seismicity in darker crossed-hatch, Zone 2 of moderate seismicity in horizontal hatch, Zone 3 of low seismicity in vertical hatch, and no seismicity in blank areas.
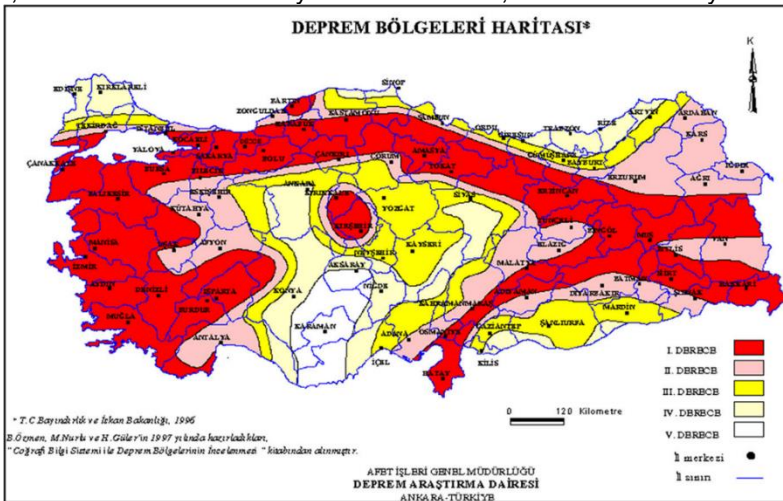
(c) Zone 1 in red of the highest seismicity, pink, yellow, and light yellow are Zone 2, 3, and 4, respectively, of decreasing seismic hazard, and blank areas of no seismicity.

Figure 2.9. Evolution of the seismic zonation maps in Türkiye: (a) 1945, (b) 1963, and (c) 1996 (Akkar et al. 2018).

Joint PVRR: 2023 Türkiye Earthquake Sequence
PRJ-3824 | Released: 3/29/2023
Building Resilience through Reconnaissance

31

Figure 2.10. Seismic Hazard Map of Türkiye (2018). PGA values are shown for DBE (DD2), a recurrence period of 475 years, or 10% probability of exceedance in 50 years (AFAD 2023d).
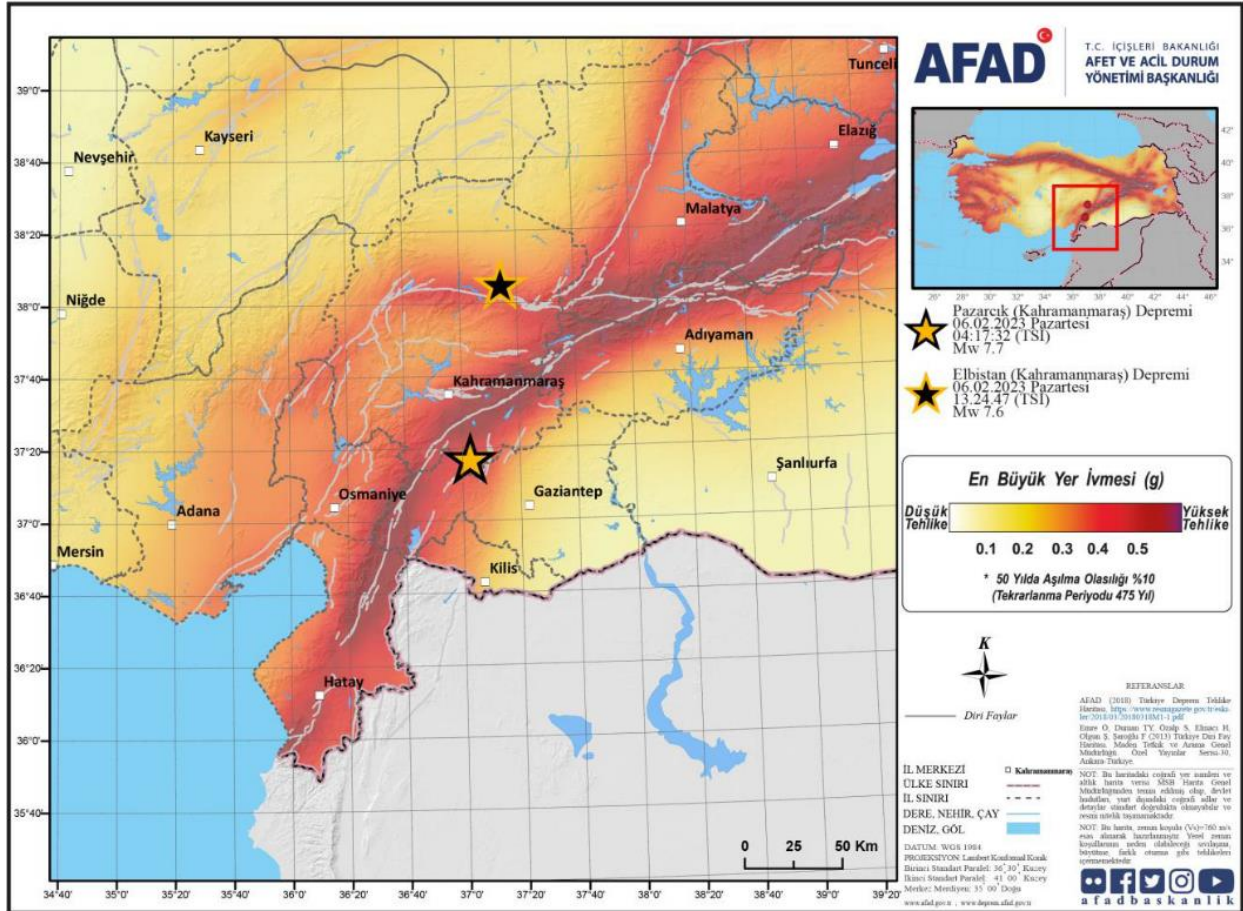
Figure 2.11. Design PGA in fraction of g's corresponding to a 10% probability of exceedance in 50 years (475-year return period) in the affected region (AFAD 2023e).

2.3.2. Syria

According to the 1996 Syrian Code Appendix I (Seismic Design), a design PGA value of 0.4g covers all Western Syria (Edlib, Aleppo, Escondaron, Latekia, Tartus, Daraa as well as some parts of Hama, Homs, Damascus, and Swaida) for a 1000-year return period (El Ssayed et al. 2012). The seismic hazard parameters were updated in the 2013 Syrian Code (Appendix 2: Seismic Design) to a PGA value ranging from 0.25g to 0.4g depending on the location and geologic nature of the region. Thus, currently the design PGA in Idlib is still 0.4g, but lower in Aleppo (0.25g in downtown and 0.3g in the West of Aleppo). The maps in Figure 2.12 show the seismic hazard level for PGA in Syria for the DBE and Maximum Considered Earthquake (MCE) (i.e., 475- and 1000-year return periods, respectively). Note that the 1,000-year return period is the maximum event that is considered in Syria, which is different from Türkiye and the US where a 2475-year return period event is the maximum considered earthquake.

Joint PVRR: 2023 Türkiye Earthquake Sequence
PRJ-3824 | Released: 3/29/2023
Building Resilience through Reconnaissance

33
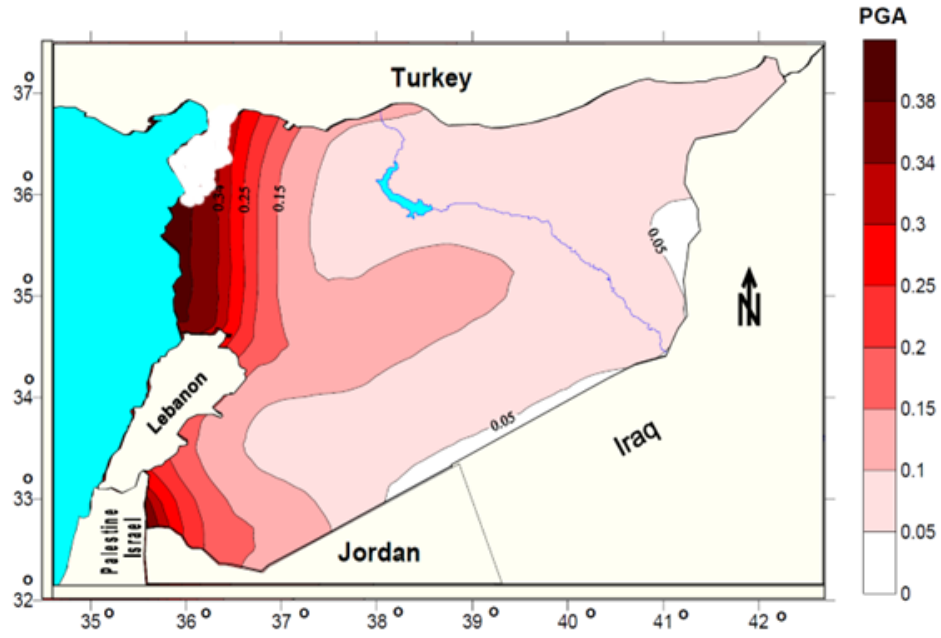
(a) 475 years.
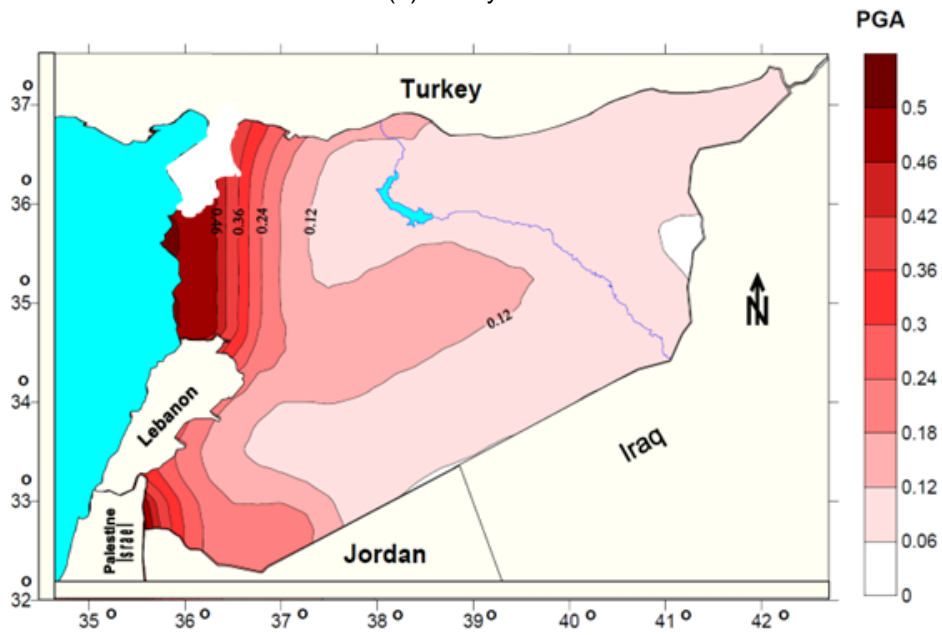
(b) 1000 years.

Figure 2.12. Seismic hazard maps of Syria showing distributions of PGA for different return periods (ElSsayed et al. 2012).

Joint PVRR: 2023 Türkiye Earthquake Sequence
PRJ-3824 | Released: 3/29/2023
Building Resilience through Reconnaissance

34

2.4. Recorded Ground Motions

2.4.1. Türkiye

The Turkish National Strong Motion Network (TNSMN), operated by AFAD, is the official strong motion network of Türkiye. This network comprises more than 800 accelerograph stations in Türkiye and Cyprus. Figure 2.13 shows the geographical distribution of these stations.
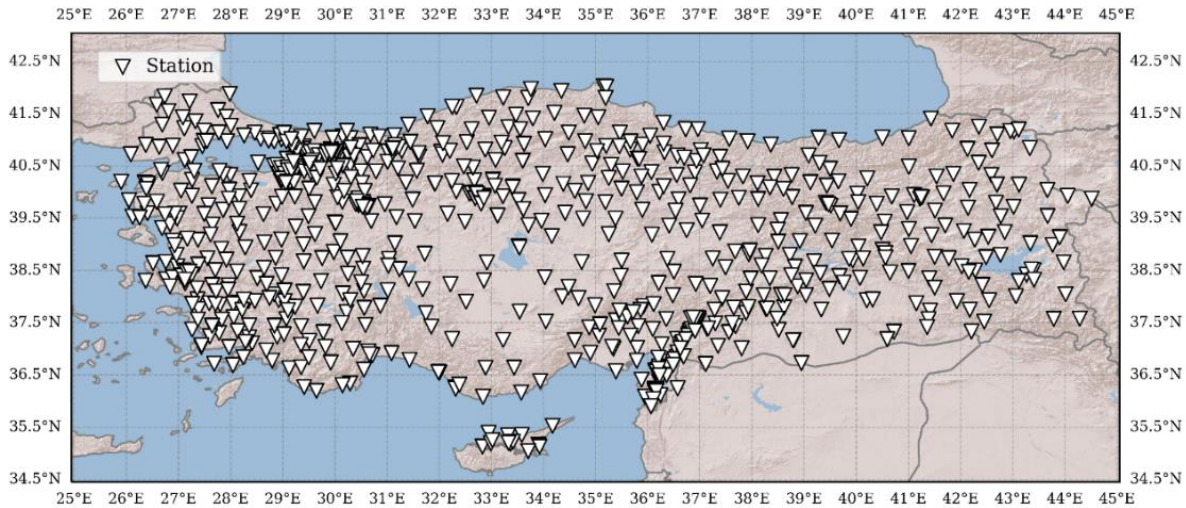
Figure 2.13. Geographical distribution of TNSMN accelerograph stations.

2.4.1.1. Mw 7.7 earthquake at 01:17 UTC

Figure 2.14 presents the shakemap for PGA estimated by AFAD (red coloring indicating highest measured intensity adjacent to the trace of the EAF portion North of the DSF, refer to Figure 2.3). Figure 2.15 zooms in on some of the stations of interest throughout this region. Coloring of the stations is consistent with the PGA levels in the legend of Figure 2.14. The corrected PGAs from the 17 stations in the vicinity of the epicenter of the Mw 7.7 event are summarized in Tables 2.1 and 2.2. Only stations with data vetted as reliable are included. The data are organized in descending order from the largest recorded horizontal geometric mean PGA. The maximum recorded horizontal PGA for a random component was 1347 cm/s^2 (1.37g), observed 146 km from the epicenter along the north-south direction at station 3129. In contrast, the horizontal geomean PGA at the station closest to the epicenter (No. 4616) was 0.58g.

Because of the bilateral nature of the rupture in this event (one rupture directivity occurring towards the south to Hatay and another occurring towards the east towards Malatya) very large PGA and PGV values were recorded at significantly large epicentral distances. For example, 1.3g PGA was recorded at an epicentral distance of 143 km due to combined effects of forward directivity, basin effects, and site amplification. Other distance parameters, e.g., Joyner-Boore distance (shortest horizontal distance from the recording site to the vertical projection of the rupture on the surface) or the closest distance from the recording site to the ruptured area, are more meaningful to represent the ground shaking due to this earthquake. This is particularly the case given that the fault rupture length was larger than 100 km, with some preliminary satellite

Joint PVRR: 2023 Türkiye Earthquake Sequence
PRJ-3824 | Released: 3/29/2023
Building Resilience through Reconnaissance

35

images showing a rupture length of 300 km. The GMMs discussed in the following use the Joyner-Boore distance. The GMMs use distances relative to the epicenter (R_{epi}) or hypocenter (R_{hyp}), relative to the closest point to the fault rupture (R_{rup}) or its surface projection (R_{jb}).

The quadratic mean of the as-recorded PGA and spectral accelerations are compared in Figures 2.16 to 2.19 to the GMMs developed by Akkar et al. (2014) and Boore et al. (2011) for a stiff soil condition (Vs30=500 m/s). For the implementation of the GMM by Boore et al. (2011), the regional coefficients for Türkiye were used. The comparisons for PGA and spectral acceleration Sa(T=0.50 s) for the Akkar et al. (2014) GMM are shown in Figures 2.16 and 2.17, respectively, while the comparisons for PGA and Sa(T=0.5 s) for the Boore et al. (2011) GMM are shown in Figures 2.18 and 2.19, respectively. For the calculation of the normalized residual, a default Vs30=500 m/s is used unless it is reported for the stations by TNSMN. Notice the overprediction (negative residual) trend increases with distance for both GMMs. Furthermore, the slope is steeper for the T=0.50 s case.
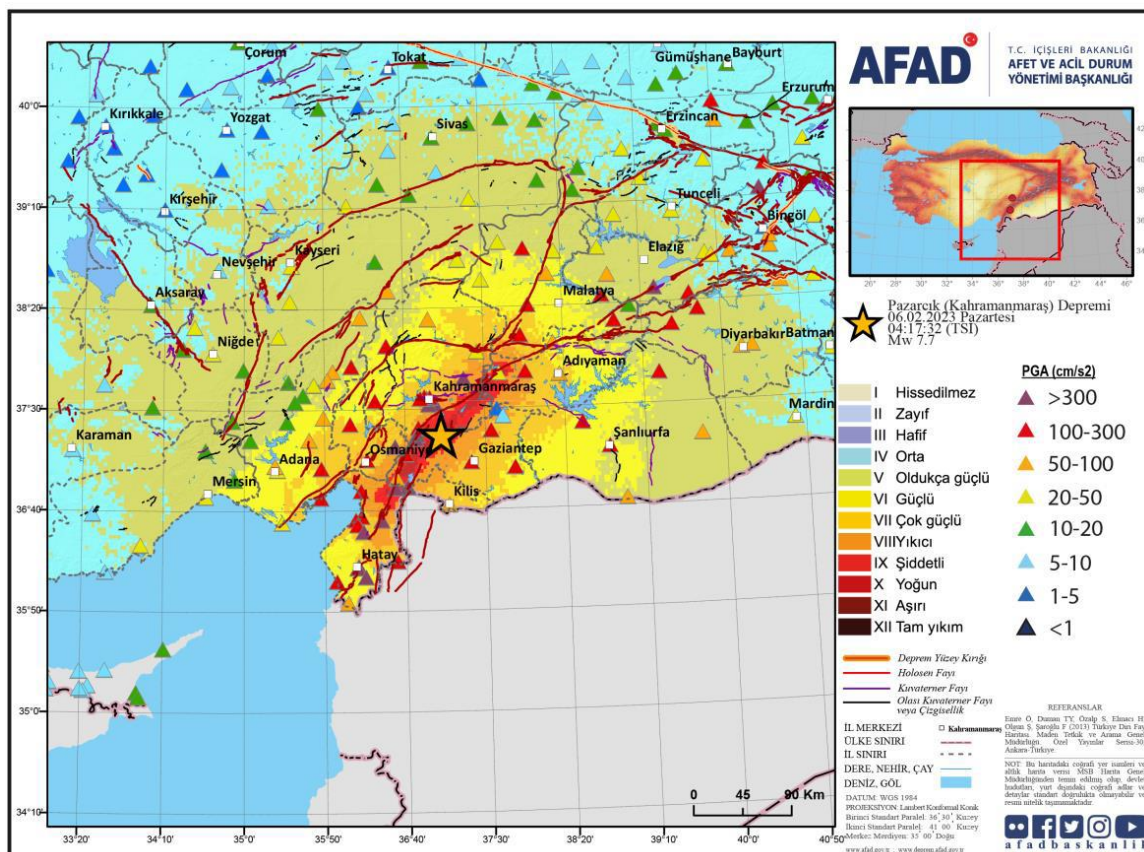
Figure 2.14. AFAD shakemap for the Mw 7.7 event at 01:17 UTC (1st event). Shakemap presents the AFAD-RED (AFAD-Rapid Earthquake Damage) estimations. Stations with triangles have the color-legend presenting the corresponding PGA records (AFAD 2023e).

Joint PVRR: 2023 Türkiye Earthquake Sequence
PRJ-3824 | Released: 3/29/2023
Building Resilience through Reconnaissance

36

(a) Northern region to the EAF

(b) Southern region to the EAF

Figure 2.15. Maps of some of the recording stations of interest. Data prepared by A. Dilsiz, after AFAD (2023b). Coloring of the stations is consistent with legend in Figure 2.14.

Joint PVRR: 2023 Türkiye Earthquake Sequence
PRJ-3824 | Released: 3/29/2023
Building Resilience through Reconnaissance

37

**Table 2.1.** Location of stations of interest for the Mw 7.7 event.

Code	Province	District	Soil Class	Vs30 (m/s)	Long.	Lat.	R_{epi} (km)
3129	Hatay	Defne	ZB	447	36.134	36.191	146.4
3126	Hatay	Merkez	ZC	350	36.138	36.220	143.5
2708	Gaziantep	İslahiye	ZB	523	36.648	37.099	40.8
3135	Hatay	Arsuz	ZB	460	35.883	36.409	142.2
3141	Hatay	Merkez	ZC	338	36.220	36.373	125.4
3125	Hatay	Merkez	ZB	448	36.133	36.238	142.1
3138	Hatay	Hassa	ZB	618	36.511	36.803	71.7
3142	Hatay	Kırıkhan	ZB	539	36.366	36.498	106.5
3123	Hatay	Merkez	ZB	470	36.160	36.214	143
4616	Kahramanmaraş	Türkoğlu	ZB	390	36.838	37.376	20.5
3131	Hatay	Merkez	ZB	567	36.163	36.191	145
4624	Kahramanmaraş	Onikişubat	ZC	280	36.918	37.536	29.7
4620	Kahramanmaraş	Onikişubat	ZB	484	36.899	37.586	35.5
2703	Gaziantep	Merkez	ZA	758	37.350	37.058	37.3
125	Adana	Ceyhan	ZC	208	35.796	37.015	114.6
4405	Malatya	Hekimhan	ZB	579	37.940	38.811	186.6
3112	Hatay	İskenderun	ZC	233	36.148	36.588	111.3

Joint PVRR: 2023 Türkiye Earthquake Sequence
PRJ-3824 | Released: 3/29/2023
Building Resilience through Reconnaissance

38

Table 2.2. PGA values at stations of interest for the Mw 7.7 event.

Code	PGA_NS (g)	PGA_EW (g)	PGA_UD (g)	Geomean PGA_Hor (g)
3129	1.37	1.23	0.72	1.30
3126	1.21	1.02	0.96	1.11
2708	1.32	0.93	0.69	1.11
3135	0.76	1.34	0.59	1.01
3141	1.01	0.85	0.68	0.93
3125	0.79	1.09	1.08	0.93
3138	0.91	0.77	1.25	0.83
3142	0.65	0.75	0.48	0.70
3123	0.67	0.59	0.86	0.63
4616	0.68	0.50	0.39	0.58
3131	0.36	0.36	0.15	0.36
4624	0.36	0.32	0.16	0.34
4620	0.30	0.32	0.19	0.31
2703	0.16	0.16	0.08	0.16
125	0.13	0.09	0.04	0.11
4405	0.08	0.12	0.07	0.10
3112	0.10	0.08	0.09	0.09

Joint PVRR: 2023 Türkiye Earthquake Sequence
PRJ-3824 | Released: 3/29/2023
Building Resilience through Reconnaissance

39
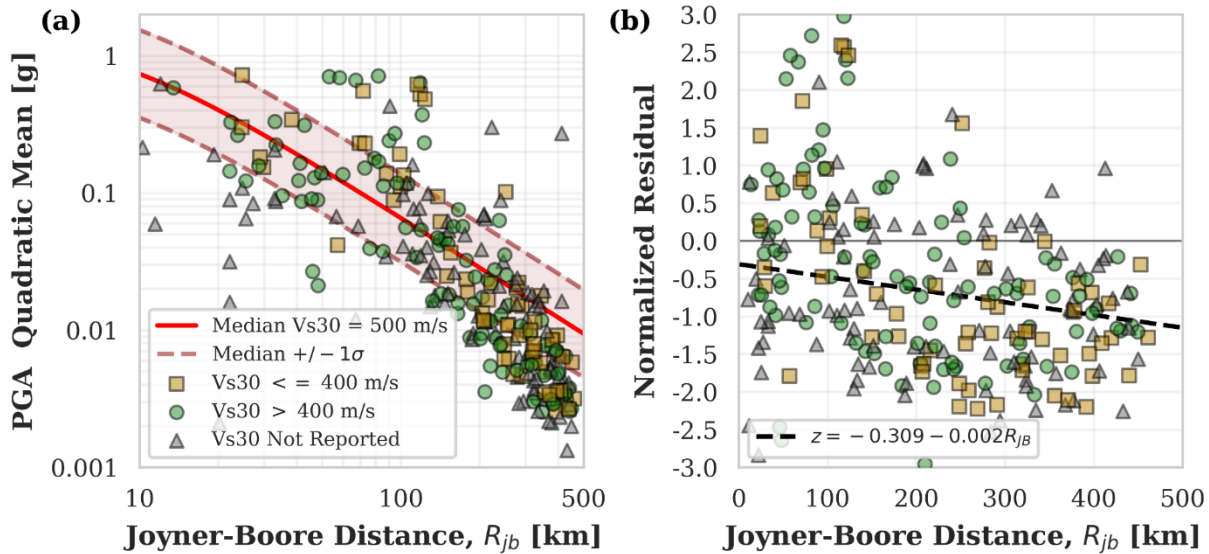
Figure 2.16. Comparison of the recorded PGA quadratic mean to predictions by the Akkar et al. (2014) GMM: (a) Attenuation for reference sites Vs30=500 m/s; (b) Normalized residuals as a function of distance.
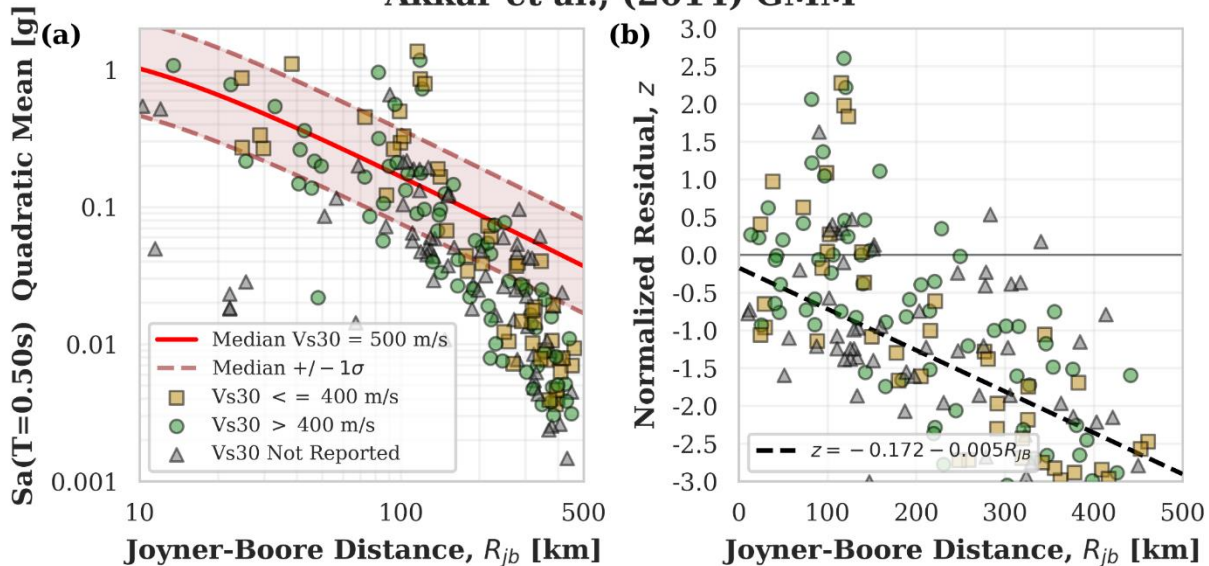
Figure 2.17. Comparison of the spectral acceleration at T=0.50 s quadratic mean to predictions by the Akkar et al. (2014) GMM: (a) Attenuation for reference sites Vs30=500 m/s; (b) Normalized residuals as a function of distance.

Joint PVRR: 2023 Türkiye Earthquake Sequence
PRJ-3824 | Released: 3/29/2023
Building Resilience through Reconnaissance

40
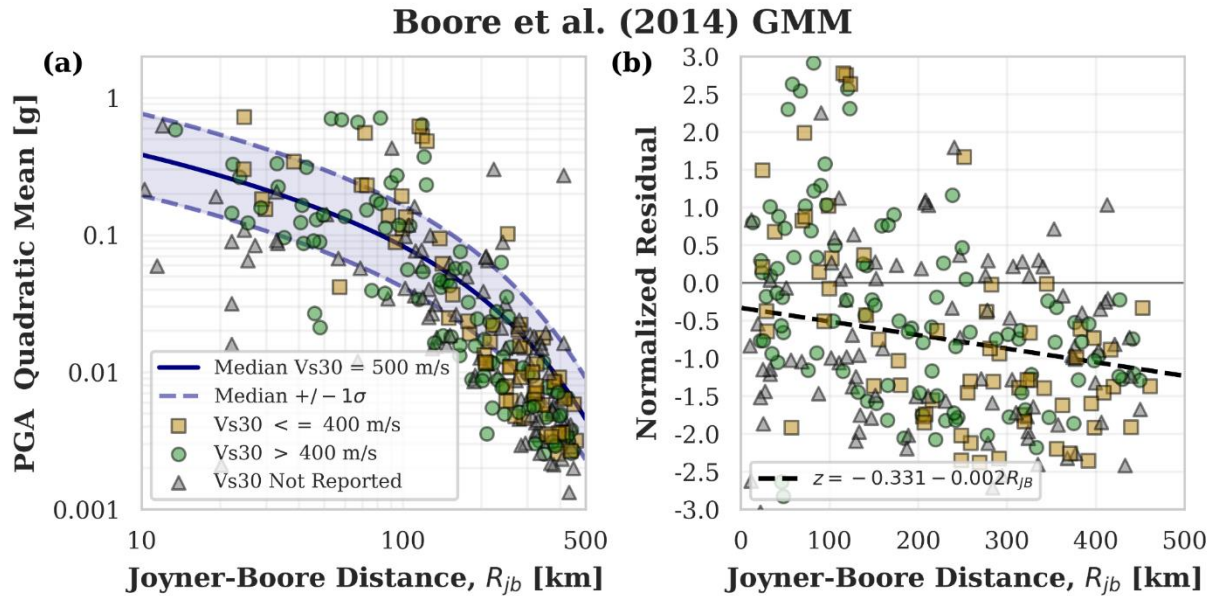
Figure 2.18. Comparison of the recorded PGA quadratic mean to predictions by the Boore et al. (2011) GMM: (a) Attenuation for reference sites 500 m/s; (b) Normalized residuals as a function of distance.
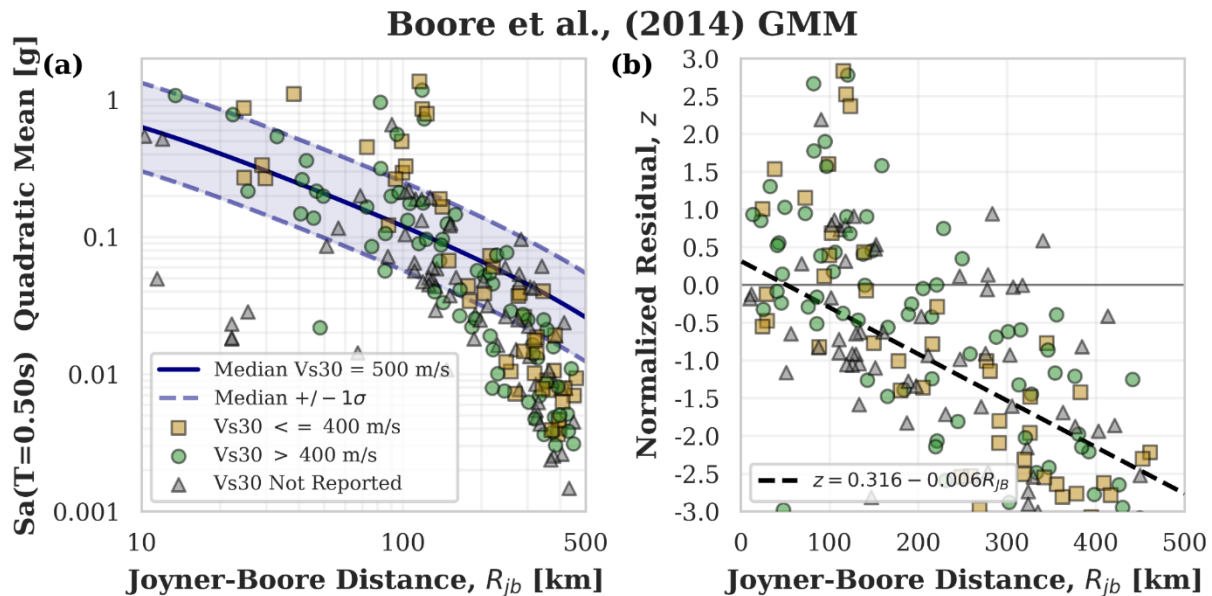
Figure 2.19. Comparison of the spectral acceleration at T=0.50 s quadratic mean to predictions by the Boore et al. (2011) GMM: (a) Attenuation for reference sites Vs30=500 m/s; (b) Normalized residuals as a function of distance.

Joint PVRR: 2023 Türkiye Earthquake Sequence
PRJ-3824 | Released: 3/29/2023
Building Resilience through Reconnaissance

41

2.4.1.2. Mw 7.6 earthquake at 10:24 UTC

Figure 2.20 presents the shakemap for PGA estimated by AFAD for the Mw 7.6 event. The color scaling is similar to that in Figure 2.14. Note the lower maximum intensities recorded for this second event, as compared to the Mw 7.7 event. The PGAs from the nine closest stations for the Mw 7.6 event that have both been automatically and manually processed are listed in Table 2.3. The maximum PGA of 637.93 cm/s^2 (0.65g) is observed at 36.5 km from the epicenter at station 4612.
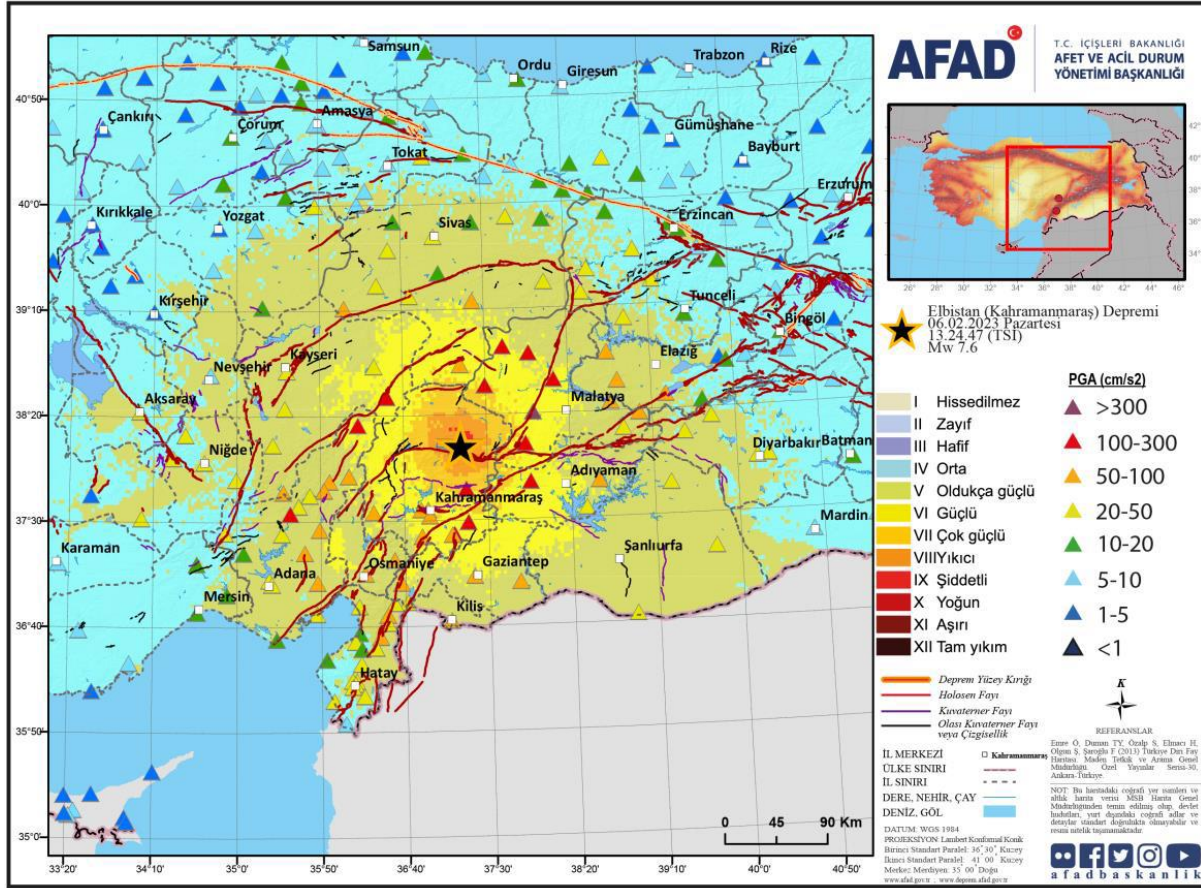
Figure 2.20. AFAD shakemap for the Mw 7.6 event at 10:24 UTC (2nd event). Shakemap presents the AFAD-RED estimations. Stations with triangles have the color-legend presenting the corresponding PGA records (AFAD 2023b).

Joint PVRR: 2023 Türkiye Earthquake Sequence
PRJ-3824 | Released: 3/29/2023
Building Resilience through Reconnaissance

42

Table 2.3. Recorded PGA values at stations closer to the epicenter of the Mw 7.6 event (AFAD, 2023b). Data obtained on 2-7-2023.

Station Code	Repi (km)	Longitude	Latitude	PGA_NS (g)	PGA_EW (g)	PGA_UD (g)
4611	38.2	37.2843	37.7472	0.20	0.14	0.07
4409	56.9	37.4908	38.5606	0.22	0.15	0.06
4612	66.70	36.4819	38.0240	0.65	0.53	0.38
213	68.7	37.9296	37.7967	0.12	0.13	0.07
4406	70.2	37.9738	38.3439	0.44	0.38	0.29
5807	70.9	37.2475	38.7269	0.09	0.07	0.05
3802	77.4	36.5036	38.4781	0.20	0.22	0.12
129	91.8	36.2109	38.2592	0.15	0.17	0.08
4410	94.6	37.6790	38.8668	0.11	0.13	0.05

2.4.2. Syria

The first seismic station was installed in Damascus University in 1978 after the establishment of the National Geologic Directorate, under the Ministry of Oil and Metallurgic Wealth. The number of seismic stations increased to nine stations in 1995 (Nadoor, 2016). The National Earthquake Center (NEC) was established by Decree N54 on December 26, 2004, and started operation in 2005. NEC was essential in updating Syrian Seismic Maps and the development of the 2005 Seismic Code Appendix 2. The NEC added more seismic stations to the network reaching a total of 27 prior to the 2011 revolution and war. The entire network was destroyed during the war except for the two stations in Damascus and Tartus. In 2019, the NEC started repair and/or reinstallation of some of these stations. However, due to the sanctions on Syria, it was prohibited to import transmitters and receivers for these stations. Therefore, they are currently not connected with the central station in Damascus and are only registering the seismic events locally with no telemetry. The map in Figure 2.21 shows the current and older seismic station locations. No information is available regarding currently operational seismic stations in Northwestern Syria, where the current earthquake sequence had the most effect. At the time of publishing this report, the ground motion records from the Syrian seismic stations for this earthquake sequence were not available. Moreover, since most of the stations were previously damaged and/or are using older technology, their records may not be reliable.

Joint PVRR: 2023 Türkiye Earthquake Sequence
PRJ-3824 | Released: 3/29/2023
Building Resilience through Reconnaissance

43
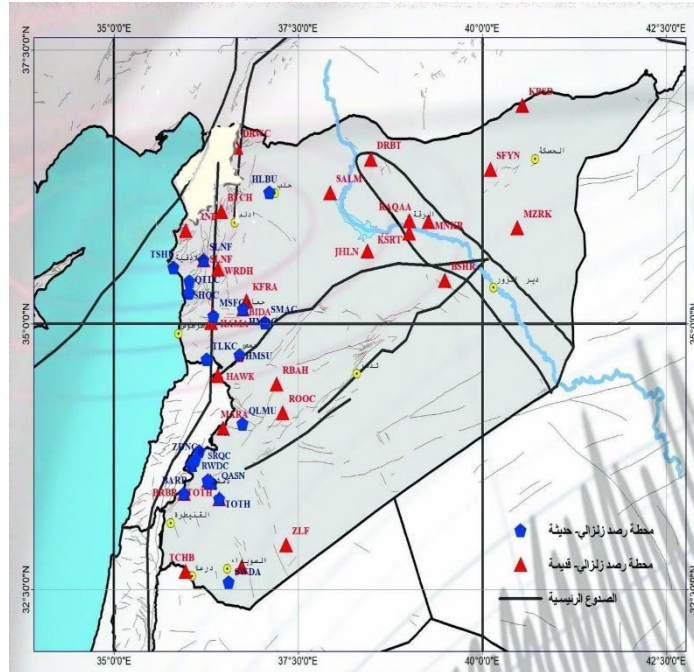
Figure 2.21. A map of the seismic recording stations in Syria. The blue markers show the operational stations at the time of the event, while the red markers show older stations (Source: SNEC - Syrian National Earthquake Center).

2.5. Response Spectra

The response spectra of selected ground motion records are presented in this section. The response spectra of the Mw 7.7 and Mw 7.6 earthquakes are provided in comparison with the corresponding design spectra at the location of the corresponding stations. The design spectra are plotted using the mapped spectral coefficients, which are taken from the seismic hazard map at the station locations. Moreover, the design spectra are plotted for both MCE (DD-1) and DBE (DD-2) level earthquakes according to the Türkiye Building Seismic Code (TBSC 2018). The DBE-level earthquake is defined as the uniform hazard spectra with a 475-year recurrence period (10% probability of exceedance in 50 years), while the MCE has a 2475-year recurrence period (2% probability of exceedance in 50 years).

As seen in Figures 2.22 to 2.27, the spectral accelerations obtained from the ground motions at the locations of the recording stations are larger than the design spectra at the MCE level for a significant portion of natural periods. It should be noted that non-essential (i.e., residential and commercial) buildings are designed and constructed according to the DBE level.

2.5.1. Mw 7.7 Event (at 01:17 UTC)

Figure 2.22 shows the response spectra at station TK.4616 (20.5 km from the epicenter, and 4 km away from the fault rupture) for the Mw 7.7 event at 01:17 UTC. This station is located in Türkoğlu district of Kahramanmaraş, and the soil characteristics are class ZB according to Eurocode 8 (shear wave velocity Vs30=390 m/s). The highest spectral accelerations of 2.5g and

Joint PVRR: 2023 Türkiye Earthquake Sequence
PRJ-3824 | Released: 3/29/2023
*Building Resilience through Reconnaissance*

44

1.38g are observed in the N-S direction at periods of 0.32 s and 0.65 s, respectively. Due to strong spectral content at short periods, a building at this location with a period of 0.1 to 0.75 s (typically 1 to 7 stories) will experience very intense shaking (larger than 1g). Additionally, there is strong spectral content (>1g) in the E-W direction at periods of 0.10 to 0.60 s.

Comparison of the response spectra for both horizontal components of this ground motion against the DBE and MCE indicates that except for the short period region (T<0.1 s), the response spectra at this location clearly exceed the design levels. For structures with periods larger than 0.4 s, it exceeds the MCE levels as well. Even in cases when the seismic hazard is accurately characterized, the current design philosophy of ductility-based design, adopted in the current and earlier versions of the Turkish Building Seismic Code (TBSC) and the seismic regulations of similar codes and standards around the world (including capacity design, confinement, and adequate detailing), aims at ensuring collapse prevention due to brittle failures and ensuring large levels of ductile response at damaged locations before failure. However, when the shaking experienced significantly exceeds the design levels, the provided ductility and energy dissipation capacity delivered by these principles of seismic design may not be sufficient and can lead to collapse. Based on judgment informed by benchmark studies of several code-conforming building systems, a maximum tolerable collapse risk of 10% is specified in FEMA P695 under MCE ground motions, and a collapse risk of 1% in 50 years is specified in the ASCE 07-22 provisions to define the seismic design parameters. Therefore, even code-compliant buildings could collapse when subjected to this intense motion.

Furthermore, it is possible that seismic detailing required by the code might not have been followed in the actual construction. For earthquake-resistant buildings, some degree of damage is expected when they are subjected to the design earthquake intensity, and this damage is generally repairable. However, when the shaking level significantly exceeds the design levels, such seismic design details may not be adequate to prevent collapse. This may explain the collapse of several mid-rise buildings in Kahramanmaras.

Finally, around 50% of the building stock in this area was constructed before 2000 and are more vulnerable under the experienced excessive levels of shaking. Another important factor related to the observed collapses is the demand that resulted from a Mw 7.7 earthquake followed by another earthquake (Mw 7.6) of a comparable size, and the high intensity aftershocks in between.

Joint PVRR: 2023 Türkiye Earthquake Sequence
PRJ-3824 | Released: 3/29/2023
Building Resilience through Reconnaissance

45

Figure 2.22. Spectral acceleration of the Mw 7.7 earthquake in comparison with the design spectra of DBE (DD-2) and MCE (DD-1) for horizontal components at station TK.4616.

The above discussion holds for stations 4612 (20 km epicentral distance) and 3123 (143 km epicentral distance) in Kahramanmaras and Hatay, respectively, with the difference that these are sites with softer soils with ground motions exceeding MCE levels at periods larger than 1.00 s. In particular, the ground motion in Hatay was multiple times larger than the MCE levels. This explains the widespread destruction observed in this city. Another major factor that might have contributed to the collapse of some relatively newer structures that were supposed to be earthquake-resistant is the cascading hazard effect from the strong aftershocks, especially the second earthquake of Mw 7.6. Several mid-rise buildings that survived the main shock (per the design intent), collapsed during the Mw 7.6 earthquake. It is likely that damage and inelastic behavior caused by the Mw 7.7 earthquake weakened these buildings. Strong aftershocks and the second major event within a few hours of the mainshock imposed large demands on the already "plastic" structures with significant strength and stiffness degradation. This sequence of seismic events is not considered by the code collapse prevention intent of a "10% probability of collapse in the MCE".

Figure 2.23 shows the response spectra at station TK.3123, which has R_{epi}=143 km and R_{rup}=20 km for the Mw 7.7 earthquake. This station is located in Hatay city center, and the soil characteristics are given as class ZB according to Eurocode 8, based on the shear wave velocity Vs30=470 m/s. Spectral accelerations larger than 1g and up to 2g are observed in both N-S and E-W directions at periods up to 2.00 s. Moreover, strong spectral content (larger than 0.5g) is observed for longer periods between 1.50 and 3.50 s. Mid- to high-rise buildings typically have natural periods in this range, and hence experienced severe shaking in both N-S and E-W directions. As mentioned above, the discussion on the possible reasons for the extensive destruction seems to be valid for buildings in this location as well.

Joint PVRR: 2023 Türkiye Earthquake Sequence
PRJ-3824 | Released: 3/29/2023
Building Resilience through Reconnaissance

46

Figure 2.23. Spectral acceleration of Mw 7.7 earthquake compared with the design spectra of DBE (DD-2) and MCE (DD-1) for horizontal components at station TK.3123.

Two more response spectra comparisons with the corresponding design spectra at the site are presented in Figures 2.24 and 2.25 for stations TK.2708 and TK.3138, respectively. TK.2708 is in Islahiye district of Gaziantep (R_{epi}=41 km and R_{rup}=2 km) and TK.3138 is in Hassa district of Hatay (R_{epi}=72 km and R_{rup}=1.3 km). The soil characteristics are given as class ZB according to Eurocode 8 for both stations with Vs30=523 m/s and 618 m/s for Islahiye and Hassa stations, respectively. High spectral accelerations > 1g and as large as 2g are observed in N-S and E-W directions at periods up to 1.7 s, for both stations. The peak spectral acceleration reached 2.9g at a period of 0.85 s at Hassa station (N-S direction). Moreover, strong spectral content (>0.5g) exists for long periods up to 2.50 and 3.00 s. Without exception, the response spectra are significantly larger than the design spectra. As discussed above, spectral accelerations are significantly larger than DBE and even MCE levels for roughly the full range of possible natural periods of buildings in the region. The high spectral content at periods larger than 1.00 s observed in Figures 2.23 to 2.25 suggest potential significant local site amplification and potential basin effects.

Other response quantities of interest in earthquake engineering applications, in addition to spectral accelerations, include spectral velocities and displacements. Particularly, it has been shown that spectral velocities (or their approximate values referred to as spectral pseudovelocities) are related to strain energy and maximum stresses, providing an effective measure of the potential damage and destructiveness of a ground motion (Villaverde 2009). Figure 2.26 shows the pseudovelocity and spectral displacement response spectra for records measured at stations TK.3125, TK.3141, and TK.3135 and a 5% damping ratio (percentage of critical damping).

Joint PVRR: 2023 Türkiye Earthquake Sequence
PRJ-3824 | Released: 3/29/2023
Building Resilience through Reconnaissance

47

Figure 2.24. Spectral acceleration of Mw 7.7 earthquake compared with the design spectra of DBE (DD-2) and MCE (DD-1) for horizontal components at TK.2708.
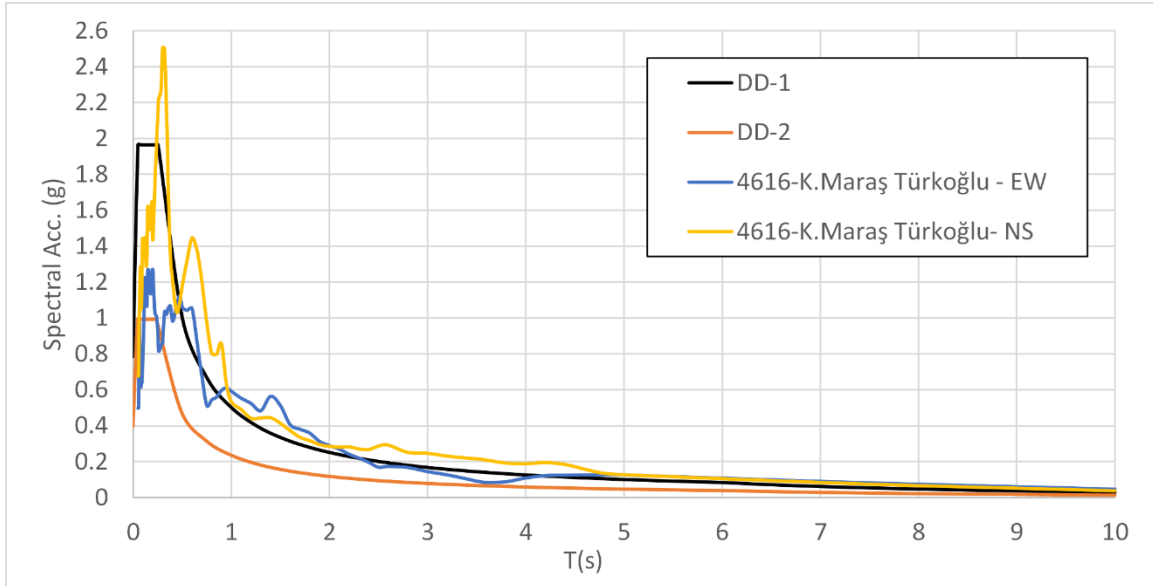

Figure 2.25. Spectral acceleration of Mw 7.7 earthquake compared with the design spectra of DBE (DD-2) and MCE (DD-1) for horizontal components at TK.3138.

Joint PVRR: 2023 Türkiye Earthquake Sequence
PRJ-3824 | Released: 3/29/2023
Building Resilience through Reconnaissance

48

Figure 2.26. Spectral pseudovelocity (PSV) and spectral displacement (SD) response spectra of the Mw 7.7 earthquake for horizontal components at TK.3125, TK.3141, and TK.3135.

2.5.2. Mw 7.6 Event (at 10:24 UTC)

For the Mw 7.6 event that occurred approximately 9 hours after the Mw 7.7 event, two comparisons between response spectra and design spectra are presented in Figures 2.27 and 2.28 for stations TK.4612 and TK.4406, respectively. TK.4612 is in Göksun district of Kahramanmaraş (R_{epi}=66.7 km) and TK.4406 is in Akçadağ district of Malatya (R_{epi}=70 km). The soil characteristics are given as class ZC and ZA per Eurocode 8, and the shear wave velocities Vs30=246 m/s and 815 m/s for Göksun and Akçadağ stations, respectively.

The strong motion duration D5-95 at this station are 25.91 s (E-W) and 20.15 s (N-S) [https://tadas.afad.gov.tr/waveform-detail/275963]. The Vs30 at TK.4612 (Göksun seismometer location) indicates soft soil which has a tendency of higher shaking at longer periods. Figure 2.27 shows large spectral content at longer periods (> 0.3 s) in both directions. In the N-S direction, the spectral accelerations exceed 1g for periods of 1.00 to 2.00 s with the potential of causing heavy damage in high-rise buildings (10 stories and higher). This aligns with reports that "the downtown district with taller buildings was hit particularly hard, while residential areas outside the city center had less apparent destruction" (Abraham et al. 2023).

Comparing the response spectra at TK.4612 with the hazard spectra indicates that observed shaking exceeds the DBE level hazard spectra (10% exceedance in 50 years, or 475-year return period) at almost all periods and exceeds the MCE level hazard spectra (2% exceedance in 50 years, or 2475-year return period) at all periods above about 0.50 s. Engineered structures that are designed to resist seismic forces are typically designed to prevent collapse at MCE-level shaking. As a result, tall buildings at this location that would have been engineered to prevent collapse at MCE levels could experience heavy damage or collapse in this earthquake given that the shaking exceeded the MCE levels by a factor of 2 to 3 for certain periods.

The impact of the earthquake sequence on buildings is clearly location dependent. For the same earthquake, the observed response spectra at station TK.4406 in Akçadağ (Figure 2.27) do not exceed the MCE levels at any value of natural period. However, the DBE level is exceeded by the observed response spectra. As a result, engineered buildings at this location may be able to withstand this shaking without collapse, albeit while sustaining moderate to heavy damage.

Joint PVRR: 2023 Türkiye Earthquake Sequence
PRJ-3824 | Released: 3/29/2023
Building Resilience through Reconnaissance

49

However, it should be noted that this second event occurred only nine hours after the first large event. As discussed above, high shaking levels as shown by the response spectra, structural system degradation during long duration of shaking from the two main events and aftershocks, and the occurrence of the earthquake sequence with strong multiple aftershocks, should all be considered altogether.
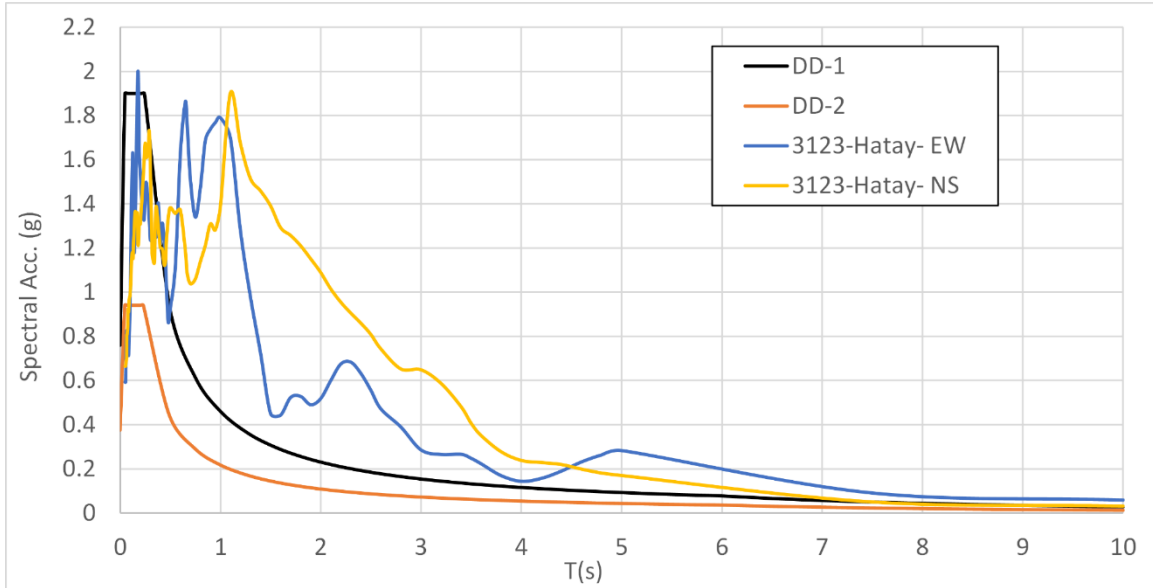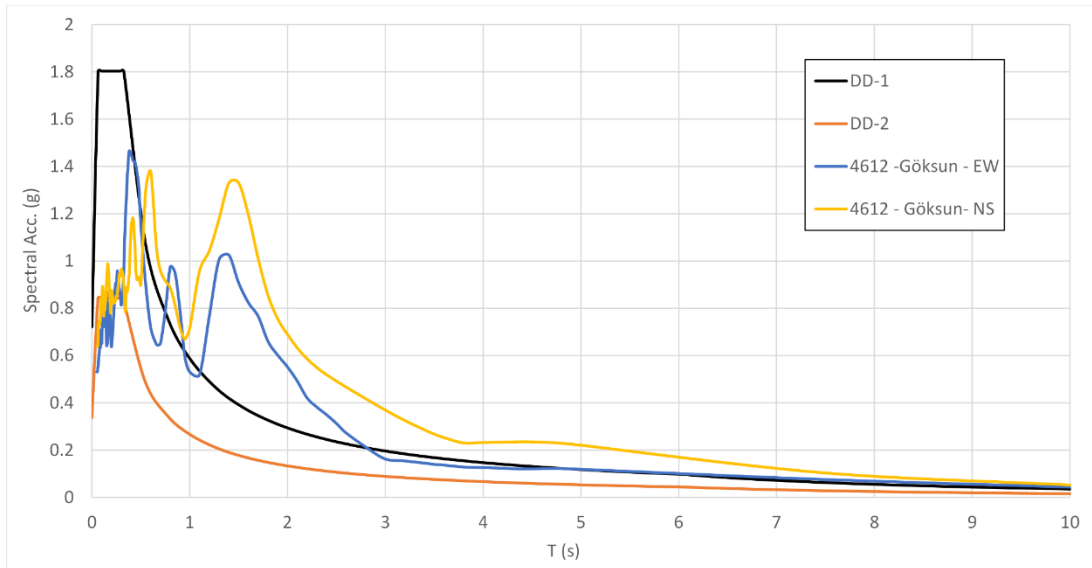

Figure 2.27. Spectral acceleration of Mw 7.6 earthquake in comparison with the design spectra of DBE (DD-2) and MCE (DD-1) for horizontal components at station TK.4612.
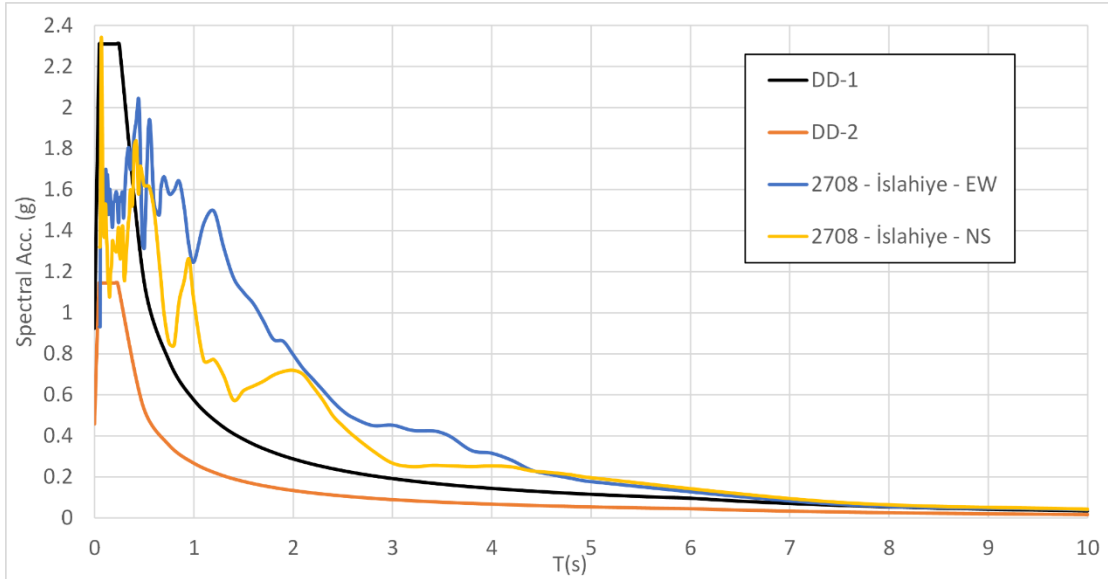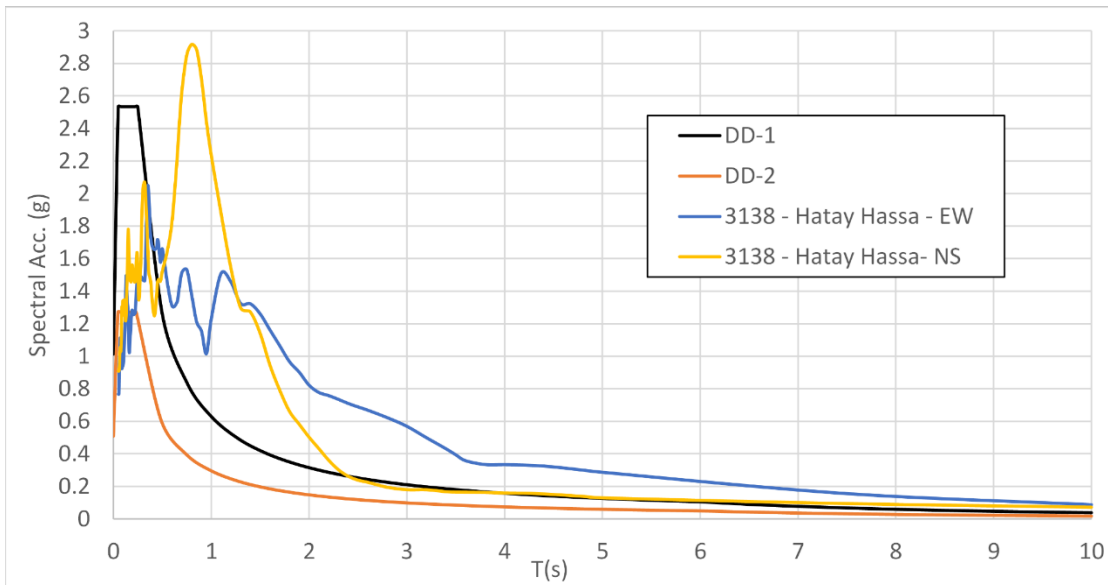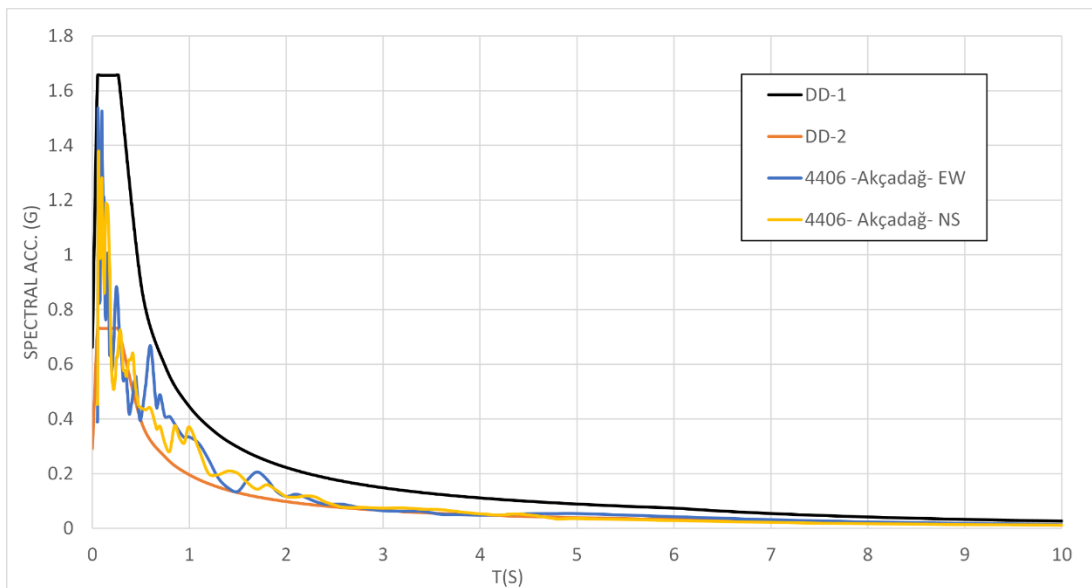

Figure 2.28. Spectral acceleration of Mw 7.6 earthquake in comparison with the design spectra of DBE (DD-2) and MCE (DD-1) for horizontal components at station TK.4406.
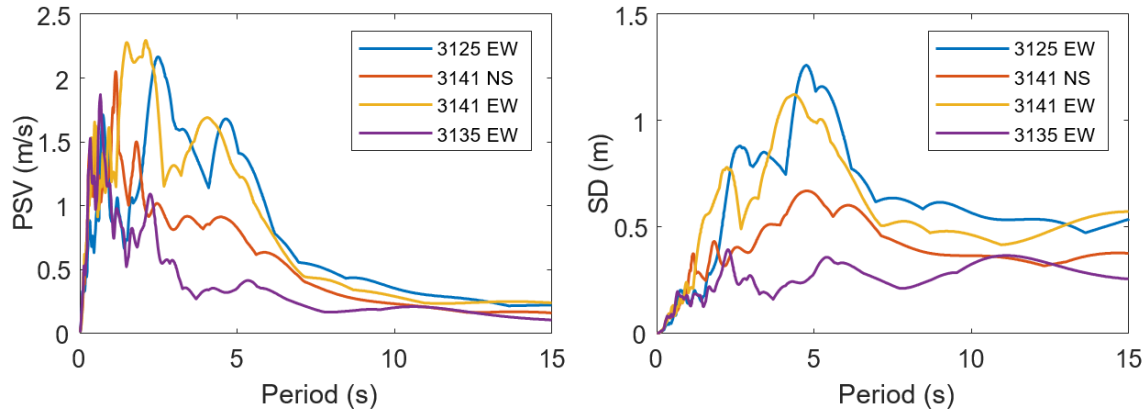
Joint PVRR: 2023 Türkiye Earthquake Sequence
PRJ-3824 | Released: 3/29/2023
Building Resilience through Reconnaissance

50

3.   Local Codes and Construction Practices

In this chapter, the regulations on the seismic resistant design and the construction practices in the two countries affected by the earthquake sequence, Türkiye & Syria, are discussed.

3.1. Türkiye

Earthquake-resistant design of buildings in Türkiye is regulated by the Turkish Building Seismic Code, TBSC (2018). Prior to the latest revision in 2018, TBSC has undergone seven revisions (1947, 1953, 1961, 1968, 1975, 1998, and 2007). Most of these revisions were based on the advancements in earthquake engineering and lessons learned from the earthquakes around the world and particularly in Türkiye. For example, the 2007 version of the code was highly influenced by the observations made after the 1999 Kocaeli and Duzce earthquakes (Sezen et al. 2023). Moreover, the seismic assessment of existing buildings was added to the code for the first time in this version. The current version (2018) of the code includes state-of-the-art earthquake engineering principles such as performance-based design, design of high-rise and base-isolated buildings, and Probabilistic Seismic Hazard Analysis (PSHA). In addition, seismic hazard maps are available for the entire country corresponding to DBE and MCE levels (Sezen et al. 2023). The TBSC sets standards for building design, construction, and building inspection to ensure safety and stability during earthquakes. Some key requirements of TBSC (2018) are:

1. <u>Seismic hazard assessments</u>: TBSC requires that the seismic hazard of a building site be considered in the design process. For the construction site, the mapped spectral coefficients are used for generating design spectra for different seismic hazard levels (e.g., DBE and MCE). The spectral acceleration coefficients are obtained from the Seismic Hazard Map (Section 2.3), which accompanies TBSC. The design spectra also consider local site parameters (e.g., local site class defined by the Vs30 information). According to the code, site specific seismic hazard assessment is also possible, and it is a requirement for construction on very loose soil conditions.
2. <u>Structural design</u>: TBSC sets specific design requirements for different building types and structures, e.g., use of seismic-resistant materials, provision of adequate reinforcement, and improvement of seismic-resistant detailing, to ensure ductile behavior of RC buildings.
3. <u>Foundation design</u>: TBSC sets requirements for the design of foundations, including the use of deep foundations, pile foundations, or raft foundations, to ensure that they can resist the forces generated during an earthquake.
4. <u>Performance Acceptance Criteria</u>: TBSC sets performance acceptance criteria for different levels of performance such as immediate occupancy, life safety, and collapse prevention for different seismic hazard levels (e.g., DBE and MCE). These criteria are defined for both design of new buildings and existing ones.

The lessons learned from the 1999 Kocaeli and Duzce earthquakes led to a post-1999 active period for the implementation of earthquake engineering principles in the whole country. Besides code development, utmost priority was placed on the transformation of old and vulnerable building inventory. Two of the new legislative actions for this purpose are "Building Supervision System" regulation in 2001 and "Urban Transformation" in 2012. The use of ready mixed concrete and deformed reinforcement bars became more widespread. Based on these developments, the buildings constructed after 2000 are assumed to have enhanced quality and considered to be less vulnerable to earthquake events. The Turkish Statistical Institute (TÜIK) recently provided

Joint PVRR: 2023 Türkiye Earthquake Sequence
PRJ-3824 | Released: 3/29/2023
Building Resilience through Reconnaissance

51

data on the 2021 building stock grouped by construction period. Table 3.1 shows the data for buildings in cities most affected by the 2023 earthquake sequence.

Table 3.1. Distribution of buildings (%) in affected cities per construction period (TÜIK 2023).

Province	1980 and before	1981-2000	2001 and later	Unknown
Şanlıurfa	5.5	18.5	61	14.9
Diyarbakır	6.5	26.6	58.1	8.8
K.Maraş	11.7	26.9	58.1	3.3
Adıyaman	8.7	23.6	52.3	15.4
Kilis	11.2	21.7	52.3	14.9
Gaziantep	6.6	25.9	51.6	15.9
Hatay	13.5	32.6	50	3.9
Malatya	14	28.1	48.4	9.5
Osmaniye	10.5	25.7	46.5	17.3
Adana	13	34.8	38.7	13.5

Building data from TÜIK and field studies in Gaziantep city, where the first earthquake hit, reveal that almost two-thirds of the residential buildings are masonry and one-third are Reinforced Concrete (RC). Most masonry buildings are 1 to 2 story structures, whereas RC buildings are mostly 1 to 4 stories, although some mid-rise and high-rise buildings exist. Most of the buildings built between 1980 and 2000 are regarded as non- or low-engineered structures. The Kocaeli and Duzce earthquakes in 1999, which resulted in significant building damage and collapses, led to major changes in the seismic design practices, which were enacted in the 2007 version of the TBSC. However, there is evidence that even post-2000 and post-2007, RC and masonry buildings were not properly designed and detailed for adequate ductility and seismic resistance.

The observations from the recent Mw 6.1 Duzce Earthquake on November 23, 2022, showed the importance of taking action to reduce the number of buildings with seismic deficiencies. The majority of the buildings in the Duzce region affected by the November 23, 2022 earthquake were new and constructed following the lessons learned from the 1999 Kocaeli earthquake. Effectively, they replaced the older buildings that were designed and constructed before 1999. Similarly, many buildings, including government and school buildings in the region, have been retrofitted since 1999. The low level of damage observed during the 2022 Duzce earthquake demonstrated the effectiveness of code-specified seismic design requirements on the newer buildings with four or less stories and is a testimony to the effectiveness of the retrofit measures taken since 1999 (Sezen et al. 2023).

According to the observations from previous earthquakes, insufficient engineering design and construction quality are major contributing reasons for the failure of buildings in Türkiye during recent earthquakes. These deficiencies are manifest in many undesirable structural flaws, such as weak column-strong beam, soft-story, non-ductile detailing of structural members and connections, lack of strength of lateral load carrying systems, and discontinuous frames. Moreover, removal of the load carrying system members, insufficient geotechnical site investigations, and poor foundation design can be added to the reasons for the observed damage of structural systems.

Joint PVRR: 2023 Türkiye Earthquake Sequence
PRJ-3824 | Released: 3/29/2023
Building Resilience through Reconnaissance

52

3.2. Syria

3.2.1. Code Development

The first RC building code in Syria is the 1977 "Arab Code for Reinforced Concrete Structures," which was based on the French Code. This code included the first basic seismic design provisions. The basis of the current structural concrete building code is the 1992 "Arab Syrian Code for the Design and Construction of Reinforced Concrete Structures," also known as "The Base Code" and its first revision took place in 1995, which adopted the Uniform Building Code UBC-85 for seismic loads and seismic calculations based on the Equivalent Static Method.

The second version of the Base Code published in 1995 planned for three appendices to separate and improve the seismic provisions. These are: Appendix 1 published in 1996 "Conditions and Precautions for the Design and Construction of Earthquake-Resistant Buildings", Appendix 2 published in 1997 "Seismic Assessment of Existing Buildings", and Appendix 3 published in 2000 "Strengthening of Existing Buildings for Seismic Resistance".

In 2004, the third version of the code was published, in which the Syrian Seismic Map was updated. After the establishment of the National Earthquake Center (NEC), a new appendix was published in 2005, merging the previous three appendices into Appendix 2 "Design and Construction of Earthquake-Resistant Buildings and Structures." In this appendix, it was possible to conduct seismic analysis either by the First Equivalent Static Method in the Base Code (2004), or by the Second Equivalent Static Method in Appendix 2 (2005) which was based on UBC-97. Appendix 2 (2005) also offered the Response Spectrum Analysis and the Response History Dynamic Analysis methods based on the nature of the structure and its intended use. The current design spectrum of the Syrian Code is shown in Figure 3.1. Both the 2004 Base Code and the Seismic Appendix 2 were reapproved in 2012 and 2013, respectively, with some modifications. The current RC building code is the fourth version of the 2012 Base Code, with the 2013 seismic design Appendix 2, both reapproved in the 2018 Code version. The seismic design Appendix in 2013 updated the use of the UBC-97 Code Equivalent Static Method, and offered, as an alternative, the Improved Equivalent Static Method (based on mode shapes following the ASCE 7-10 Standard, and the IBC 2009 Code).
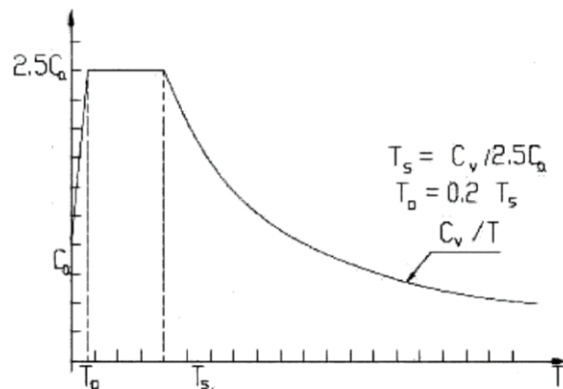
Figure 3.1. Current design response spectrum (spectral acceleration versus natural period) in Syria (Source: Arab Syrian Code for Design and Construction of Reinforced Concrete Buildings (2013), Appendix 2: Design of Earthquake-Resistant Buildings and Structures).

Joint PVRR: 2023 Türkiye Earthquake Sequence
PRJ-3824 | Released: 3/29/2023
Building Resilience through Reconnaissance

53

The first code provisions to introduce seismic details in concrete construction was the 1996 Appendix 1. Thus, it is reasonable to assume that any building constructed prior to 2000 lacks seismic details and can be considered non-ductile. In the 2018 seismic design Appendix 2, the design of RC moment frames generally follows similar practices to US codes for ordinary, intermediate, and special moment frames. However, two more local categories are added: 1) local intermediate moment frames (constructed with relative ease in Syria) and 2) local special moment frames (constructed with more difficulty in Syria). Moreover, Appendix 2 required shear walls for critical buildings like hospitals, public buildings, and high-rise buildings. In the Syrian Code, low-rise, mid-rise, and high-rise buildings are 1 to 6, 7 to 12, and 12 or more stories, respectively.

It is noteworthy that the seismic design/provisions in the Syrian Code were considered optional to adopt until 2008 and that the unreinforced non-ductile bearing wall systems made of masonry and concrete are permitted by the Syrian Code in low-rise buildings up to six stories. Despite the presence of the above-mentioned elaborate building codes that include seismic design provisions since 1996, it is important to highlight that earthquake-resistant construction found little to no implementation in Syria due to several economic, societal, and political reasons.

3.2.2. Construction Practices

Figure 3.2 shows an example of common flawed practices in non-engineered buildings promoted through a local "Reconciliation Law", which allowed building owners to register the building with little or no structural review or building inspection/assessment. Furthermore, permits were granted to recently registered buildings of less than 6 stories to allow construction of additional stories (up to 6) despite being non-engineered buildings with unknown column and foundation capacity. Those additional floors were built completely from hollow concrete block bearing walls, and solid slabs that are 60 to 80 mm thick with no beams and insufficient reinforcing bars.

Figure 3.2. An Aleppo City mid-rise non-engineered building before and after the earthquakes, (Source: Salah Haj Ismail personal Archive).

Joint PVRR: 2023 Türkiye Earthquake Sequence
PRJ-3824 | Released: 3/29/2023
Building Resilience through Reconnaissance

54

Another example is related to earthquake-resistant designed public buildings and hospitals. In this case, as-built conditions were substantially different from the structural drawings. For instance, the local special moment frames were usually built with substandard quality, reinforcement quantity and details, such as using smaller diameter reinforcing bars or even removing the reinforcement totally from some members.

Figure 3.3. The structure of Aleppo military Hospital, Aleppo City - Construction was not compatible with the study (Source: Salah Haj Ismail personal Archive).

Based on the inspection of damage photographs, information from Syrian engineers, the above code development history and construction practices analysis, and the post-war rebuilding practices in the earthquake affected regions, following _preliminary_ observations can be made:

- It is reasonable to assume that most building stock in the earthquake affected areas is non-ductile concrete systems with masonry infill walls or unreinforced bearing masonry wall systems.

- The non-ductile concrete systems for multi-story low-rise and mid-rise buildings are either beam and slab gravity frames (may be designed for wind loads in some cases) or flat plates or ribbed/joisted slabs with hollow blocks with no or shallow spandrel beams. It is noteworthy that the ribbed slabs with no projected/drop beams and the flat plates, in the absence of seismic design and structural walls, are most vulnerable to severe damage and collapse even with moderate earthquake shaking. The seismic vulnerability of such vulnerable buildings becomes even higher with low-quality materials and non-engineered construction.

Joint PVRR: 2023 Türkiye Earthquake Sequence
PRJ-3824 | Released: 3/29/2023
Building Resilience through Reconnaissance

55

- The multi-story low-rise and mid-rise non-ductile concrete systems in Northern Syria are evidently thin joist slabs with hollow blocks or flat plates, with no drop beams and no or very shallow spandrel beams that are slightly deeper than the slabs. Columns are apparently thin with extremely low reinforcement ratios, small diameter reinforcing bars and poor confinement (refer to Figure 3.3). These buildings appear to be non-engineered or poorly engineered at best with no shear walls, perhaps built post 2011 war. Concrete quality appears low from inspection of damaged photographs. For the low-rise buildings (1 to 2 stories) in these areas, unreinforced masonry seems more common.

Figure 3.3. Damaged RC column with severe deficiency of reinforcement (Source: Personal image by Eng. M. Zakaria member of damage assessment commision).

- Similar practices can be observed in other Syrian areas, except that buildings have more stories. The buildings are older and the use of slab and beam non-ductile concrete frames with infill walls and the unreinforced bearing wall masonry system (both are considered the mainstream construction methods in pre-2011 era) seem to be more common. Moreover, no shear walls can be observed in any building type.

Joint PVRR: 2023 Türkiye Earthquake Sequence
PRJ-3824 | Released: 3/29/2023
Building Resilience through Reconnaissance

56

4. Building Performance

In this section, typical building damage and collapses are documented, organized by occupancy for residential, commercial, government facilities, schools, hospitals, religious, and historical buildings. Residential buildings are sub-categorized by country, Türkiye & Syria, due to differences in construction practices, codes, and regulations. Additional examples are provided in the Media Repository, which will be published after this report in the same DesignSafe to document a wider collection of georeferenced visual evidence cataloged by occupancy.

Many buildings collapsed, partially collapsed, or were severely damaged in this earthquake sequence. According to data from the Türkiye Ministry of Environment, Urbanization and Climate Change as of February 19, the number of buildings in different damaged states are listed in Table 4.1 for nine of the impacted cities in Türkiye. Figures 4.1 and 4.2 show the map of collapsed, partially collapsed, and severely damaged buildings in several cities in Türkiye.

In Syria, severe building damages and hundreds of building collapses resulted from the two main events and the aftershocks in Northern Syria. More than 22,000 buildings were affected by the events. At the time of publication of this report, damage assessment by structural engineers in Syria has provided preliminary rapid visual assessment numbers of the "red-tagged" unsafe buildings to be demolished as 400 buildings in Northern Syria and 275 buildings in other areas. Moreover, the corresponding human loss and building damage statistics are as follows (Source: White Helmet Press Conference; Syrian News and Press Agency) :
1) Fatalities: 3,688 (2,274 Northern Syria & 1,414 other areas)
2) Injuries: 14,777 (12,420 Northern Syria & 2,357 other areas)
3) Complete building collapses: 762 (552 Northern Syria & 210 other areas)
4) Severe damage/Partial collapses: 2,090 (1,570 Northern Syria & 520 other areas)
5) Moderate/minor damage/cracking: 19,187 (12,750 Northern Syria & 6,437 other areas)

4.1. Residential Buildings

Due to the differences in construction practices, codes and regulations, findings are presented separately herein for Türkiye and Syria. While there are numerous photographs and videos documenting the damage experienced by single- and multi-family residential buildings following the earthquake sequence, this section presents selected cases that represent observed typical failure mechanisms. Aerial views of the extent of destruction in some cities in Türkiye are shown in Figure 4.3.

4.1.1. Türkiye

Several single-family and mixed-use multi-family RC buildings collapsed due to the presence of soft/weak first stories. Observations from photographs in the referenced figures are as follows:

Joint PVRR: 2023 Türkiye Earthquake Sequence
PRJ-3824 | Released: 3/29/2023
Building Resilience through Reconnaissance

57

Table 4.1. Number of buildings in various damaged states in the earthquake-impacted cities of Türkiye (Source: Türkiye Ministry of Environment, Urbanization and Climate Change, Feb. 19).

Damage State	# Buildings	%	# Buildings	%	# Buildings	%
	Adana		Adiyaman		Diyarbakir	
Total	10,916	100.00	54,149	100.00	38,357	100.00
No Damage	7,871	72.11	16,190	29.90	22,933	59.79
Light Damage	2,370	21.71	17,618	32.54	9,282	24.20
Moderate Damage	601	5.51	7,897	14.58	5,199	13.55
Severe Damage	56	0.51	8,611	15.90	710	1.85
Partial Collapse	5	0.05	1,001	1.85	54	0.14
Collapse	13	0.12	2,832	5.23	179	0.47
	Gaziantep		Hatay		Kahramanmaras	
Total	209,746	100.00	142,284	100.00	106,649	100.00
No Damage	125,209	59.70	70,393	49.47	40,255	37.75
Light Damage	38,313	18.27	33,493	23.54	30,595	28.69
Moderate Damage	32,351	15.42	9,964	7.00	15,733	14.75
Severe Damage	9,121	4.35	19,005	13.36	13,260	12.43
Partial Collapse	1,492	0.71	3,286	2.31	2,842	2.66
Collapse	3,260	1.55	6,143	4.32	3,964	3.72
	Malatya		Osmaniye		Sanliurfa	
Total	55,259	100.00	52,104	100.00	54,191	100.00
No Damage	14,436	26.12	33,338	63.98	26,554	49.00
Light Damage	14,861	26.89	10,934	20.98	18,885	34.85
Moderate Damage	11,413	20.65	4,344	8.34	8,213	15.16
Severe Damage	11,917	21.57	2,947	5.66	421	0.78
Partial Collapse	349	0.63	303	0.58	48	0.09
Collapse	2,283	4.13	238	0.46	70	0.13

Joint PVRR: 2023 Türkiye Earthquake Sequence
PRJ-3824 | Released: 3/29/2023
Building Resilience through Reconnaissance

58
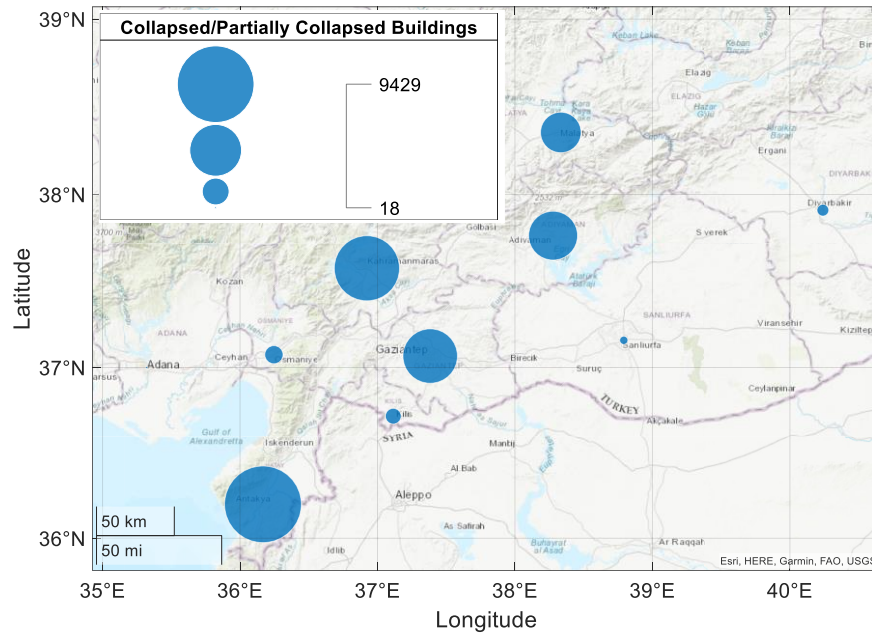
Figure 4.1. Total number of completely and partially collapsed buildings in several cities in Türkiye impacted by the earthquake sequence (Türkiye Ministry of Environment, Urbanization and Climate Change).
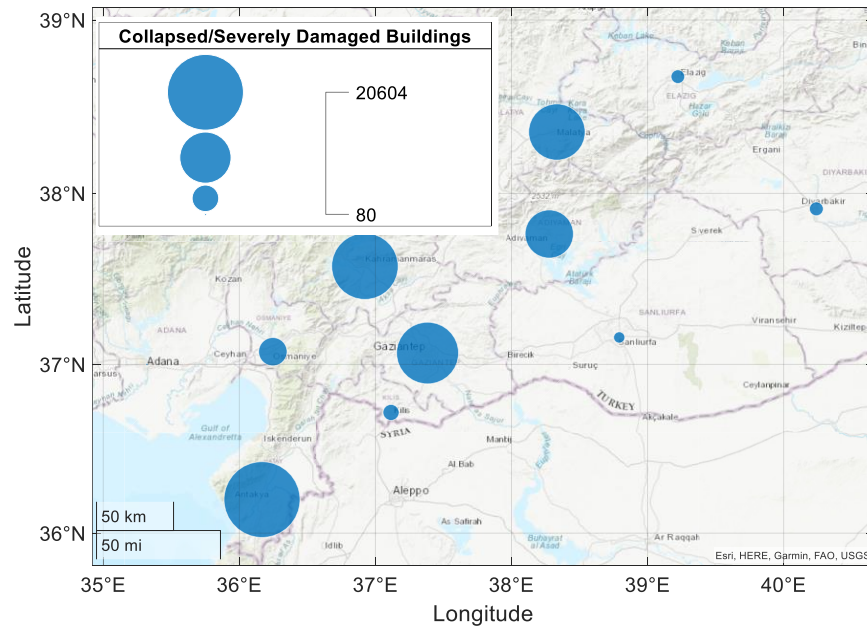
Figure 4.2. Total number of collapsed and severely damaged buildings in several cities in Türkiye impacted by the earthquake sequence (Türkiye Ministry of Environment, Urbanization and Climate Change).

Joint PVRR: 2023 Türkiye Earthquake Sequence
PRJ-3824 | Released: 3/29/2023
Building Resilience through Reconnaissance

59

Figure 4.3. Aerial views of the extent of damage in some cities in Türkiye after the earthquakes: a) and b) show mid-rise RC residential buildings that have collapsed in a side-sway manner, while nominally identical buildings in the same developments are damaged but have not collapsed; c) shows two corner RC buildings that have collapsed, possibly due to torsional eccentricity; d) shows a single high-rise building that has collapsed among other similar high-rise buildings that did not collapse (Source: (a) Getty Images via BBC, (b) Independent, (c) Getty Images via CNN, (d) Getty Images via CNN).

(1) The first story of the 5-story building in Figure 4.4 is much taller than the other stories, leading to a soft story. The intact columns of the collapsed building in the above stories show that most of the lateral displacements concentrated at the soft first story, resulting in eventual collapse of the structure. It is observed that the adjacent building, with glass façades at the first two stories, has also high potential to have soft stories because of the glass façades or openings at the first two stories and the infill walls at the upper stories. This adjacent building has not collapsed. The differences in the concrete and reinforcing bar strength, quantity, and detailing could be the reasons why one building collapsed and the adjacent one did not. However, another reason can be the potential pounding of the first floor of the standing building at a location above the mid-height of the first story corner column of the collapsed building. This additional shear force could have led to the collapse

Joint PVRR: 2023 Türkiye Earthquake Sequence
PRJ-3824 | Released: 3/29/2023
Building Resilience through Reconnaissance

60

of the corner column, leading to a progressive collapse. Another set of adjacent buildings with inadequate seismic gap is shown in Figure 4.5, where one of the buildings collapsed. Insufficient seismic gap results in increased damage when the adjacent buildings have different periods (e.g., due to different number of stories) and the consequent pounding of buildings due to the asynchronous motions. Collapse of weak/soft story (due to glass façades of stores at the first story) of adjacent buildings with different number of stories and with insufficient seismic gap is observed in Figure 4.6.
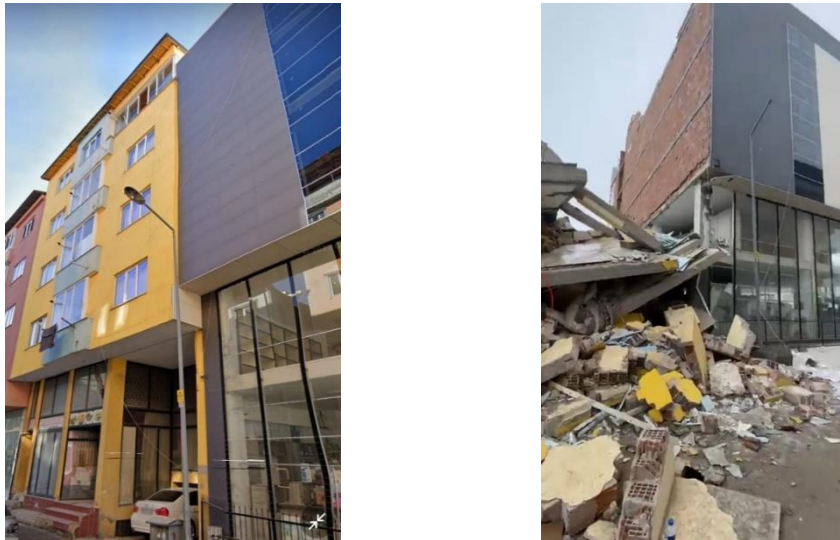
(a) Before (Source: Google Maps).   (b) After (Source: Eren Uslu via Twitter).

Figure 4.4. Collapse of a 5-story RC building in Afsin, Kahramanmaras.

Figure 4.5. Ruins of a collapsed building showing no seismic gap between adjacent buildings, Malatya (Source: Darkwebhaber via Twitter).

Joint PVRR: 2023 Türkiye Earthquake Sequence
PRJ-3824 | Released: 3/29/2023
Building Resilience through Reconnaissance

61

Figure 4.6. Collapse of buildings due to weak/soft story & pounding. The short 2-story building located between two mid-rise buildings, without adequate seismic separation, likely led to pounding between the roof slab of the 2-story building and the mid-height of the adjacent buildings. This has resulted in partial collapse of the building on the left and total collapse of the building on the right along with collapse of the 2-story (Source: New York Times 2023).

(2) The building in Figure 4.7 has larger openings at the first story, with infill walls at the upper stories, resulting in a weak and soft first story. It is observed that the first two stories of this building collapsed, where the second story collapse likely occurred due to the impact of the first story collapse. Out of plane wall failures in all stories of the exterior bay indicate larger accelerations experienced by these walls due to torsional irregularity and the twist of the building. This building collapsed after the second earthquake (Mw 7.5 in Elbistan).

(a) Before (Source: Google Maps).   (b) After (Source: Kece, Local Assessor).

Figure 4.7. Soft-story failure of a 5-story RC building with masonry infill walls in Elbistan.

(3) The 6-story building in Figure 4.8 is a mixed-use building with a pharmacy and a grocery store at the first story, and residential occupancies at the upper stories. The window openings at the first story and the infill walls at the upper stories resulted in a weak and soft first story, leading to collapse of the first story. It is likely that the first story glass façades were only at the front of the building, with infill walls at the back and sides. This nonuniform distribution of infill walls around the perimeter could have increased the torsional response during ground shaking.

(4) The 7-story mixed use RC building in Figure 4.9 likely collapsed due to similar reasons as indicated for the collapse of the 6-story mixed use building in Figure 4.8. It is located on a street corner with shopfront openings on both streets, and presumably solid fire walls on the back sides of the building. The torsional effects during ground shaking would impose large shear and bending demands on the front corner column (yellow color in Figure 4.9a). The video of this event indicates that failure of this column initiated total collapse of the building.

(5) Other examples of collapses due to potential weak/soft stories are provided in Figures 4.10 and 4.11. RC frames with unreinforced masonry infill walls is a common structural topology in Türkiye. In low levels of excitation, these infill walls add to the stiffness and strength of the structure, providing beneficial contributions. However, even in cases where the infill walls are uniformly distributed along the height of the structure and there are no initial soft or weak stories, brittle failure of the infill walls due to in-plane/out-of-plane interaction can lead to the formation of soft stories during an earthquake (Günay and Mosalam 2015), leading to eventual collapse. Considering the two strong earthquakes (Mw 7.8 and Mw 7.5) and the aftershocks between them, the formation of soft stories due to infill walls in the first event could have led to the collapse of these structures during the second event, as shown in Figures 4.4 to 4.10.
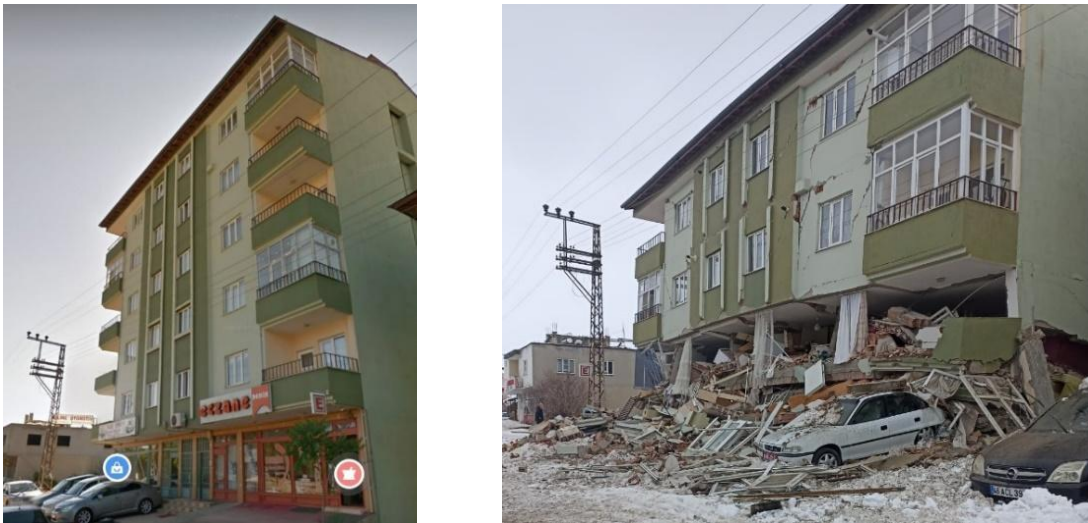
(a) Before (Source: Google Maps).   (b) After (Source: Demirkapu, Local Assessor).

Figure 4.8. Soft-story failure of a 6-story RC building in Afsin, Kahramanmaras during the Mw 7.5 earthquake in Elbistan.

**Joint PVRR: 2023 Türkiye Earthquake Sequence**
PRJ-3824 | Released: 3/29/2023
Building Resilience through Reconnaissance

63

(a) Building prior to collapse.   (b) Collapse of weak/soft story prior to gravity collapse.

Figure 4.9. Images from collapse videos of a 7-story mixed use building in Sanliurfa during the Mw 7.5 earthquake in Elbistan (Source:https://www.youtube.com/watch?v=l_KC0RMZQbI).

(a) Hatay.   (b) Elbistan.

Figure 4.10. Soft-story collapse of residential buildings in different cities (Sources: The Insider Paper via Twitter & AlertaNews24 via Twitter).

Joint PVRR: 2023 Türkiye Earthquake Sequence
PRJ-3824 | Released: 3/29/2023
Building Resilience through Reconnaissance

64

Figure 4.11. Güçlü Bahçe residential building complete collapse in Hatay (Source: Twitter).

(6) It is noted that the infill walls of the collapsed buildings discussed above were not isolated from the bounding frames, which is the main reason why the infill walls were an important factor in the formation of weak and soft stories. Although the current version of the TBSC includes provisions for the inclusion of the infill walls for identification of vertical irregularities and suggests methods for isolating the infill walls from the frames, such isolation and inclusion of infill walls in numerical models are not required. Revisions in the TBSC for explicit consideration of infill walls and their isolation from the frames should be revisited.

(7) In some of the collapsed buildings, it is possible that the presence of soft and weak stories is accompanied by other characteristics of low ductility response (e.g., inadequate seismic detailing such as lack of confinement at the beam- and column-ends and insufficient transverse reinforcement at beam-column joints).

(8) The particular issue with the detrimental effects of infill walls at large shaking is not specific to only Türkiye. In addition to their effect on the stiffness of upper stories, masonry infill walls, both at the exterior and interior walls of each floor, add considerable mass to the building, resulting in larger inertial forces developed during ground shaking. Poor behavior of RC frame structures with masonry infill walls was observed in several previous earthquakes in the world as well (Braga et al. 2011; Manfredi et al. 2014; Marinković et al. 2022).

(9) The 7-story building on a 2-story podium in Figure 4.12 is a mixed-use building, where the podium is used as a commercial space and the 7-story building has residential units. The first story of the podium structure has glass façades and is weaker and softer than the second story of the podium. This is a potential reason for the collapse of this building. As observed from the right figure, all stories of the 7-story building collapsed, likely due to the impact of the podium collapse.

Joint PVRR: 2023 Türkiye Earthquake Sequence
PRJ-3824 | Released: 3/29/2023
Building Resilience through Reconnaissance

65

(a) Source: Google Street View (37.575, 36.93) 2018.

(b) Source: The Guardian - Anadolu Agency/Getty Images.

Figure 4.12. Collapse of a 7-story mixed-use building in Kahramanmaraş.

(10) The 2-story buildings in Figure 4.13 might have collapsed due to the combined effect of soft and weak stories and accompanying torsional response.

Figure 4.13. First story collapse of single-family RC residential buildings in Tevekkelli possibly due to weak and soft-story failures (Source: Veryansin TV 2023).

An important reason for the collapses in the earthquake sequence is that such buildings were subjected to two large magnitude earthquakes (Mw 7.8 and Mw 7.5) and major aftershocks in between. Figure 4.14 shows a severely damaged building after the first earthquake that continued to collapse hours later during an aftershock putting at risk the lives of first responders.

Joint PVRR: 2023 Türkiye Earthquake Sequence
PRJ-3824 | Released: 3/29/2023
Building Resilience through Reconnaissance

66

Figure 4.14. Partially collapsed building showing major diagonal cracks (refer to the insert) on the remaining towers, Diyarbakir (Source: Getty Images).

Modern principles of earthquake design were implemented in the TBSC, starting with the 1998 version of the code. The 1999 Kocaeli and Duzce earthquakes, which resulted in significant building damage and collapses, led to major changes in seismic design, which were further reflected in the 2007 version of the TBSC. Therefore, the buildings in the region can be categorized as pre-2000 (not up to date with modern seismic codes) and post-2000 (supposed to be designed according to the modern principles of seismic design). There is evidence that even post-2000 and post-2007 RC and masonry buildings collapsed. As noted earlier, there are several reasons for these collapses, including: (a) the ground motions exceeding MCE levels, (b) several large motions experienced by the buildings back-to-back in a sequence, (c) possibility of buildings not designed according to the code, and (d) possibility of the construction and material quality not following the intended design. Regarding the last two reasons, when buildings are designed as seismically resistant, some degree of repairable damage is expected due to higher earthquake levels than what was considered in the design of these buildings. However, when the shaking level significantly exceeds the design levels as the case here in this earthquake sequence, details of construction become a major factor to distinguish between collapse and other levels of damage.

An RC residential building with shear walls, newly constructed in 2022, had a catastrophic collapse as shown in before and after images in Figure 4.15. Another new residential RC building with shear walls collapsed while it was under construction (Figure 4.16). In this figure, shear walls are oriented along one direction of the building. Extensive concrete crushing is visible at the shear wall base, denoting sliding-shear failure, as well as diagonal concrete crushing (e.g., refer to the third wall after the corner column), suggesting a combined flexure-shear diagonal failure. Furthermore, an axial failure of a corner beam-column joint is visible, with a possible under-design or shortage of sufficient confinement. Significant beam yielding along the orthogonal direction to

Joint PVRR: 2023 Türkiye Earthquake Sequence
PRJ-3824 | Released: 3/29/2023
Building Resilience through Reconnaissance

67

the building lateral collapse in the shear wall direction might have led to shear and axial failure of the joint.

Figure 4.15. New residential towers before the earthquake sequence and during collapse due to the second earthquake (Mw 7.5), Bostanbasi, Malatya (38.32189N, 38.24656E) (Source: Google Maps & Ibrahim Haskologlu via Twitter).

Figure 4.16. Collapse of an RC building under construction (Source: Earthquake Engineering Association Turkey).

Joint PVRR: 2023 Türkiye Earthquake Sequence
PRJ-3824 | Released: 3/29/2023
Building Resilience through Reconnaissance

68

Another building that has collapsed on its side is shown in Figure 4.17. There are several potential reasons for this failure: (1) Inadequate foundation, or (2) Initiation of the collapse of the structure from one side, resulting in the toppling of the structure. It is noted that this type of collapse due to the second reason is known as sidesway collapse, which occurs due to lateral dynamic instability at large lateral displacements, when the lateral strength of the structure degrades significantly. This type of collapse is different from the ones discussed in earlier images, where the RC buildings mostly collapsed by losing gravity load carrying capacity, much before reaching these excessive lateral displacements. This difference is conceptually demonstrated in Figure 4.18. The sidesway collapse might have occurred in buildings with larger displacement capacities, which have been exceeded by the large demands in this earthquake sequence, while the gravity collapse occurred in buildings with less deformation capacity (ductility) due to presence of vertical irregularities, insufficient confinement, weak-column/strong-beam proportions, or other characteristics of nonductile concrete buildings.

In addition to the numerous failures shown above, Figure 4.19 (b) and (c) show that half of a 15-story mixed-use concrete building collapsed by separation from the other half. This collapse was reported to occur after a Mw 6.1 aftershock. From the top view of the building, an excessive reentrant corner can be seen in the middle. This reentrant corner could have led to excessive stress concentrations at that portion of the building (FEMA-P154, 2012). This may have caused the splitting of one half of the building from the other contributing to the collapse of the split half. It is also noted that the same reentrant corner is present in similar buildings in the neighborhood that are standing, hinting at possible other structural issues of this collapsed building.

Figure 4.17. Potential sidesway collapse of the Rönesans residence, Hatay (Source: AFP via Middle East Eye).

Joint PVRR: 2023 Türkiye Earthquake Sequence
PRJ-3824 | Released: 3/29/2023
Building Resilience through Reconnaissance

69
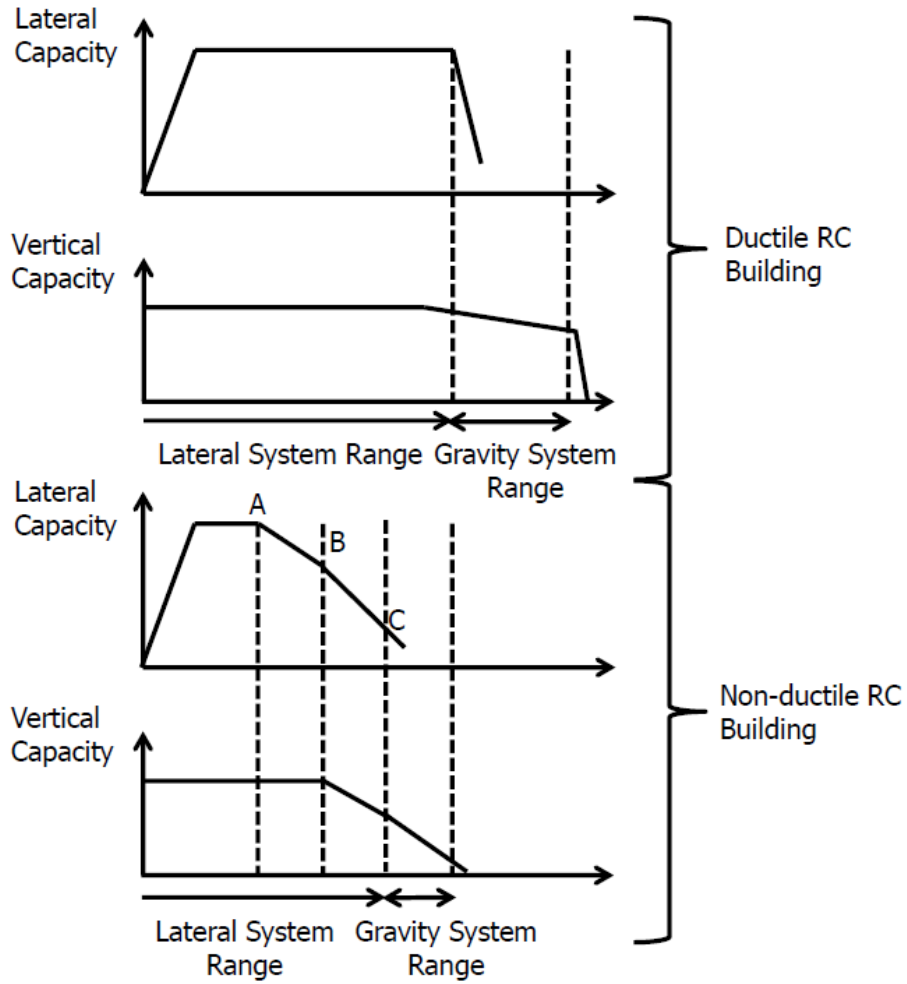
Figure 4.18. Lateral and vertical responses of RC buildings (Mosalam and Günay 2014; Holmes 2000).

Joint PVRR: 2023 Türkiye Earthquake Sequence
PRJ-3824 | Released: 3/29/2023
Building Resilience through Reconnaissance

70

(a) Google Street View "before the earthquake sequence".
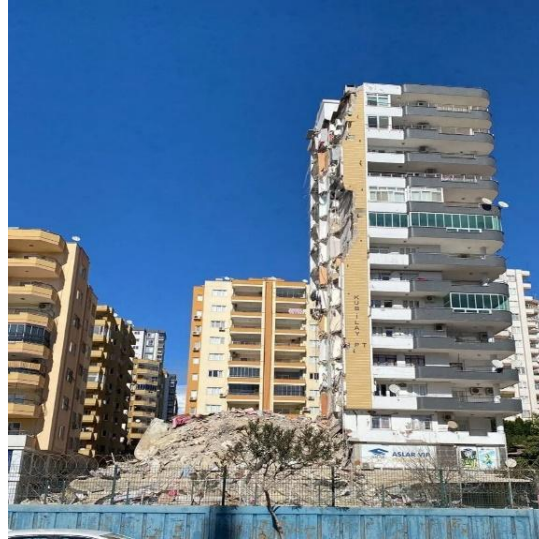
(b) Front view "after the earthquake sequence".

(c) Aerial View of collapsed building (Source: NTV 2023).

Figure 4.19. Partial collapse of a 15-story concrete mixed-use building, Adana (37.049N 35.275E).

Another partially collapsed building is shown in Figure 4.20. It is possible that the failure in the corner of this building took place due to a combined effect of the two horizontal components of the ground motions at the location of the building. Increased shear forces due to plan torsion irregularity could have contributed to the occurrence of such failure.

Joint PVRR: 2023 Türkiye Earthquake Sequence
PRJ-3824 | Released: 3/29/2023
Building Resilience through Reconnaissance

71

Figure 4.20. Partially collapsed of a multi-story building in Kahramanmaras, February 6 (Source: Ihlas News Agency (IHA) via Reuters 2023a).

4.1.2. Syria

As discussed in Section 3, it is likely that most building stock in the earthquake impacted regions in Syria is non-engineered, poorly engineered, or at best gravity-designed non-ductile systems. The heaviest damage and the most collapses occurred in 4 cities in Syria (Aleppo, Latakia, Idlib, and Hama) and in 40 towns and villages in Northern Syria (Idlib) and its countryside (Reef Idlib), Aleppo and its countryside (Reef Aleppo)), with the most damage concentrated in Jendeyres near Afrin, and Harem near Idlib. As mentioned in Section 3, non-ductile concrete frames, non-ductile concrete ribbed slabs with hollow blocks and no drop beams, and non-ductile concrete flat plates are the most common RC systems for mid-rise buildings (all RC systems included heavy masonry infills) while the unreinforced masonry bearing walls is more common in low-rise buildings up to 6 stories. Many buildings in Syria that were damaged during the war are believed to have been rebuilt by individuals with low-quality materials. Such buildings are expected to be more vulnerable to collapse from earthquake shaking (Naddaf 2023; Mroue and Chehaeb 2023). There is past evidence of the collapse of war-damaged residential buildings in Aleppo and consequential casualties (Reuters 2023b). It is unfortunate that the ground motion records by the Syrian stations are not available by the time of publication of this report to help correlate damage to ground motion site spectra. Several unreinforced masonry multi-family buildings (low-rise and mid-rise) collapsed with a soft-story mechanism or out-of-plane (OOP) masonry failure as presented in Figures 4.21 to 4.23 (refer to shown arrows). Moreover, video evidence showed OOP failure of masonry infills leading to structural collapse.

Joint PVRR: 2023 Türkiye Earthquake Sequence
PRJ-3824 | Released: 3/29/2023
Building Resilience through Reconnaissance

72

Figure 4.21. Soft-story collapse of a multi-family low-rise unreinforced masonry building in Aleppo (Source: RAMI AL SAYED/AFP).

Figure 4.22. Collapse of a multi-family low-rise unreinforced masonry building in Aleppo (Source: Getty Images).

Joint PVRR: 2023 Türkiye Earthquake Sequence
PRJ-3824 | Released: 3/29/2023
Building Resilience through Reconnaissance

73

Figure 4.23. Ruins of a collapsed masonry building in Aleppo (Source: LOUAI BESHARA/AFP, Getty Images).

Non-ductile concrete construction presented severe damage and collapse in many instances and was believed to have caused the most fatalities and injuries. Examples are shown in Figures 4.24 to 4.35. Section 3 discussed the construction types and practices in the affected areas, which are important for better damage correlation. In some cases, a non-ductile concrete system is mixed with an unreinforced masonry bearing wall system within the same building, especially for the purpose of adding more floors to an existing building (refer to the building in the red rectangle in Figure 4.26). Severe damage before complete collapse due to low-quality materials made it sometimes difficult to distinguish from the debris a skeleton RC structure from a bearing wall system. For instance, while the rubble in Figure 4.26 may suggest all masonry construction, evidence of a few RC columns can still be detected as in the highlighted blue rectangle.

Joint PVRR: 2023 Türkiye Earthquake Sequence
PRJ-3824 | Released: 3/29/2023
Building Resilience through Reconnaissance

74

Figure 4.24. Ruins of a collapsed building with severely damaged RC columns (shown with arrows) in the adjacent building, Hama (Source: LOUAI BESHARA/AFP, Getty Images).

Figure 4.25. Pancaked collapse of masonry and RC buildings (shown with arrows) in Besnaya, Reef Idlib (Source: AFP via npr.org).

Joint PVRR: 2023 Türkiye Earthquake Sequence
PRJ-3824 | Released: 3/29/2023
Building Resilience through Reconnaissance

75

Figure 4.26. Collapsed masonry & RC buildings, Besnaya, Reef Idlib (Source: AFP via npr.org).

It is evident from the partial collapse photographs that some older buildings in Syria were constructed with no gap to neighboring buildings of the same height, perhaps using the neighboring building as formwork for concrete elements (Figures 4.22, 4.23 and 4.27), which may have helped avoiding total collapse or preventing collapse in some instances. Pounding effects may have been relatively reduced due to such configurations.

Joint PVRR: 2023 Türkiye Earthquake Sequence
PRJ-3824 | Released: 3/29/2023
Building Resilience through Reconnaissance

76

Figure 4.27. A partially collapsed building in Syria. Notice light column reinforcement (yellow arrow), the absence of beams and slab integrity steel (blue arrow), and poor reinforcing bars anchorage (green arrow) (Source: https://yle.fi/a/74-20016582).

The diaphragm (floor slab) failure was commonly observed in many buildings (Figures 4.27 to 4.29, 4.32 and 4.33) when the horizontal diaphragm is unable to resist lateral forces during strong shaking or it is separated from the vertical system due to anchorage failure. The absence of slab integrity reinforcement, lack of continuity reinforcement, and poor anchorage to columns are evident in these figures. Very vulnerable slab-column connection conditions resulted from the absence of beams along with poor anchorage to columns, and in many instances, it is speculated that the collapse sequence was triggered by these vulnerable connections, as shown in the red rectangles in Figure 4.28.

Joint PVRR: 2023 Türkiye Earthquake Sequence
PRJ-3824 | Released: 3/29/2023
Building Resilience through Reconnaissance

77

Figure 4.28. Slab failure in a collapsed building in Samada, Northern Syria (Source: https://news.un.org/en/story/2023/02/1133177). Notice the complete damage to the slab-column connection in the two right columns.

Pancaked collapse of multi-story non-ductile concrete buildings with ribbed slabs and no drop beams was widespread in Syria, more evident in Northern Syria's newer buildings constructed post 2012 war from low-quality materials as explained in Section 3 (Figures 4.28 to 4.35). Newer unreinforced masonry bearing wall buildings also suffered extreme damage or collapse. On the other hand, old buildings of 2 to 3 stories in Syria (even made from adobe or stone masonry) resisted the strong shaking well, with some cracks and light damage, likely due to relatively higher quality of construction and materials prior to 2012.
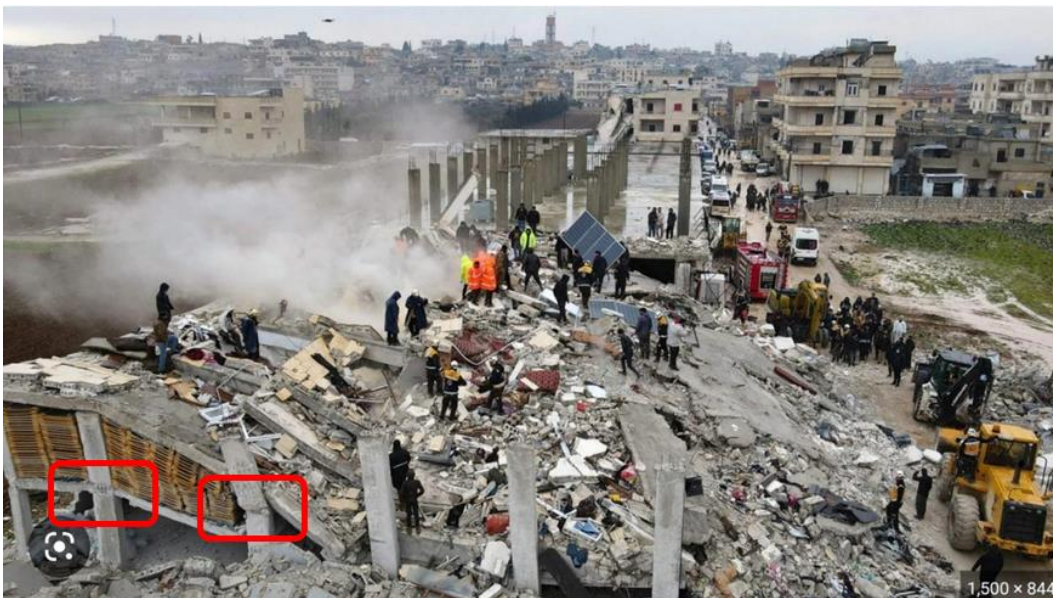

Figure 4.29. A collapsed building in Samada, Northern Syria (Source: Reuters). Notice the light column reinforcement and separation of slab from columns (in red rectangles) in the collapsed building.

Joint PVRR: 2023 Türkiye Earthquake Sequence
PRJ-3824 | Released: 3/29/2023
Building Resilience through Reconnaissance

78

In concrete buildings that experienced severe damage or partial or total collapse, some common deficiencies can be observed from the collapse photographs, most of which are common in non-ductile concrete buildings, but some are considered excessive due to poor construction quality:

- Concrete quality/strength appears very low by visual inspection of texture and color, as well as the severity of crushing following collapse. Syrian engineers contacted after the event confirmed the low quality of the concrete used. This can be observed in Figures 4.25, 4.26 and 4.30 to 4.32.

- Thin RC column sections, suggesting no seismic design was conducted, and even in some cases appearing to be under-designed for gravity loads. This is common in non-engineered buildings. Thin columns can be observed in many damaged buildings; examples are seen in Figures 4.26 to 4.29, 4.31, and 4.32.

- Many buildings had lightly reinforced column sections, with no or little transverse reinforcement, and potentially inadequate lap splices located immediately above the slabs. Examples of such deficiencies can be observed in Figures 4.27 to 4.32.

- Absence of drop (projected) beams below the ribbed slab and flat plate systems. This creates a slab-column connection situation (no beam-column joints) which is known to perform poorly under severe earthquake shaking unless well reinforced. This condition can be observed in Figures 4.27 to 4.29, 4.32, and 4.33.

- Absence of seismic details throughout as seen on most photographs of damage. These include insufficient anchorage, development length, and continuity of slab reinforcement, and absence of integrity reinforcement. Refer to Figures 4.27 to 4.29, and 4.32 to 4.35.

- The orientation of the column section in several buildings is in one direction for all columns, rendering the weak-axis direction of the building, in the absence of shear walls, very vulnerable even to moderate shaking. These columns are often extremely thin in one direction. This can be observed in the columns at the right side of the building in Figure 4.30, the exterior columns in Figure 4.31, and all columns in the building in Figure 4.33.

- The use of heavy masonry infills either made of stone bricks or hollow concrete blocks. This practice results in high mass buildings which induce large seismic forces during ground shaking, becoming destructive in the absence of a seismic-resistant lateral system. This is a typical construction practice in the Mediterranean, Middle East, and Eastern Europe. Evidence of such practice is shown throughout this section's photographs.

- Absence of shear wall throughout, even in midrise 6 to 12 story buildings.

Joint PVRR: 2023 Türkiye Earthquake Sequence
PRJ-3824 | Released: 3/29/2023
Building Resilience through Reconnaissance

79

Figure 4.30. Collapsed building (foreground) and a partially collapsed RC building (background) in Jandires, Northern Syria (Source: Reuters).

Figure 4.31. Collapsed buildings in Harem, Reef Idlib, Northern Syria (Source: wsiu.org 2023).

Joint PVRR: 2023 Türkiye Earthquake Sequence
PRJ-3824 | Released: 3/29/2023
Building Resilience through Reconnaissance

80

Figure 4.32. Collapsed RC building in Idlib. Notice the poor or absent confinement in columns, small and light longitudinal column bars, and poor concrete quality (Source: Anas Alkharboutli/picture alliance via CNN).

Figure 4.33. Collapsed concrete slab without beams and lacking continuity and integrity reinforcement. Note also the extremely narrow columns in one direction (Source: The Telegraph, 2023b).

Joint PVRR: 2023 Türkiye Earthquake Sequence
PRJ-3824 | Released: 3/29/2023
Building Resilience through Reconnaissance

81

Figure 4.34. Pancaked concrete ribbed slab failure, likely built on unreinforced masonry bearing walls in Jinderis, Northern Syria. Notice the ribbed slab RC construction of the right neighboring building (Source: NPASyria).

Figure 4.35. Collapsed concrete building near Idlib, Northern Syria. Notice the poor reinforcement of the columns (Source: AFP).

Figure 4.36 shows the damage assessment via satellite pictures taken by the UN satellite in the affected regions in Northern Syria. This aerial assessment can be correlated to the damage assessment conducted by Syrian rapid screening field teams.

Joint PVRR: 2023 Türkiye Earthquake Sequence
PRJ-3824 | Released: 3/29/2023
Building Resilience through Reconnaissance

82
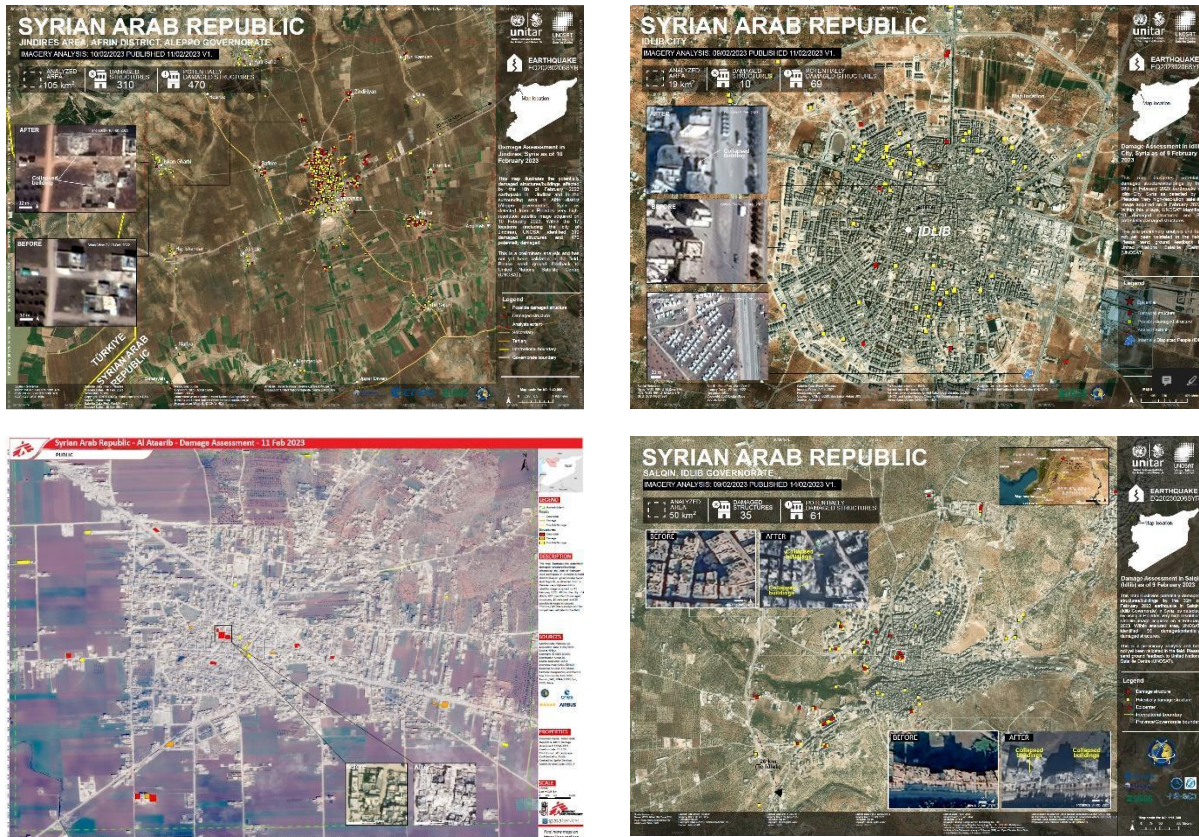
Figure 4.36. Damage assessment by UN satellite imagery of Northern Syria (Source: Reliefweb (left), Reliefweb (right)).

4.2. Commercial Buildings

Several partial and total collapses of commercial buildings were reported in Türkiye. In Malatya, Hotel Avsar (a 10-story RC building) and Trend Garden Residence (an 8-story RC building) completely collapsed (Figures 4.37 and 4.38). According to Google Earth data, the buildings had been renovated during the past two years and appear new. However, Google Earth imagery shows that the buildings have existed at least since 2001. Therefore, these buildings are in the category of pre-2000 buildings in Türkiye that were not designed according to the advances in the 1998 version of the TBSC. This can be one of the reasons for the observed collapse. Malatya was close to the end of the fault rupture in both the Mw 7.8 and Mw 7.5 earthquakes, impacted by forward directivity. The large displacement demands due to the forward directivity effects during these two events and the strong aftershocks in between likely contributed to the observed collapse.

Joint PVRR: 2023 Türkiye Earthquake Sequence
PRJ-3824 | Released: 3/29/2023
Building Resilience through Reconnaissance

83

Figure 4.37. Before and after photographs of Hotel Avsar showing the building collapse in Malatya (38.3516N 38.3002E) (Source: NY Times and Yedinoktabir via Twitter).

Figure 4.38. Before and after photographs of Trend Garden Residence showing the building collapse in Malatya, the pancake collapse of all stories suggests major structural problems. (38.347N 38.283E) (Source: NY Times).

4.3. Government Facilities

Government facilities play a key role during extreme events like earthquakes. The continuing functionality of these facilities is essential. Some of the government buildings in Türkiye experienced extensive damage and some collapsed. For instance, Figure 4.39 shows the collapse of a municipality building in Adiyaman, Türkiye. Figure 4.40 shows the collapse of the first story and extensive damage to the second and third stories of a municipality building in Afsin, Türkiye.

Joint PVRR: 2023 Türkiye Earthquake Sequence
PRJ-3824 | Released: 3/29/2023
Building Resilience through Reconnaissance

84

Figure 4.39. Adiyaman municipality building before and after the earthquake sequence (38.2441N, 36.9151E) (Source: Twitter).

Figure 4.40. Afsin-Kahramanmaras municipality building before (Source: Google Map) and after (Source: Twitter) the earthquake sequence (38.2441N, 36.9151E). The collapse of one wing of this building with an L-shape plan might be due to torsional effects and plan irregularity.

4.3. Masonry Buildings

It is likely that unreinforced masonry is more prevalent in rural areas than in cities. Despite damage and collapse reports from rural areas in social media, to date, there is only limited visual evidence of damaged unreinforced masonry buildings. At the time of writing this report, the rescue efforts are ongoing with difficulties in accessing rural areas. The immense rescue needs in the highly populated areas and the lack of access in reaching rural areas might explain the lack of visual evidence from these regions. With the available information, damage to a few masonry buildings is discussed in this section.

Figure 4.41 shows the partial collapse of Ciftarslan House external enclosure wall in Kahramanmaraş province. This house is a 2-story structure built in 1928 and is part of the Turkish architectural heritage that has survived for nearly a hundred years. According to Paköz (2019), this house is a part-masonry and part-timber structure. The lower floor perimeter walls of the house were built of stone masonry, and the intermediate and upper floor walls were made of wooden frames filled with adobe material. After the earthquake sequence, no visible cracks were recognized in the house facade. However, part of its enclosure wall collapsed. This collapse might

Joint PVRR: 2023 Türkiye Earthquake Sequence
PRJ-3824 | Released: 3/29/2023
Building Resilience through Reconnaissance

85

be due to an out of plane (OOP) bending mechanism of the very tall walls without transverse restraining elements.

(a) Pre-earthquake sequence. (b) Post-earthquake sequence.

Figure 4.41. Damage in a masonry structure in Kahramanmaraş province, 37.5870N 36.9307E (Source: Twitter).

Turkish media has reported that 200 houses in Malatya province have been declared unusable. The rural area buildings were apparently built with adobe masonry walls and earth slabs supported by wooden beams, and experienced severe damage during the earthquake sequence (Figure 4.42). The buildings were used as residences or barns. There was one casualty in this historical neighborhood, which was known as a symbol of the region due to these old buildings. Figure 4.42(a) depicts an OOP failure mode of one of the house façades. The standing walls exhibit a vertical failure plane which may indicate the lack of horizontal bond elements and a poor connection between perpendicular walls.

(a) Severely damaged house. (b) Collapsed house.

Figure 4.42. Damage in masonry structures in Kozluca District, Malatya province, 38.3840N 37.6836E (Source: EN SON HABER).

Joint PVRR: 2023 Türkiye Earthquake Sequence
PRJ-3824 | Released: 3/29/2023
Building Resilience through Reconnaissance

86

4.4. Schools

4.4.1. Schools in Türkiye

In Türkiye, the educational system was suspended (unplanned school closure) from February 6 to 20 to determine the damage to the city schools where the impact of the earthquake sequence was felt. Schools were closed in the provinces of Diyarbakır, Batman, Siirt, Mardin, Şırnak, Kahramanmaraş, Adana, Hatay, Şanlıurfa, Osmaniye, Gaziantep, Kilis, Malatya, and Elazığ (TGRT HABER 2023). In addition, school buildings and education facilities with minor or no damage became shelters for thousands of victims (Adejumo 2023).

On February 13, the Turkish Minister of Education stated that among the 20,868 buildings in the custody of the Ministry of National Education, at least 24 schools were destroyed and 83 were severely damaged (MEB 2023). Due to the time of occurrence of the earthquake, most of the schools were probably empty, which meant that the severe damage and collapse of the school buildings, fortunately, did not result in deaths or injuries.

Figure 4.43 shows the total collapse due to the failure of the first floor of a 4-story school building located in Elbistan, Kahramanmaraş in Southern Türkiye. From the image before the earthquake, the school was a regular building in plan and height. The post-earthquake image shows that the structure was an RC moment resisting frame in one direction and a shear wall system in the other direction. Although it is not clear from the images, a problem with this type of schools is the short columns due to partial height infill walls, which could have played a role in the observed collapse.

(a) Before the earthquake sequence.   (b) Collapse after the earthquake sequence.

Figure 4.43. Vocational and Technical Anatolian High School collapse due to crushed first floor, 38.2578 N 36.9286 E (Source: (a) Google Maps and (b) Reddit).

In Antakya, Hatay province, a school building collapsed. Figure 4.44 shows this building with a lateral load resisting system composed of moment resisting frames with unreinforced masonry infill walls. In the pre-earthquake image, the building had a reduced footprint and open two-story frame with possible captive column effects, which may have contributed to the observed collapse.

Joint PVRR: 2023 Türkiye Earthquake Sequence
PRJ-3824 | Released: 3/29/2023
Building Resilience through Reconnaissance

87

(a) Before the earthquake sequence.   (b) After the earthquake sequence.

Figure 4.44. Collapsed building of the "REAL SUCCESS COURSE CENTER" school in Antakya, Hatay province, 36.1853N 36.1210E (Source: (a) Google maps, (b) Twitter).

The Gazi middle school was an RC structure with unreinforced masonry infill walls. Figure 4.45a depicts the left wing of the building, it had three stories, while the right wing had four stories with shorter story heights. At a façade level, both parts were connected by middle-height horizontal panels, which coincided with the story heights of the right wing. Figure 4.45b shows these panels were severely damaged, which suggests there was no seismic joint between the two wings of the structure, despite their irregularities in story height. Several ground-floor vertical elements in the left wing of the building collapsed.

(a) Before the earthquake sequence.   (b) After the earthquake sequence.

Figure 4.45. Partial collapse of the Gazi Primary School in Kahramanmaras province, 37.5754N, 36.9239E (Source: (a) Google Maps, (b) Facebook).

4.4.2. Schools in Syria

A considerable number of school buildings in Syria were affected by this earthquake sequence. At the time of writing this report, the Syrian Minister of Education indicated that damage has been observed in at least 248 schools. The affected schools are mainly located in the urban area of

Joint PVRR: 2023 Türkiye Earthquake Sequence
PRJ-3824 | Released: 3/29/2023
Building Resilience through Reconnaissance

88

TarFGtous (99), Aleppo (71), Lattakia (50), Hama (27), and in the rural area of Idleb (1) (SANA 2023). In addition, UNRWA (United Nations Relief and Works Agency) for Palestine Refugees in the Near East has informed that one of its schools in Neirab has also been affected by the earthquake sequence (Source: Twitter). Among the identified buildings, reports by the Directors of Education of the most affected provinces have indicated that four schools are completely damaged in Aleppo, five are at risk of collapse in Lattakia, and other facilities urgently need intervention and repair. Schools that withstood the earthquake sequence with minor damage have been allocated as shelter centers for the victims (Aawsat 2023). Additionally, the educational system was suspended (unplanned school closure) from February 6 to 10 to determine the damage to the city schools where the impact of the earthquake sequence was felt.

The severity of the structural damage to schools is still being assessed, and related visual evidence is scarce at the moment of writing this report due to efforts that might be primarily addressed to more pressing needs. Figure 4.46 shows the partial collapse of a Cilician Armenian high school in Aleppo, Syria. This structure, built in 1921, is a double-leaf masonry construction with transversal connections made with regular-shaped stone blocks. The observed damage suggests that some top-floor walls experienced an OOP bending failure mechanism, leading to the falling of stone blocks and the partial collapse of the roof structure.

Figure 4.46. Damage at a Cilician Armenian high school of Aleppo, 36.2082°N, 37.1559°E (Source: Massis Post).

According to local news, the most affected schools in Aleppo were the Martyr Judy Amanous School, the Michael Nehme School Complex, and the Martyr Gian Kindergarten located in the neighborhood of Ashrafieh and the Halima Al-Saadia School located in the neighborhood of Sheikh Maqsoud (ANHA 2023). Figure 4.47 shows some images of the damage documented at Martyr Gian Kindergarten, where the wreckage of the damaged walls, water gushing out from broken water lines, and a fallen non-structural component can be observed.

Joint PVRR: 2023 Türkiye Earthquake Sequence
PRJ-3824 | Released: 3/29/2023
Building Resilience through Reconnaissance

89

(a) Wreckage of damaged walls.

(b) Broken water lines.

(c) Fallen non-structural component.

Figure 4.47. Damage documented at Martyr Gian Kindergarten (Source: ANHA).

Figure 4.48 depicts the damage observed at Martyr Judy Amanous School, an RC building complex with masonry infill walls. It can be observed that the façade tiling was severely damaged, probably triggered by a lack of support anchoring and tiling joints. This is particularly important because, during a seismic event, the falling non-structural elements can cause serious injury to people evacuating the buildings. A shear failure mechanism is observed in concrete beams and an OOP bending failure in the enclosing walls. It is important to comment that geographical localization of the damaged schools and visual evidence of the infrastructure before the earthquake sequence has not been easy to obtain, as services like Google Street View are restricted in Syria.

Figure 4.48. Damage at Martyr Judy Amanous School (Source: ANHA).

Joint PVRR: 2023 Türkiye Earthquake Sequence
PRJ-3824 | Released: 3/29/2023
Building Resilience through Reconnaissance

90

4.5. Hospitals and Health Care

Damage to hospitals in the affected region was significant, and World Health Organization (WHO) spokeswoman Harris mentioned impacts on health care in Türkiye and Syria as "*huge long-term*" issues (Francis and Nadhir, 2023). Hundreds of medical facilities were damaged, disrupting treatment capacities across large regions. These levels of hospital system's damage were critical since tens of thousands of people were injured, as reported in Section 1.1, putting heavy strains on the affected healthcare system.

Several hospital buildings experienced complete failure with patients and medical staff inside the destroyed facilities. Reports from the Turkish Ministry of Health indicate that at least 15 hospitals were severely damaged or collapsed, and about half of them are in the most affected area (Reliefweb 2023c). In addition, the Turkish health minister reported that on February 8, 77 field hospitals were set up across 10 regions (Francis and Nadhir, 2023).

Hatay province is one of the most affected regions after the earthquake sequence. Its government announced that two state hospitals were completely destroyed, one of the three private hospitals collapsed, and the City Hospital was damaged (TGRT HABER 2023). Figure 4.49 shows collapsed hospitals in Hatay province. The images suggest that the buildings were old, thus they very likely did not meet the structural provisions required in the current TBSC.

(a) Şanlıurfa City Hospital (Source: Twitter).

(b) ICUs building, state hospital, Iskenderun (Source: Twitter, BBC).

Figure 4.49. Collapsed buildings of state hospitals in Hatay province where rescue teams were needed to take survivors from the rubble.

Block A of Iskenderun State Hospital in Dumlupınar neighborhood collapsed. It was built in 1968 and included Intensive Care Units (ICUs), physical therapy department, polyclinic services, and administrative units (Oksijen 2023). Figures 4.50 and 4.51 show two views of a complete collapse of an RC structure, which was detached from the main building. Government officials claimed it was an old building that was supposed to be retrofitted in 2023 (NTV 2023c). Figure 4.52 depicts further examples of damage to structural and non-structural components within "Block A" building.

Joint PVRR: 2023 Türkiye Earthquake Sequence
PRJ-3824 | Released: 3/29/2023
Building Resilience through Reconnaissance

91

(a) Before the earthquake sequence (Source: Google Street View).

(b) After the earthquake sequence showing three fully collapsed stories of the RC structure (Source: Reuters via ARAB NEWS).

Figure 4.50. Structural collapse in Iskenderun State Hospital, Hatay province, 36.5820N, 36.1738E where doctors report people trapped inside the damaged structure.

(a) Before the earthquake sequence (Google Street View).

(b) After the earthquake sequence (Reuters via RGRU).

Figure 4.51. Entrance to the Iskenderun State Hospital, 36.5820N 36.1738E. The 5-story reinforced concrete building which collapsed was adjacent, but not structurally joined, to another five-story building which survived.

Joint PVRR: 2023 Türkiye Earthquake Sequence
PRJ-3824 | Released: 3/29/2023
Building Resilience through Reconnaissance

92

(a) Exposed reinforcing bars in beams and columns with evidence of corrosion, which could limit the ductility of the connection during the earthquake sequence (Reuters via zawya.com).

(b) Fallen panels from the ceiling and blocked corridor, indicating loss of functionality and giving evidence of the significant interior damage that can occur even if the exterior looks undamaged (extracted from Reuters via Twitter).

Figure 4.52. Structural and non-structural damage to "Block A" building of Iskenderun State Hospital in Hatay province, 36.5820N 36.1738E.

Antakya Academy Hospital in Hatay province and the old 750-bed Antakya State Hospital were destroyed. In the Academy Hospital, people remained under the rubble (Figure 4.53), and in the old building of the Antakya State Hospital, users from social media claimed that more than 70 people died under the rubble (Twitter 2023p). Starting from 2016, the regional hospital services were offered in the new facilities of Hatay Training and Research Hospital. Figures 4.54 and 4.55 show the collapsed hospital, which was built in 1939.

Joint PVRR: 2023 Türkiye Earthquake Sequence
PRJ-3824 | Released: 3/29/2023
Building Resilience through Reconnaissance

93

(a) Pre-earthquake view (Google Maps)

(b) Post-earthquake (3 of 9 stories fully collapsed, with the southern portion more damaged than the northern portion) (Source: Twitter).

Figure 4.53. Structural collapse of the building of Antakya Academy Hospital in Hatay province, 36.2354N 36.1694E.

View of the southeast corner of the collapsed facility (Source: DepoPhotos via Birgun.net).

View of the northeast side of the collapsed facility (Source: Twitter).

Figure 4.54. Structural collapse of the building of Old Antakya State Hospital in Hatay province, 36.2149N 36.1374E. Similar to many other collapsed buildings, the collapse mechanism is gravity collapse, with the collapse of vertical members primarily centered in the middle third of the structure and lower stories, along with out-of-plane wall failures in the upper stories.

(a) Post-earthquake view from the west of the hospital ([Twitter](#)), showing minimal structural tie-in between the collapsed and still standing portions of the northwest wings of the hospital.

(b) Satellite image, centered on the hospital, showing adjacent infrastructure without total structural failure ([Twitter](#)).

Figure 4.55. Collapsed old building of Antakya State Hospital, Hatay province, Türkiye.

According to the Turkish news and social media publications, Göksun State Hospital in Kahramanmaraş province was severely damaged after the earthquakes. It was delivering emergency healthcare assistance in a tent at the hospital garden ([Sözcü](#) 2023). Figure 4.56 shows the hospital before and after the earthquake sequence.

(a) Pre-earthquake ([Google Street View](#)).　　　(b) Post-earthquake ([Twitter](#)).

Figure 4.56. Göksun State Hospital, Kahramanmaraş province, 38.0294N 36.5506E.

Although several healthcare facilities suffered significant damage and some of them collapsed, most seismically protected buildings remained functional. There were 11 base-isolated hospitals within 200 km from the epicenter of the Mw 7.8 earthquake. In addition, there was one more base-isolated hospital within 200 km from the epicenter of the Mw 7.5 event (information courtesy of Omer Ülker, Turkish Association of Seismic Isolation). These hospitals included those in the

Joint PVRR: 2023 Türkiye Earthquake Sequence
PRJ-3824 | Released: 3/29/2023
Building Resilience through Reconnaissance

95

provinces of Adana (1), Elazig (1), Hatay (1), Malatya (3), Adiyaman (1), Osmaniye (2), Diyarbakir (1), and Kahramanmaras (1) (refer to Figures 4.57 and 4.58). The type and number of seismic base-isolators used in these hospitals are reported in Table 4.2, where the hospitals are listed according to rough proximity from the epicenter of the M7.8 event. All hospitals have curved surface slider (CSS) isolation systems; ten use dual-curvature pendulum bearings and two use triple-pendulum bearings. Seven of the hospitals with pendulum-based isolators have an RC moment-resisting frame structure over the isolation level.

Turkish news reported that not even slight damage occurred in State Hospitals of Kahramanmaras Elbistan, Hatay Dörtyol, and Malatya Battalgazi and Maternity and Children's State hospital in Malatya. They have also been used as shelter facilities for the earthquake victims (Hurriyet Daily News 2023).

A team of 5 members of the Deprem Izolasyon Derneği, (DID), and Turkish Association for Seismic Isolation (TASI) have traveled to the region and conducted initial reconnaissance. They visited each of these 12 hospitals over the course of 3 days. Their initial assessment indicates that all base-isolated hospitals were operational after the earthquake sequence, and most importantly allowed the facilities to serve their emergency response function in the aftermath of the extraordinary destruction. One hospital experienced some minor, non-structural damage. Movements of 2 cm to 16 cm were observed based on physical evidence at the isolation interfaces (Personal communications from Bahadir Sadan of DID, and Special Newsletter from ASSISi (Anti-Seismic Systems International Society), dated February 16, 2023). A detailed report will be released by DID on these observations (did.org.tr). Only one of the 12 facilities is seismically instrumented, and at this time data are not yet available for processing or evaluation.
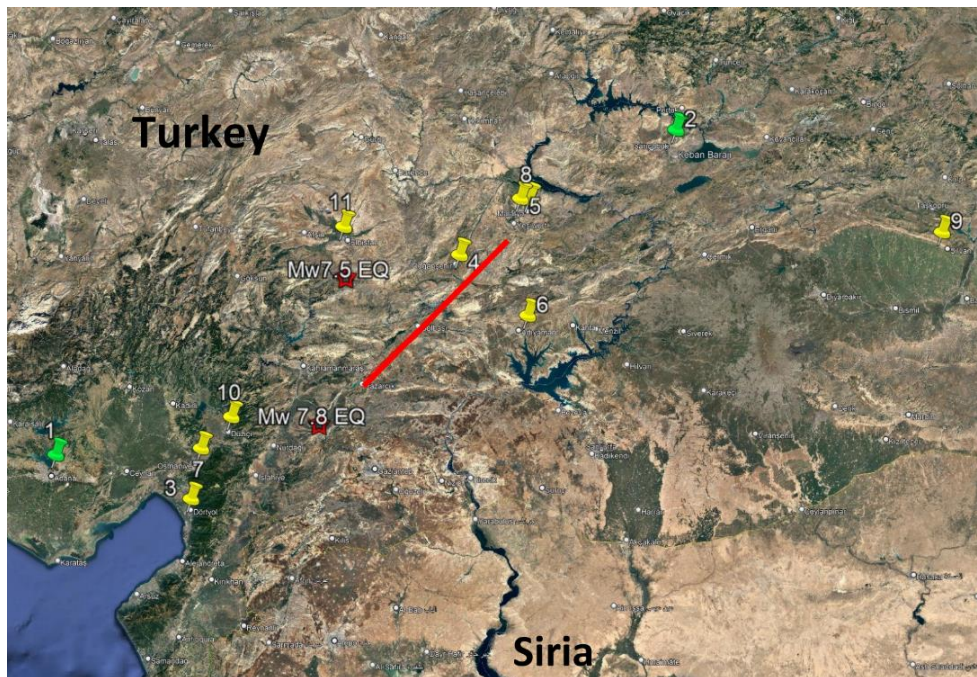

Figure 4.57. Locations of base-isolated hospitals in the regions affected by the earthquake sequence (Image courtesy of Dr. Michael C. Constantinou, University at Buffalo 2023).

Joint PVRR: 2023 Türkiye Earthquake Sequence
PRJ-3824 | Released: 3/29/2023
Building Resilience through Reconnaissance

96

Figure 4.58. Locations of base-isolated hospitals in the epicentral region (Image credit – Seismic Isolation Engineering, Inc., http://www.siecorp.com).

Table 4.2. List of base-isolated hospitals in the epicentral region.

Hospital	Type of Isolators	# of Isolators
Kahramanmaras KDC Hospital	DP or CSS	361
Osmaniye Duzici State Hospital	DP or CSS	NA
Osmaniye New State Hospital	DP or CSS	541
Hatay Dortyol State Hospital	DP or CSS	340
Kahramanmaras Elbistan State Hospital	DP or CSS	455
Malatya Dogansehir State Hospital	DP or CSS	122
Adiyaman State Hospital	DP or CSS	264
Adana Health Campus	TFP	1,552
Guney Adana Seyhan State Hospital	DP or CSS	251
Malatya State Hospital	DP or CSS	264
Malatya Battalgazi State Hospital	DP or CSS	222
Elazig Fethi Sekin City Hospital	TFP	878

DP: Double Pendulum; CSS: Curved Surface Sliders; TFP: Triple Friction Pendulum, NA: Information not available (Credit: Seismic Isolation Engineering, Inc.; http://www.siecorp.com).

A particular example of the benefits of using seismic protection systems in healthcare infrastructure is the post-earthquake response of the 1,600-beds Adana City Hospital (Figure 4.59). It has been recognized as the World's Largest Seismically Base-Isolated Hospital, with a 550,000 m^2 footprint and 1,552 seismic base-isolators (RÖNESANS 2023). After the earthquake, the hospital was able to offer 24-hour uninterrupted health services to injured people, including

Joint PVRR: 2023 Türkiye Earthquake Sequence
PRJ-3824 | Released: 3/29/2023
Building Resilience through Reconnaissance

97

up to 40 arrivals of 7-patient helicopters every day (MaviKocaeli 2023). Many patients were transferred from Hatay province, where multiple hospitals were damaged or collapsed and the reduced healthcare services in regional hospitals were extremely overwhelmed. A relevant observation was the significant number of critical patients mobilized to the functional hospitals by helicopter as access roads were overwhelmed or damaged. Thus, the building heliports and elevators became key emergency components with an essential role for the life-saving chain of patients with severe injuries. In addition, the Ministry of Health reported that patients were mobilized by the Iskenderun ship of the Ministry of National Defense (Ministry of Health 2023a). These large multi-modal patient mobilizations during the emergency response highlight the importance of coordination across large regions to deliver treatment to patients in disasters.

Figure 4.59. Adana City Hospital, 37.0301N 35.3483E (left) (Source: EPS 2023) and Frictional pendulum-type base-isolation devices in the hospital building (right) (Source: Anadolu Ajansi 2023).

On February 7, the Ministry of Health reported that hospitals in Reyhanlı, Dörtyol, Samandağ, Yayladağı, and Kırıkhan were operational and delivering treatment to injured patients. City Hospitals in Ankara and Istanbul were also operating and receiving nearly 300 wounded people, the most critical patients being transferred by helicopter ambulances. The same day, serious damage was reported in the 400-bed Adıyaman Training and Research Hospital (Figure 4.60). However, detailed information about the type of damage and its impact on functionality was not available. Official reports from the government indicated that on February 9, the hospital was operating at full capacity, according to the Ministry of Health.

Joint PVRR: 2023 Türkiye Earthquake Sequence
PRJ-3824 | Released: 3/29/2023
Building Resilience through Reconnaissance

98

Figure 4.60. Pre-earthquake image of Adıyaman Training and Research Hospital, Adıyaman province, 37.7675N 38.3228E (Source: Google Street View).

The Altinozu State Hospital (Figure 4.61) was assessed by World Health Organization (WHO) teams and reported to have heavy damage and lack of utilities (WHO, 2023). Thus, the hospital remained non-operational and unable to receive any patients from Altinozu district in Hatay province. On February 9, the government indicated that injured patients in critical conditions were transferred to other facilities.

Figure 4.61. Pre-earthquake view of Altinozu State Hospital, Hatay province, 36.1120N 36.2437E (Source: Google Street View).

In Kahramanmaraş province, a few areas of Necip Fazıl City Hospital, Maternity Hospital, and Yörük Selim State Hospitals were affected by the earthquake. However, the Ministry of Health reported that these hospitals were operational again on February 9. The state of damage to

Joint PVRR: 2023 Türkiye Earthquake Sequence
PRJ-3824 | Released: 3/29/2023
Building Resilience through Reconnaissance

99

structural or non-structural components or other causes of the interrupted operations were still unknown at the time of writing of this report. Official reports highlighted that inpatient treatment services, ICUs, and emergency departments were functional. ICUs in Artvin State Hospital (Figure 4.62) were also put into operation to receive injured patients. Conversely, emergency healthcare services in the Pazarcık State Hospital (Figure 4.63) were delivered in a tent outside the building due to the non-structural damage to the main building (Figure 4.64). Even though the building did not collapse, the extent of diagonal shear cracks in the short wall elements in Figure 4.64a indicate that significant lateral drift occurred. This would explain the collapse of ceiling tiles (Figure 4.64a) and damage to interior walls and roof elements (Figure 4.64b and c).

Figure 4.62. Pre-earthquake image of the Artvin State Hospital, Kahramanmaraş province, 37.5031N 37.3234E (Source: Google Street View).
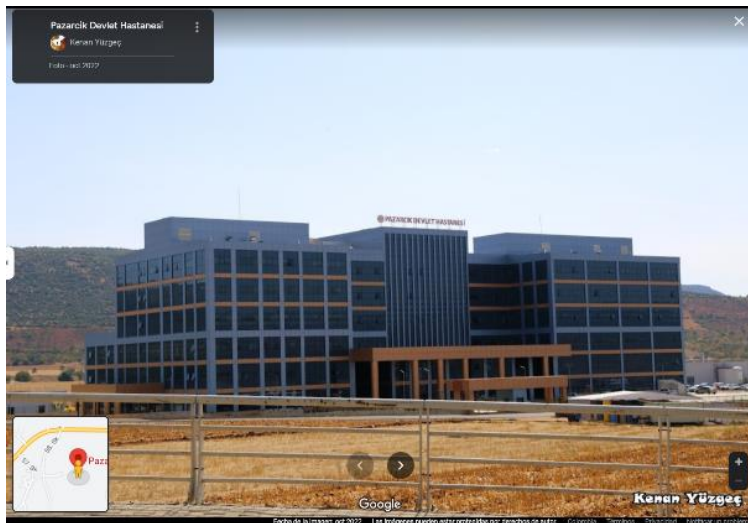

Figure 4.63. Pre-earthquake image of the Pazarcık State Hospital, Kahramanmaraş province, 41.1820N 41.8185E (Source: Google Street View).

Joint PVRR: 2023 Türkiye Earthquake Sequence
PRJ-3824 | Released: 3/29/2023
Building Resilience through Reconnaissance

100

(a) Façade walls and falling of ceiling tiles.

(b) Gypsum/plaster division walls.

(c) Cracking evident in the covering of multiple gypsum/plaster division walls.

Figure 4.64. Damage to non-structural components of Pazarcık State Hospital, built in 2018 (Source: [Twitter](#)).

4.6. Religious buildings

4.6.1. Religious buildings in Türkiye

Several mosques (Figures 4.65 to 4.68) and churches, new and historic, were damaged or partially collapsed in Türkiye due to the earthquake sequence. In particular, the city of Adiyaman suffered much of this damage.

The Yeni Camii or New Mosque, in Malatya, was extensively damaged when its roof structure and domes collapsed (Figure 4.65). The mosque was constructed on the site of the former Hacı Yusuf Mosque destroyed by an earthquake on March 3, 1894. The mosque was reconstructed on March 14, 1964, when another significant earthquake caused severe damage to the building. There were cracks in the dome and some of its walls and the top stones of the cone fell off. The

Joint PVRR: 2023 Türkiye Earthquake Sequence
PRJ-3824 | Released: 3/29/2023
Building Resilience through Reconnaissance

101

mosque was repaired as part of the restoration work carried out by the General Directorate of Foundations, and large minarets were also installed at that time.

(a) Before the earthquake sequence. (b) After the earthquake sequence.

Figure 4.65. Collapsed domes and walls, and damaged minarets of Yeni Camii, Malatya, 38.3495N 38.3180E (Source: Google Earth and DHA Photo via Ruetir 2023).

Figure 4.66 shows the partial collapse of Habib-i Neccar Mosque, Hatay, the first mosque in Anatolia. The dome was completely destroyed while the masonry walls and the courtyard roof partially collapsed. The long-span dome roof and significant vertical accelerations during this earthquake sequence may have contributed to the roof collapse of this structure, as well as the Adiyaman Ulu Grand Mosque in Adiyaman, Türkiye (Figure 4.67), which also experienced collapse of the roof and most supporting walls. Collapse sometimes initiated in the walls however, with the roofs remaining intact, as observed in damage to a mosque in Kahramanmaras, Turkiye (Figure 4.68). It is likely that the long-span dome roof structures, with large open interiors and limited number of supporting columns make these structures particularly susceptible to earthquakes, especially those containing large vertical accelerations such as those observed during this sequence.

(a) Before the earthquake sequence. (b) After the earthquake sequence.

Figure 4.66. Damage to Habib-i Neccar Mosque, the first Anatolian mosque, Hatay, Southeastern Türkiye (Sources: (a) hataygastronomi.com, (b) IHA Photos via Daily Sabah).

Joint PVRR: 2023 Türkiye Earthquake Sequence
PRJ-3824 | Released: 3/29/2023
Building Resilience through Reconnaissance

102

(a) Before the earthquake sequence.   (b) After the earthquake sequence.

Figure 4.67. Damage to the Adiyaman Ulu Grand Mosque in Adiyaman, Türkiye (Sources: (a) Twitter (b) Middle East Eye 2023).

Figure 4.68. Partial collapse of an exterior wall of a mosque in Kahramanmaras, Turkiye, while the domed roof remained intact (Source: Reuters via the Independent 2023).

The Cathedral of the Annunciation in İskenderun has partially collapsed (Figure 4.69a). The Cathedral of the Annunciation (also known as the Alexandrian Catholic Church) is a Catholic church that functions as the Cathedral of the Apostolic Vicariate of Anatolia in İskenderun. It was built between 1858 and 1871 by the Order of the Carmelites. After a fire in 1887, it was rebuilt between the years of 1888 and 1901. In İskenderun, the St. Nicholas Orthodox Church was also severely damaged (Figure 4.69b). This church is a listed heritage building whose construction began in the early 1870s and was completed in 1876. The church is a three-nave basilica with bell towers on both sides of the main entrance section. In İskenderun, media reports indicated that the Holy Forty Martyrs of Sebaste Armenian Church (*Surp Karasun Manuk Ermeni Kilisesi* - coordinates: 36.5902N 36.1704E) was also heavily damaged (Armenpress 2023). Finally, in Arsuz, the Mar Yuhanna Orthodox Church was also destroyed (Figure 4.70).

(a)

(b)

Figure 4.69. (a) Collapse of the arch roof structure of the Cathedral of the Annunciation in İskenderun (36.5876N 36.1655E) (Source: New Arab 2023); (b) Severe damage to St. Nicholas Orthodox Church in İskenderun due to out-of-plane failure of the gable end wall (36.5875N 36.1706E) (Source: haber.sat7turk.com 2023).

Figure 4.70. Collapsed Mar Yuhanna Orthodox Church in Arsuz where walls were constructed of unreinforced stone masonry (36.4120N 35.8849E) (Source: haber.sat7turk.com 2023).

4.6.2. Religious buildings in Syria

Several mosques and churches in Syria collapsed or were partially damaged during the earthquake sequence. Figure 4.71 shows damage to a historic mosque minaret made of unreinforced stone masonry in Aleppo. Figure 4.72 shows the collapse of a mosque in a residential area in Idlib, Northwestern Syria. The heavy dome roof appears to have been supported on a long-span roof supported by rectangular reinforced concrete columns with inadequate reinforcement. Some of these columns are visible in Figure 4.72 without any evidence of reinforcing bars extending from the column segments.

(a) Photograph from July 3, 2016.   (b) Photograph from February 6, 2023.

Figure 4.71. Collapse of the roof structure on the minaret, and partial collapse of unreinforced masonry walls of a mosque inside UNESCO-listed citadel in Ancient city of Aleppo (36.1994N 37.1622E) (Sources: (a) AFP via Time of Israel 2023; (b) AFP via Middle East Eye 2023).

Figure 4.72 Collapsed mosque in Idlib, Northwest Syria (Source: Getty Images via Foreign Policy, 2023). The heavy dome roof appears to have been supported on a long-span roof supported by rectangular reinforced concrete columns with inadequate reinforcement.

Joint PVRR: 2023 Türkiye Earthquake Sequence
PRJ-3824 | Released: 3/29/2023
Building Resilience through Reconnaissance

105

4.7. Nonstructural Components and Building Contents

There was a varying level of structural response in this earthquake sequence from complete collapse to no damage and fully functional structures. For structures with light/no structural damage, nonstructural damage becomes important as nonstructural components and building contents can be costly to repair or replace impacting the building functionality and resulting in downtime. In addition, damage to some nonstructural components can endanger the life of people escaping the building and prevent the first responders entering the building. For instance, as shown in Figures 4.52b and 4.73, ceiling system and parapet failure can be a falling object hazard, and in some cases they completely shut down the egress of the building.

Figure 4.73. Examples of nonstructural components (bricks and parapets), which can be a falling hazard, in a residential building in Hatay, Türkiye. It was also announced that residents were stuck in the stairwell (Source: Ozgur via Twitter 2023).

Figure 4.74 shows the damage to the façade of the Mersin City hospital in Mersin, Türkiye. Vertically spanning nonstructural components and systems such as façade, curtain walls, and the stair system are exposed to multi-support excitation due to attachment at multiple levels within a building. Therefore, it is essential to design these nonstructural systems such that they are drift compatible.

Joint PVRR: 2023 Türkiye Earthquake Sequence
PRJ-3824 | Released: 3/29/2023
Building Resilience through Reconnaissance

106

Figure 4.74. Damage to Mersin City Hospital, Türkiye (Source: Twitter).

Exterior and interior infill walls experienced extensive damage during the earthquake sequence. Figure 4.75 shows the typical damage of nonstructural infill walls. These types of infill walls are reported in many buildings with low to high level damage to the structural system. The building shown in this figure was carefully inspected by a team on the site, and the building is reported to have medium level damage. Proper design of nonstructural infill walls would mitigate the damage level to these drift-sensitive nonstructural systems. The structure in Figure 4.75 can be considered as a case where the infill walls provided beneficial effects to the structural response.

(a) Exterior walls.

(b) Interior wall.

Figure 4.75. Damage to non-structural infill walls (Source: Demirkapu, Local Assessor).

Joint PVRR: 2023 Türkiye Earthquake Sequence
PRJ-3824 | Released: 3/29/2023
Building Resilience through Reconnaissance

107

Other nonstructural damage is shown in Figure 4.76 for items fallen off shelving units at a store in Gaziantep, Türkiye. Moreover, Figure 4.77 shows broken window panes (refer to the arrows) of a building in Aleppo, Syria, due to out-of-plane accelerations, which can be a falling hazard.

Figure 4.76. Items fallen off shelving units at a store in Gaziantep, Türkiye (Left: Before earthquake sequence; Right: After earthquake sequence) (Extracted from Twitter video).

Figure 4.77. Broken window panes, Aleppo, Syria (Source: LOUAI BESHARA/AFP via Getty Images 2023).

4.8. Stairwells

Stairs are the primary means of ingress and egress for a building during and after extreme events like earthquakes. Significant damage to the stair systems have been reported in previous earthquakes such as the 2008 Wenchuan Earthquake (Li and Mosalam 2013) and 2011 Christchurch earthquake (Bull 2011). During the Mw 7.8 and Mw 7.5 earthquake sequence in Türkiye, damage to stairwells and stairwell collapse were reported. As shown in Figure 4.78, the

Joint PVRR: 2023 Türkiye Earthquake Sequence
PRJ-3824 | Released: 3/29/2023
Building Resilience through Reconnaissance

108

residential building received significant damage, but the building did not collapse. However, the residents of these buildings were not able to evacuate the building due to the collapse of stairwells. Therefore, the functionality and serviceability of these buildings were compromised, and the life of the residents were endangered.

(a) Residents had difficulty exiting the building due to stairwell collapse (Source: Tommy Shelby via Twitter).

(b) Residents sought help from a rescue team as they were stuck inside the building due to stairwell collapse (Source: Husamettin Dogan via Twitter).

Figure 4.78. Damage to structural and nonstructural systems of residential buildings, Hatay, Türkiye.

Significant damage to the Yesilhisar municipality building and stair flight was reported (see Figure 4.79). Yesilhisar municipality building is approximately 250 km away from Elbistan, and 290 km away from Pazarcik Kahramanmaras.

Joint PVRR: 2023 Türkiye Earthquake Sequence
PRJ-3824 | Released: 3/29/2023
Building Resilience through Reconnaissance

109

(a) Diagonal tension cracks of building exterior wall.   (b) Crack parallel to stair run direction.

Figure 4.79. Damage to Yesilhisar municipality building, Kayseri, Türkiye (Source: Only53.com 2023).

In Malatya, Türkiye, a steel stair tower which was intended to be used for a fire emergency stood alone, while the building adjacent to this stair tower collapsed (Figure 4.80). It was an emergency stair attached to the exterior of the building on each level.
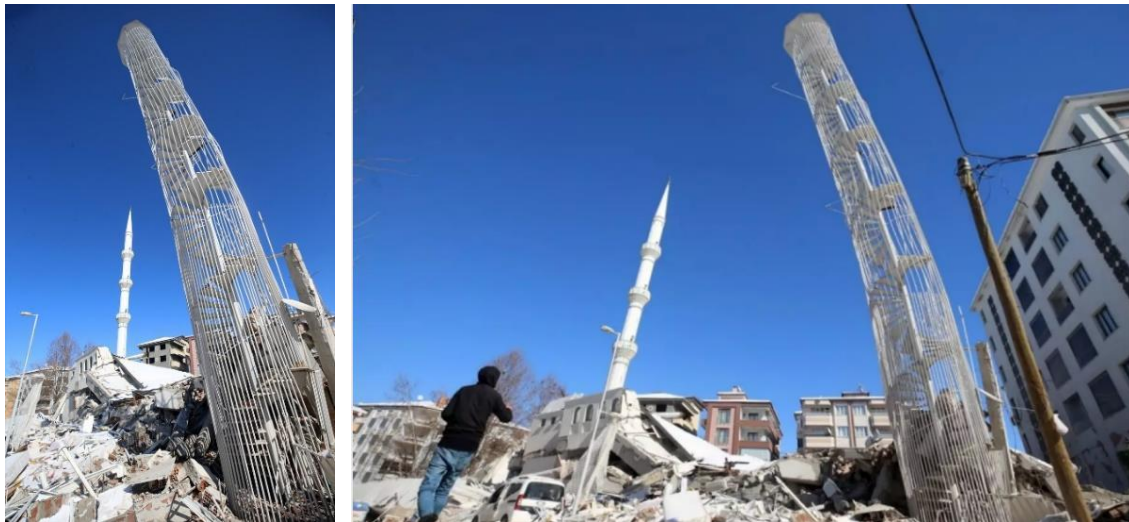

Figure 4.80. A 5-story RC building collapsed, but the steel stair stood alone, Malatya, Türkiye (Source: TRHaber 2023).

Joint PVRR: 2023 Türkiye Earthquake Sequence
PRJ-3824 | Released: 3/29/2023
Building Resilience through Reconnaissance

110

4.9. Historical Structures

Gaziantep Castle, located in the heart of the city, closest to the epicenter, was constructed as an observation point during the Hittite Empire, fortified during the Roman Empire, and expanded under Byzantine Emperor Justinian I in the 6th century. Although the castle withstood centuries of invasions, it was badly damaged in this earthquake sequence (Figure 4.81) (NPR 2023). The unreinforced masonry walls present a significant mass that induces large internal forces during ground shaking. The shear strength of an unreinforced masonry wall is relatively low, and appears to have been exceeded in many areas around the perimeter wall of this castle. These walls often consist of neatly stacked exterior stone plies, enclosing loose rubble masonry on the interior of the wall as is visible in Figure 4.81 (d(and (e). This construction is effective against cannonball impact, but susceptible to collapse during ground shaking.
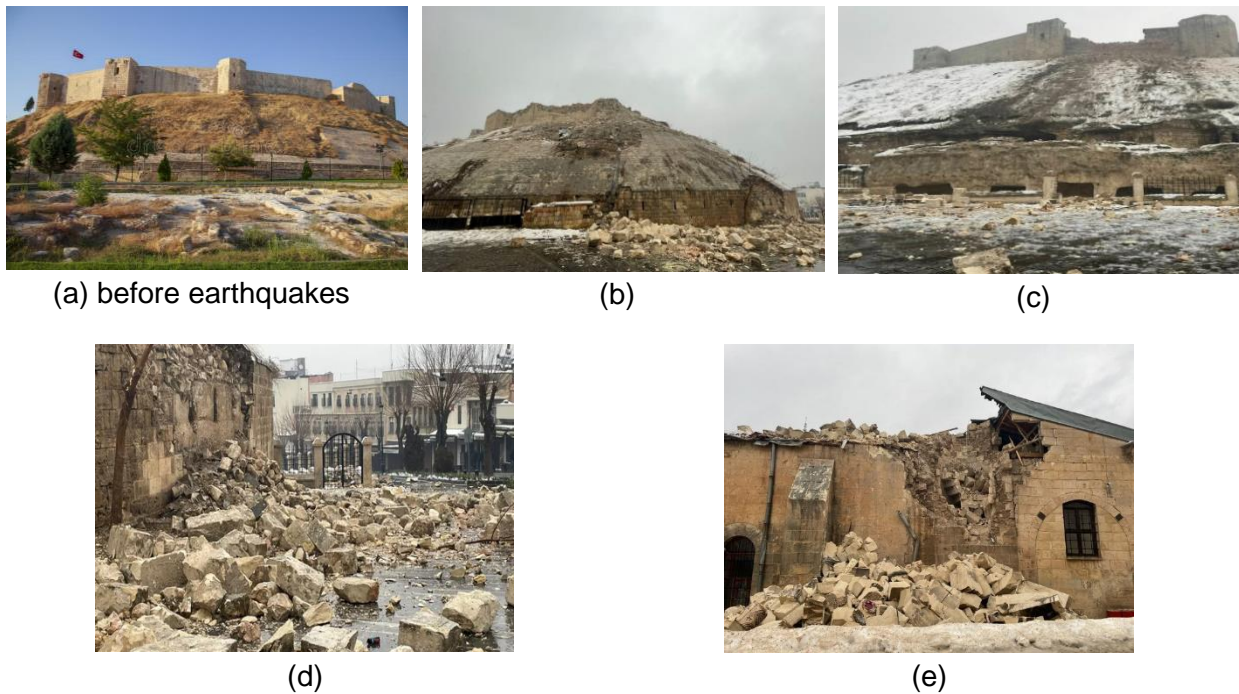

(a) before earthquakes

(b)

(c)

(d)

(e)

Figure 4.81. Gaziantep Castle damage (Source: (a) and (b) Thomas van Linge via Twitter, (c) and (d) Getty Images via TheGuardian.com, (e) Getty Images via Smithsonian 2023).

Joint PVRR: 2023 Türkiye Earthquake Sequence
PRJ-3824 | Released: 3/29/2023
Building Resilience through Reconnaissance

111

5. Infrastructure Performance

Table 5.1 provides a summary of the performance of various classes of infrastructure. Specific illustrations of infrastructure performance are provided in the subsections that follow.

Table 5.1. Summary of performance by infrastructure class.

Roads & Bridges	Road damage occurred throughout the impacted region due to the earthquake sequence. Roads were also closed due to inclement weather that occurred immediately after the earthquake sequence. A few bridges and tunnels were damaged, namely, Erkenek tunnel, Bulan 3 Bridge (collapsed), and Recepbey Bridge (collapsed).
Power	30 substations were damaged in the earthquake sequence causing power outages throughout Gaziantep, Hatay, and Kilis.
Telecommunication	Phone lines were down in the southern provinces after the earthquake sequence and internet outages were widespread throughout Osmaniye, Hatay, and Adiyaman.

5.1. Roads and Bridges

5.1.1. Road damage and closures

Damage to the Tarsus-Adana–Gaziantep (TAG) Highway occurred due to the Mw 7.8 earthquake. Traffic along the Osmaniye-Gaziantep West Junction portion of the TAGHighway was diverted to the D-400 state road (Demirci 2023). Figure 5.1 shows representative damage of roadways observed after the Mw 7.8 earthquake along the TAG Highway. In several places, cracking of pavement (e.g., Figures 5.1(a-c)) due to seismic compression and vertical settlement induced distortional shearing caused surface failures (Figure 5.2). Vertical settlement of the pavement could be associated with the cyclic softening of materials due to large shear strain imposed by the earthquake sequence. Differential movement of a road near the Tevekkelli village on the Kahramanmaraş-Gaziantep Highway was also observed (Figure 5.3). This movement was measured to be approximately 3 meters.

Joint PVRR: 2023 Türkiye Earthquake Sequence
PRJ-3824 | Released: 3/29/2023
Building Resilience through Reconnaissance

112

(a)

(b)

(c)

(d)

Figure 5.1. Damage to Tarsus-Adana-Gaziantep (TAG) Highway (Expat Guide Türkiye 2023).

Figure 5.2. Surface failure of roadway (Source: Channel News Asia).

Joint PVRR: 2023 Türkiye Earthquake Sequence
PRJ-3824 | Released: 3/29/2023
Building Resilience through Reconnaissance

113

Figure 5.3. Shifting (differential movement) of the roadway near the Tevekkelli village (Source: Veryansin TV).

On February 8, 2023, Karayollari Genel Mudurlugu (General Directorate of Highways) announced that all major arteries in the country were open for travel and no destinations were closed due to earthquake damage. Some roadways remained closed due to inclement weather. Table 5.2 lists a summary of road closures and bridge collapses as of February 6, 2023 at 6:29 pm local time, around 14 hours after the earthquake. The reopening sequence for roadway closures is cataloged in Appendix A. Notable closures included Gaziantep Narli Nurdagi, Osmaniye to Gaziantep, Osmaniye to Nurdagi, the Erkenek tunnel (east of Malatya Golbasi), Bulan 3 bridge (due to collapse between Adiyaman and Celikhan), and Recepbey bridge (due to collapse between Adiyaman and Celikhan Surgu). In the case of damage to the Erkenek tunnel on February 7 (per General Directorate of Highways Tweet), concrete spalling was noted and the tunnel was operated on one tube to accommodate two way traffic. Considering only a few road closures and damaged bridges, the overall performance of the roads, highways, and bridges is acceptable for such a major earthquake sequence.

Joint PVRR: 2023 Türkiye Earthquake Sequence
PRJ-3824 | Released: 3/29/2023
Building Resilience through Reconnaissance

114

Table 5.2. Summary of road closures and bridge collapses as of February 6, 2023 at 6:29 pm.

Short name	Distance (km)	Date of closure	Time	Reason	Notes
Bahce - Gaziantep junction	40+000	February 6	05:00 pm	Collapses on the road	-
Malatya - Golbasi - 5th District	76+000, 78+000	February 6	05:00 pm	Concrete spalling on Erkenek tunnel	-
Malatya - Yazihan	61+000; 62+3000	February 6	05:00 pm	Bridge joint openings	Tohma bridge, 15 spans, 517.50 m length
Adiyaman - Celikhan	49+000	February 6	05:00 pm	Bridge collapse	Bulam 3 bridge collapsed, 3 spans, 55.3 m length
Celikhan - Surgu	3+000	February 6	05:00 pm	Bridge collapse	Balikburnu bridge collapsed, single span, 14.2 m length
Hatay - Reyhanli	20+000; 22+000	February 6	05:00 pm	Collapses on the road	-
Goksun-Maras	47+825	February 6	05:00 pm	Damage to tunnel	-

5.1.1. Bridge damage

A limited number of bridges were reported to be damaged after the earthquake sequence. Figure 5.4 shows the damage at the expansion joint of a bridge on the Adana-Gaziantep Highway and the repair work which was reported to be completed on February 11, 2023 per Twitter. Extensive damage at the deck of Şekeroba bridge on the Kahramanmaraş-Osmaniye Highway (Figure 5.5) and unseating and falling girders at an overpass at Nurdağı (Figure 5.6) were reported to be the few cases of bridge damage after the earthquake sequence.

Figure 5.4. Damage and repair work of an expansion joint of a bridge on Adana-Gaziantep Highway (Source: Twitter).

Joint PVRR: 2023 Türkiye Earthquake Sequence
PRJ-3824 | Released: 3/29/2023
Building Resilience through Reconnaissance

115

Figure 5.5. Extensive damage at the deck of Şekeroba Bridge (Source: Olay53).

Figure 5.6. Unseating failure of an overpass in Gaziantep Nurdağı (Source: hurriyet.com).

5.2. Other Civil Infrastructure

5.2.1. Ports

As discussed in Section 1.2.2, fires affected the Iskenderun Port, causing considerable disruption to operations. Meanwhile, the Port of Ceyhan is where the Baku-Tiblisi-Ceyhan (BTC) crude oil from Azerbaijan is delivered to Türkiye. This port lost power, and there was a small leak in one of the storage tanks. Due to this, tanker loading operations were suspended for a day. However, the leak was fixed, and the loading operations have resumed (Perkins et al. 2023). It is noted that there was no damage to the BTC oil pipelines due to the earthquake sequence.

5.2.2. Airports

Gaziantep, Hatay, Kahramanmaraş, and Adana airports remained closed for a few days after the earthquake sequence. The Hatay Airport is closed due to a surface rupture of the tarmac (Figures 5.7 and 5.8). In addition, aftershocks have caused planes to be grounded at airports throughout the region (Aerotime Hub 2023). Flights across Türkiye were also being canceled due to adverse weather conditions.

Joint PVRR: 2023 Türkiye Earthquake Sequence
PRJ-3824 | Released: 3/29/2023
Building Resilience through Reconnaissance

116

Figure 5.7. Hatay Airport in southeastern Türkiye has suspended operations due to runway damage caused by the earthquake sequence (Source: Twitter).

Figure 5.8. Image posted on February 8 1:04 am documenting repair work on the Hatay airport runway (Source: Raillynews).

5.2.3. Railways

Deformation of the railway tracks was observed between Kahramanmaraş, Türkoğlu, and Gaziantep, İslahiye. This serves as evidence of the movement of the tectonic plate, probably at the fault location (Figure 5.9).

Joint PVRR: 2023 Türkiye Earthquake Sequence
PRJ-3824 | Released: 3/29/2023
Building Resilience through Reconnaissance

117

Figure 5.9. Deformed railway between Kahramanmaraş, Türkoğlu, and Gaziantep, İslahiye (Sources: Reddit (left) and Facebook (right)).

5.2.4. Thermal and nuclear power plants

It was reported that the Hunutlu thermal power plant was undamaged (Figure 5.10) and the personnel were safe. None of the equipment of the plant was impacted and the plant continued to provide electricity to the earthquake affected region. No damage was reported at Akkuyu nuclear power plant (Figure 5.11). This nuclear plant is under construction, which continued after a prompt operational inspection of all buildings, structures, and tower cranes was performed with no observed damage as the outcome of this inspection.

Figure 5.10. Undamaged Hunutlu thermal power plant in the Adana province (Source: Twitter).

Joint PVRR: 2023 Türkiye Earthquake Sequence
PRJ-3824 | Released: 3/29/2023
Building Resilience through Reconnaissance

118

Figure 5.11. Undamaged Akkuyu nuclear power plant (Source: World Nuclear News).

5.2.5. Industrial facilities

Satellite images show grain silos destroyed near Kırıkhan and Nurdağı (Figure 5.12). Moreover, Figure 5.13 shows damage to an industrial facility with steel tanks. Often these tanks do not have lateral bracing or adequate anchorage for seismic demands, which causes them to buckle or topple in an earthquake. However, the storage containers shown in Figure 5.13 were also impacted by a collapsed roof, which could also have contributed to the observed damage and induced the subsequent failure of the concrete stem wall surrounding the tanks.

Figure 5.12. Aerial views of the damage of grain silos near Kırıkhan (Left) and near Nurdağı (Right) (Source: CNN).

Joint PVRR: 2023 Türkiye Earthquake Sequence
PRJ-3824 | Released: 3/29/2023
Building Resilience through Reconnaissance

119

Figure 5.13. Steel storage containers damaged during the earthquake sequence due to failure of roof (Source: Mustafa Kerem Koçkar via Linkedin).

5.2.6. Lifelines

Internet connectivity was lost in all cities impacted by the event in Türkiye. The connectivity was not fully recovered as of February 8, 2023 as shown in Figure 5.14. Over 30 electrical substations were damaged due to the earthquake sequence causing power outages and blackouts reported in Antep, Hatay, and Kilis (The Telegraph, 2023). Generators and mobile power plants were provided to essential power facilities such as hospitals, soup kitchens, and general services for the public. Authorities were fearful of gas leaks and potential fires. Therefore, gas was cut off to the impacted regions to prevent fires.
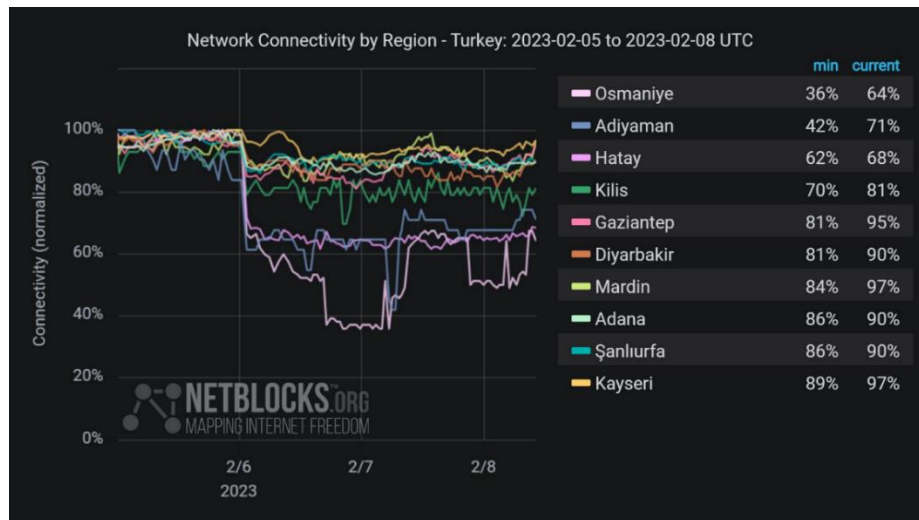
Figure 5.14. Recovery of data infrastructure in cities of Türkiye impacted by the event (Source: Twitter).

Joint PVRR: 2023 Türkiye Earthquake Sequence
PRJ-3824 | Released: 3/29/2023
Building Resilience through Reconnaissance

120

5.2.7 Oil Refineries

The Banias refinery in Syria was partially damaged due to the earthquake sequence. The main damage to the refinery was to the concrete bases of equipment, separation, and failure of furnaces' linings, displacement of the center of the gasoline reactor, in addition to the damage to the main chimneys of the power unit (Figure 5.15). Therefore, the refinery was out of service. The technical staff continued the repair work, and the distillation unit has been functioning since the afternoon of February 8, and the furnaces were started on February 9 (as they needed 48 hours for the slow drying of the tile lining).

(a)

(b)

(c)

(d)

(e)

Figure 5.15. Damage of Banias Oil Refinery in Syria (Source: Syrian Ministry of Oil and Mineral Resources).

Joint PVRR: 2023 Türkiye Earthquake Sequence
PRJ-3824 | Released: 3/29/2023
Building Resilience through Reconnaissance

121

6. Geotechnical Performance

6.1. Seismic Site Classification

Kahramanmaras city was evaluated for seismic site classification and a map was developed by Naji et al. (2020, 2021). The Kahramanmaras basin is a major geological structure developed from the collision of the Arabian and Eurasian tectonic plates over the Bitlis Suture Zone, resulting in the deposition of thick alluvial sediment of undisturbed gravel, silt, and clay. According to Gül et al. (2005), limestone and claystone overlay shallow marine deposits. As shown in Figure 6.1, geological units include outcrops from Cambrian, Triassic, Jurassic, Cretaceous, Tertiary, and Quaternary periods. Prominent soil formations in Figure 6.2 include the Golbasi formation, composed of horizontally bedded river sediments of pebble, mud, and sand, the Ahirdagi formation, a durable limestone unit, and the Pinarbasi formation, a variety of poorly bedded angular pebbles of predominantly limestone. Naji et al. (2021) collected SPT-N values from 287 boreholes from the top 30 m and measured the shear-wave velocity (V_{s30}) through Multichannel Analysis of Surface Waves (MASW) and Microtremor Array Method (MAM) measurement tests. Using 15 MASW and 10 MAM sites, the V_{s30} profile within the top 30 m (see Figure 6.3) and average values (see Figure 6.4) were attained. Using Boore et al. (2011) methodology, the V_{s30} (time-averaged shear wave velocity in the upper 30 m of the soil deposit) values were estimated from shallow velocities (V_{sd}). The values are mapped in Figures 6.4 and 6.5, along with corresponding NEHRP classifications. About 57.5% of the area is classified as soil class D, while the rest (42.5%) of the area is classified as soil class C based on SPT N30 measurements and NEHRP site classification (Figure 6.6).
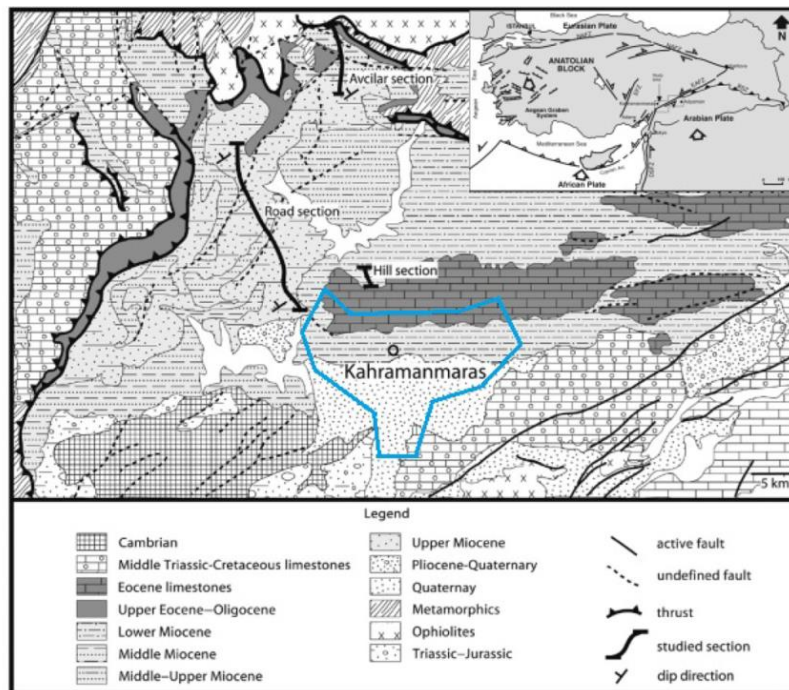

Figure 6.1. Geological map of Kahramanmaras area (modified from Yilmaz et al. 2006; Hüsing et al. 2009).
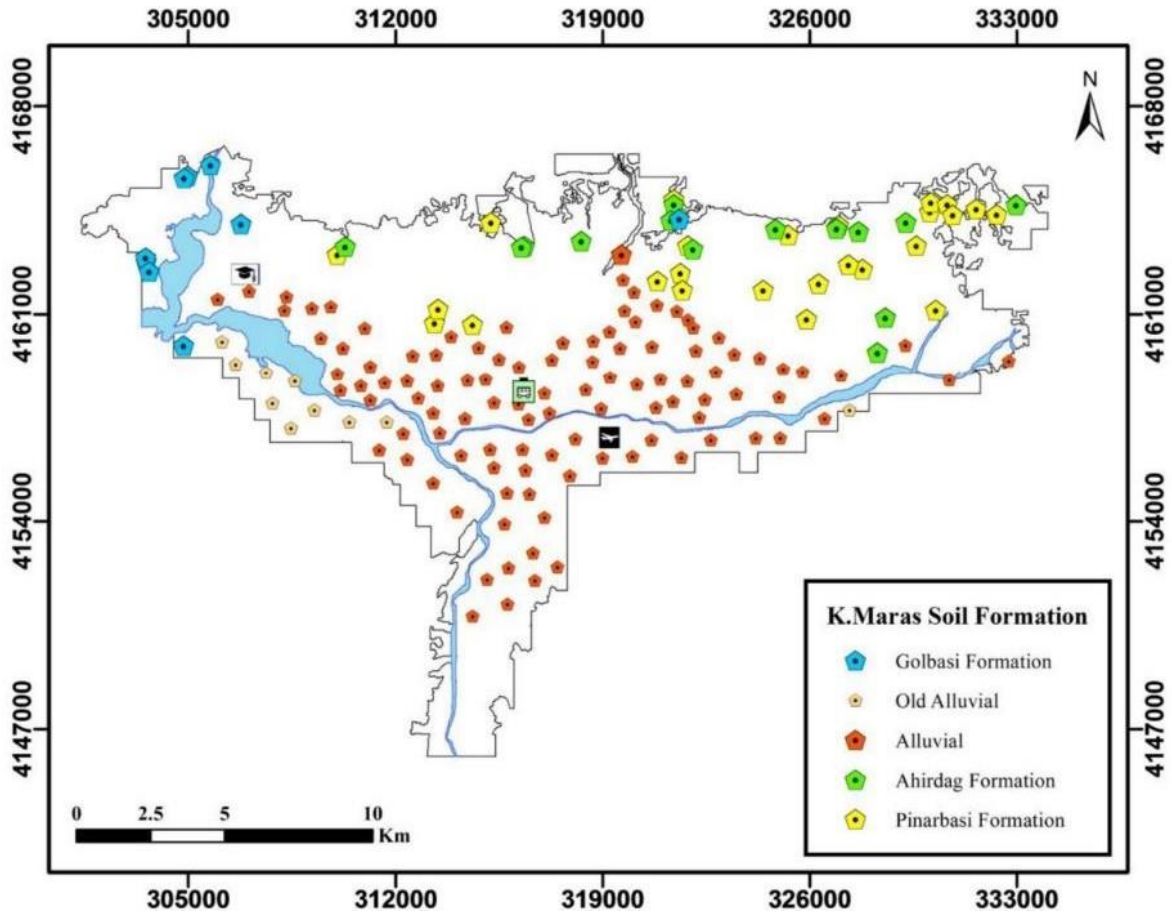
Joint PVRR: 2023 Türkiye Earthquake Sequence
PRJ-3824 | Released: 3/29/2023
Building Resilience through Reconnaissance

122

Figure 6.2. Soil formations of the Kahramanmaras area (Naji et al. 2021).

Joint PVRR: 2023 Türkiye Earthquake Sequence
PRJ-3824 | Released: 3/29/2023
Building Resilience through Reconnaissance

123
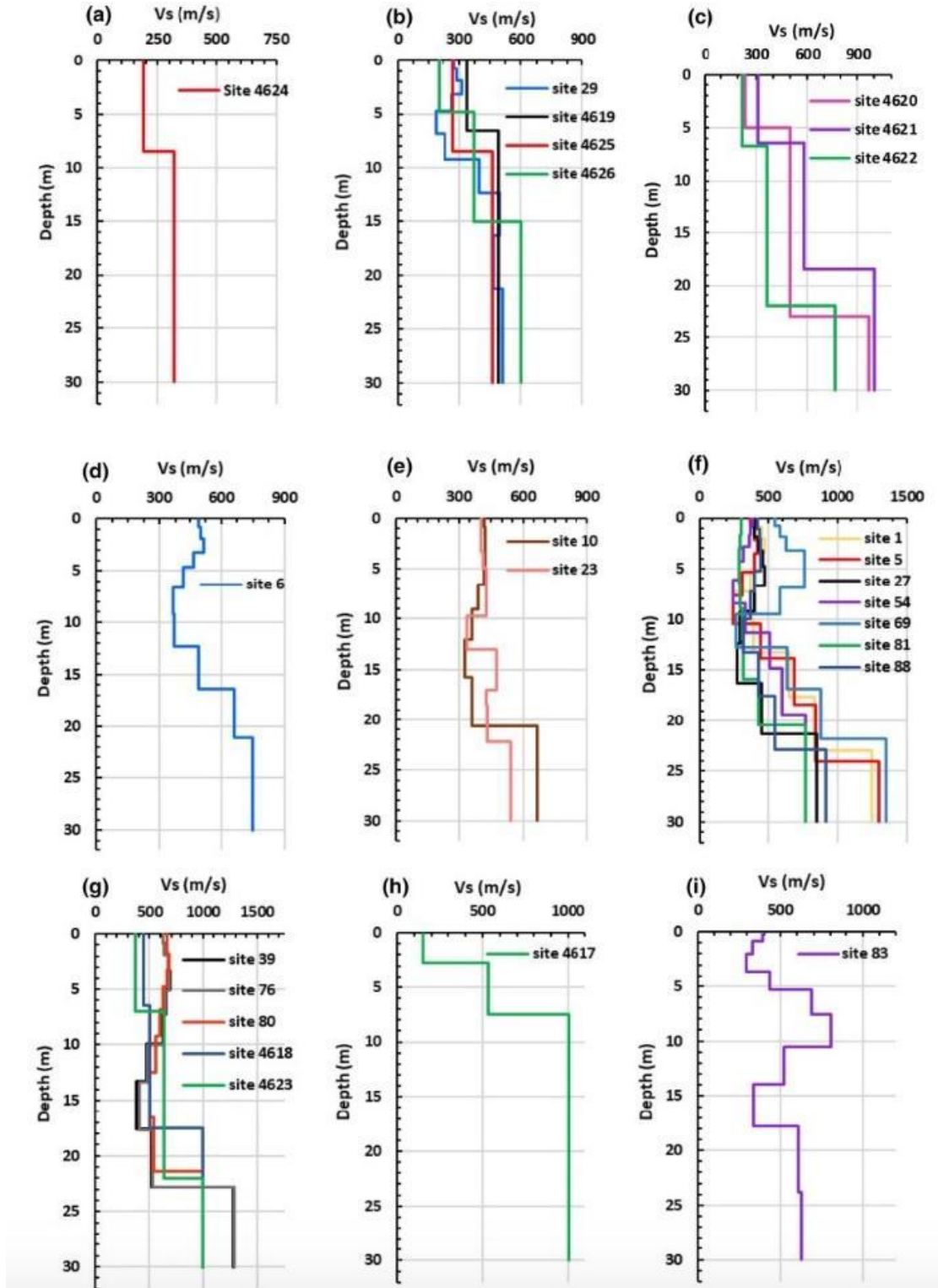
Figure 6.3. V_{s30} profiles from 25 sites (15 MASW and 10 MAM) (Naji et al. 2021).

Joint PVRR: 2023 Türkiye Earthquake Sequence
PRJ-3824 | Released: 3/29/2023
Building Resilience through Reconnaissance

124
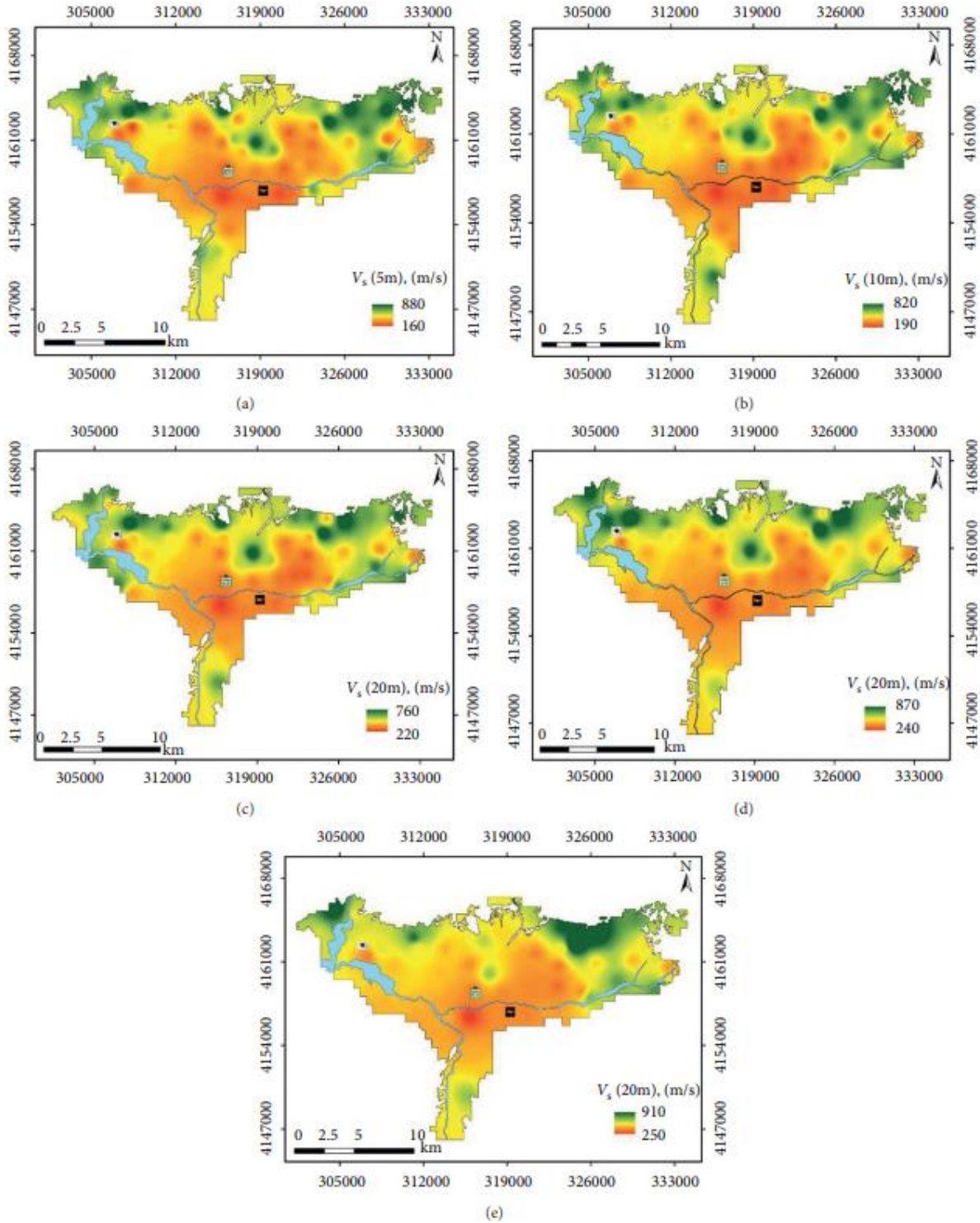
Figure 6.4. Average V_s values for the depths of: (a) 5 m, (b) 10 m, (c) 15 m, (d) 20 m, and (e) 25 m in Kahramanmaras area (Naji et al. 2020).

Joint PVRR: 2023 Türkiye Earthquake Sequence
PRJ-3824 | Released: 3/29/2023
Building Resilience through Reconnaissance

125
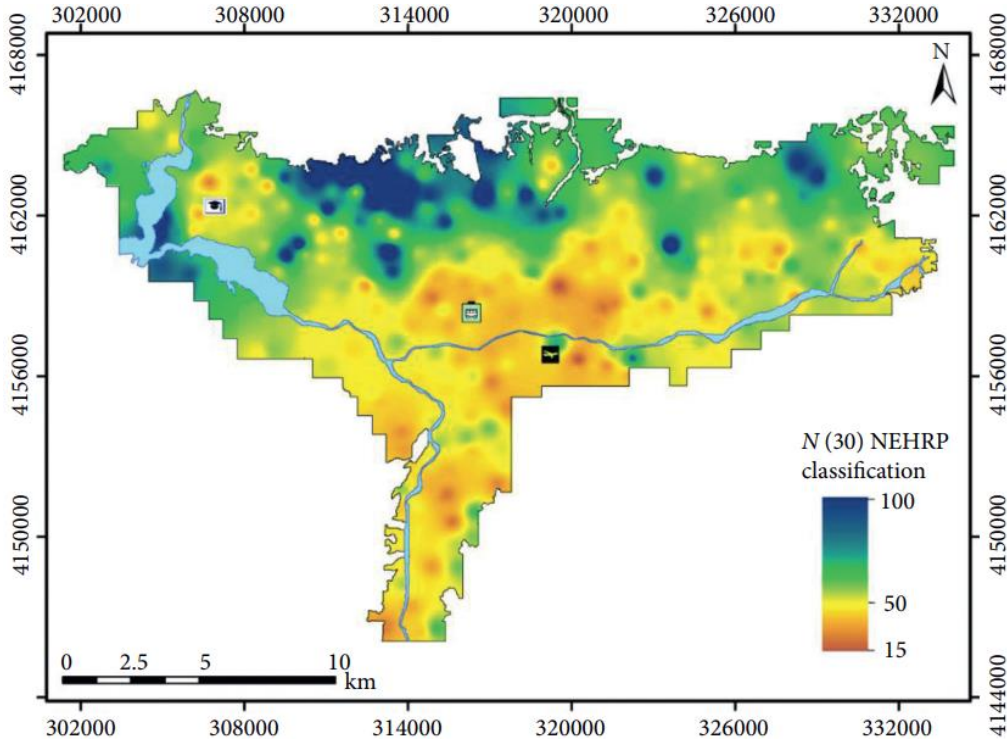
Figure 6.5. N30 based seismic site classification map in Kahramanmaras (Naji et al. 2020).
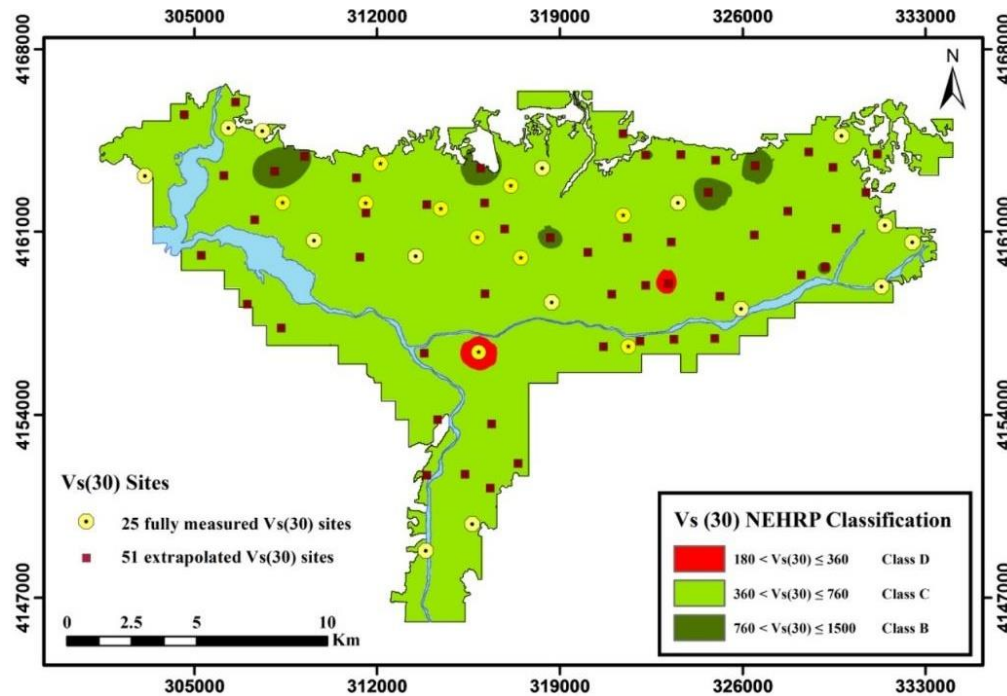
Figure 6.6. V_{S30} ranges and corresponding NEHRP classifications (Naji et al. 2021).

Joint PVRR: 2023 Türkiye Earthquake Sequence
PRJ-3824 | Released: 3/29/2023
Building Resilience through Reconnaissance

126

6.2. Liquefaction Potential

Cabalar et al. (2019) assessed the liquefaction potential of Kahramanmaras, Türkiye, based on the in situ SPT-based approach presented by Youd and Idriss (2001). The SPT blow counts from the field testing revealed that the southern part of the Kahramanmaras city has the highest liquefaction risk. The liquefaction potential of the studied area was presented using site maps at different depths below the ground surface. Their findings are presented in Figure 6.7 and are summarized as follows:

1. Liquefaction potential is not significant for shallow depths (below 3.0 m) in the studied area.

2. The depth of 6.0 m to 7.5 m was identified as the layer with highest liquefaction potential as it contains loose silty-sand in most regions of the studied area.

3. There are certain areas of the city center with the highest potential of liquefaction triggering under the effect of a large magnitude earthquake. Those areas showed high liquefaction potential in almost all depth intervals.
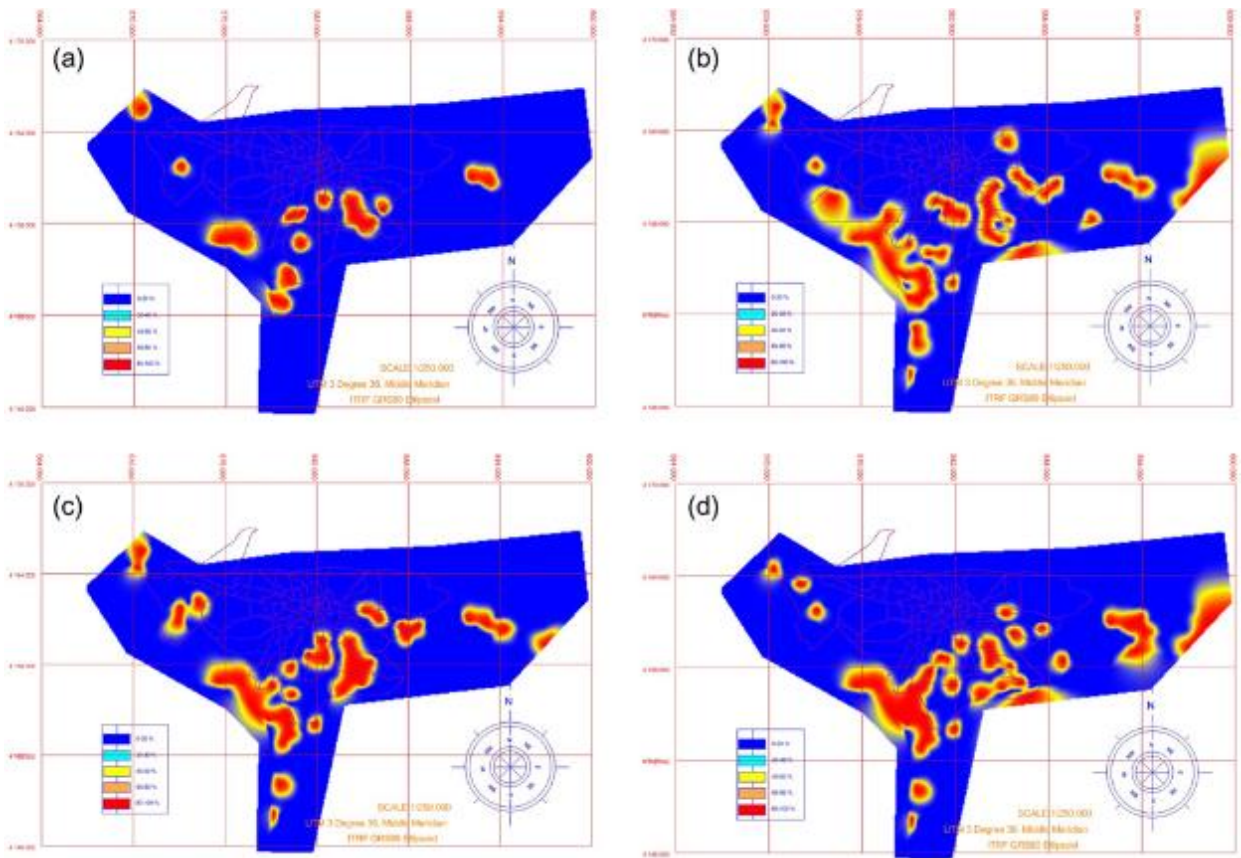

Figure 6.7. The liquefaction map for the Kahramanmaras region at depths: (a) 1.5 m to 3.0 m, (b) 6.0 m to 7.5 m, (c) 9.0 m to 10.5 m, and (d) 13.5 m to 15.0 m (Cabalar et al. 2019). Note that blue and colors indicate the smallest and largest potential for liquefaction.

Joint PVRR: 2023 Türkiye Earthquake Sequence
PRJ-3824 | Released: 3/29/2023
Building Resilience through Reconnaissance

127

6.3. Landslides

The USGS landslide inventory map shows the probability of landslides in the area (Figure 6.8). Based on this map, it is likely that some landslides will occur during strong ground shaking, and a substantial number of roads could be blocked by slope or embankment failures. This will impede the rescue work, especially in remote areas during the initial, all-important, 24-hour rescue and recovery period. In general, landslides from strike-slip earthquakes cluster close to the surface expression of the fault trace, although some can still occur at considerable distances. A lateral spreading induced landslide was observed on the road between Adana and Gaziantep following the Mw 7.8 and Mw 7.5 earthquakes on February 6 (Figure 6.9). Ground movements caused extensive damage to this roadway.
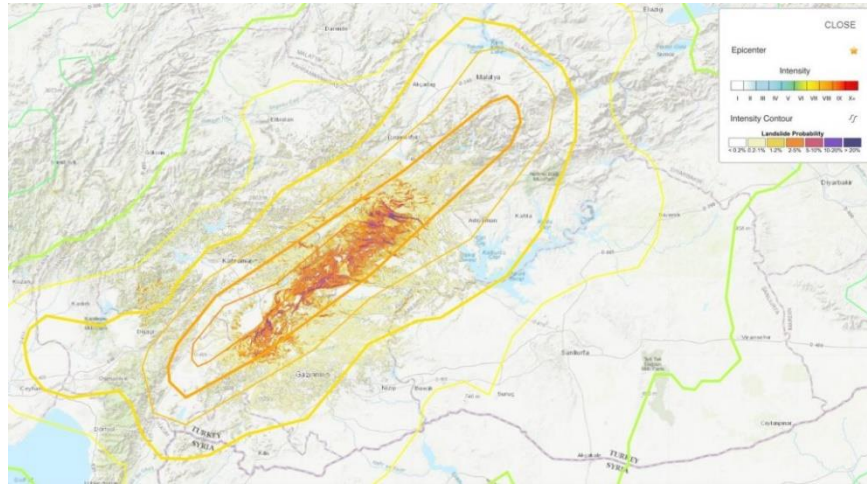
Figure 6.8. Initial USGS landslide probability map for Feb. 6, 2023 earthquake near Nurdağı in Gaziantep, Türkiye.
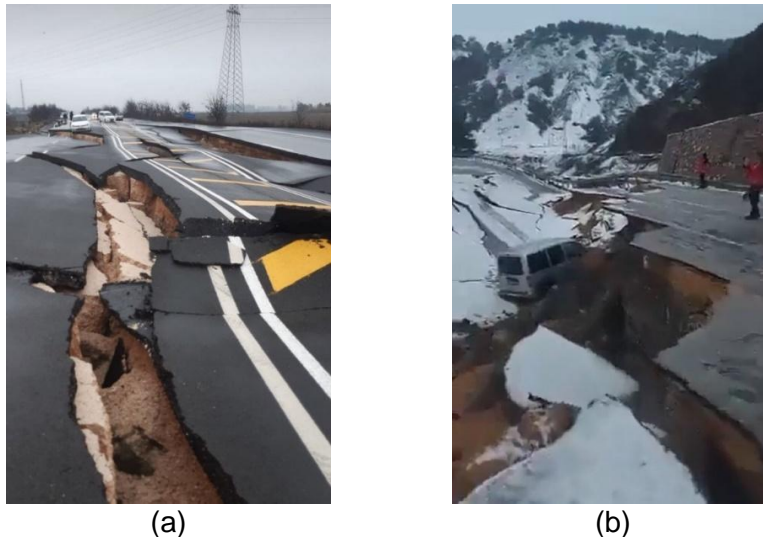

| (a) | (b) |

Figure 6.9. (a) Potential lateral spread failure (Source: Reuters via National Post). (b) Landslide & lateral spreading failure (Source: Extracted from Sokagin Sesi Gazetesi, Twitter).

Joint PVRR: 2023 Türkiye Earthquake Sequence
PRJ-3824 | Released: 3/29/2023
Building Resilience through Reconnaissance

128

Because there were sites susceptible to liquefaction-induced failure, observations of liquefaction have been reported. With time, such observations could be prominent in future field visits. For example, potential cyclic softening induced lateral spreading was observed over a long stretch of a road section (Figure 6.9). The horizontal displacement in the order of 5 ft (1.5 m) to 10 ft (3 m) can be observed. The Sultansuyu Dam in Malatya experienced significant longitudinal cracking at the crest due to a lateral spreading type failure (Figures 6.10a, b). The dam water was discharged in a controlled manner after cracks were discovered in the body axis of the dam. Longitudinal and transverse cracks were similarly observed in the Afrin dam (Figure 6.10c).

(a)

(b)

(c)

Figure 6.10. (a-b) Sultansuyu Dam with cracks along its central axis (Source: ntv.com) and (c) longitudinal and transverse cracks in the Afrin dam (Source: Syrian Television via misbar.com).

Another example of collapse of a road is observed in Figure 6.11. This is the road to the village of Koseli, which passes over the Adıyaman-Sanliurfa-Gaziantep Highway, south of Türkiye. The embankment suffered from lateral spread.

Joint PVRR: 2023 Türkiye Earthquake Sequence
PRJ-3824 | Released: 3/29/2023
Building Resilience through Reconnaissance

129

Figure 6.11. Failure of the embankment road in the village of Koseli, which passes over the Adıyaman-Sanliurfa-Gaziantep Highway in the Adıyaman province (Source: Reuters via Washington Post).

Joint PVRR: 2023 Türkiye Earthquake Sequence
PRJ-3824 | Released: 3/29/2023
Building Resilience through Reconnaissance

130

7. Recommended Response Strategy

On February 6, 2023, one of the most intense earthquakes ever recorded in Türkiye caused widespread devastation and claimed numerous lives in the country's southern region and northern Syria. The area was particularly vulnerable to a strong seismic event, with a high proportion of older concrete-framed buildings in the inventory, many completely destroyed. The infrastructure in northern Syria was already weakened due to years of airstrikes and bombardments during the civil war. Just nine hours after the first quake of magnitude 7.8, a powerful magnitude 7.5 quake struck, located approximately 60 miles north of the initial quake, according to the US Geological Survey. Although the full extent of the damage remains uncertain, this Joint Preliminary Virtual Reconnaissance Report (PVRR) between StEER and EERI LFE documents the collapse of many buildings, including apartments, hotels, and businesses, in multiple cities near the epicenters on both sides of the border. Based on the findings of this joint PVRR, the authors share the following conclusions, observations, and recommendations for future studies:

1. **Choice of Distance Parameters:** A commonly used distance parameter to qualitatively characterize the levels of shaking at a given location is the distance from the epicenter (epicentral distance). It is known that there are several issues with the use of this parameter; this earthquake provided an important demonstration of these issues. Because of the bilateral nature of the rupture in the Mw 7.8 earthquake (one rupture directivity occurring towards southwest to Hatay and another rupture directivity tending northeast towards Malatya), very large PGA and PGV values were recorded at significantly large epicentral distances. For example, 1.3g PGA and 170 cm/s PGV were recorded at an epicentral distance of 143 km due to combined effects of forward directivity, basin effects, and site amplification. Other distance parameters, such as the Joyner-Boore Distance, which is the shortest horizontal distance from the recording site to the vertical projection of the rupture onto the surface, or the closest distance from the recording site to the ruptured area should be used as an alternative to the epicentral distance.

2. **Consequences of Large-Magnitude Earthquake Sequences:** Earthquake sequences with consequent large magnitude events separated by short time intervals have been occurring at different parts of the world in recent years (e.g., 2019 Ridgecrest earthquakes, 2022 Iran earthquake sequence, and 2022 Taiwan earthquakes). The Mw 7.8 and Mw 7.5 earthquakes, along with the large magnitude aftershocks between and following these two earthquakes resulted in multiple occurrences of significant shaking in several provinces. In the province of Hatay, a Mw 6.4 earthquake on February 20 resulted in major shaking once again. The potential for cumulative effects should be characterized and considered, not only in the Turkish Building Seismic Code (TBSC), but in the US and other parts of the world. This can be conducted, for example, by implicitly accounting for the duration effect. It is known that several buildings collapsed during the aftershocks of the Mw 7.5 earthquake. The presence of these observations and available ground motion records at many stations should be used for characterizing the consequences of sequential ground motions.

3. **Soft/Weak Stories in Mixed Use Buildings:** One of the common reasons for the observed collapses in this earthquake sequence was the presence of soft/weak stories at the base of mixed-use buildings. Some of these soft/weak stories were created due to the presence of glass façades in the commercial first stories, with infill walls at the upper stories that are not isolated from the bounding frames. Three related recommendations are as follows:

Joint PVRR: 2023 Türkiye Earthquake Sequence
PRJ-3824 | Released: 3/29/2023
Building Resilience through Reconnaissance

131

a. similar buildings in other earthquake-vulnerable regions of Türkiye should be identified from tier 1 surveys using streetview panoramic imaging. Artificial intelligence methods can be used for this purpose as well;

b. cost-effective retrofit solutions should be formulated or the feasibility of demolishing these buildings and constructing new ones should be explored;

c. revisions in the TBSC for explicit modeling of infill walls and their isolation from the bounding frames should be considered.

4. **Hospital Performance and Continuity of Service:** Twelve seismically isolated hospitals in the earthquake-impacted region were operational after the earthquake sequence and most importantly allowed the facilities to serve their emergency response functions in the aftermath of the extraordinary destruction. Seismic base-isolation was employed in these hospitals according to a law that requires all hospitals in seismic regions in Türkiye to be base-isolated. The excellent operational performance of base-isolated hospitals was in major contrast with the observed collapses of hospitals that were not base-isolated. Collapse of any structure should be avoided but collapse of hospitals and other critical facilities is simply unacceptable. The reasons for collapsed hospitals should be studied and retrofit methodologies, including the possible use of base-isolation methods, should be explored.

From an operational viewpoint, hospitals were overwhelmed due to many injuries, especially those that remained functional. Many had to treat patients from different regions who were mobilized in ambulances, helicopters, and ships. It is worth visiting these hospitals to understand how they adapted their operations to maintain continuity of service and meet the high demand for medical treatment in the wake of these earthquakes, particularly during a sequence of violent earthquakes and aftershocks.

5. **Ground Motion Intensity and Code Designed Buildings**: Several ground motions recorded PGA and PGV values as large as 1.3g and 170 cm/s, exceeding the building code Maximum Considered Earthquake (MCE) levels. Related recommendations are as follows:

a. Particular reasons for these large levels of strong shaking, e.g., forward directivity, basin effects, and site amplification, need to be quantified and potential implementation/update of basin effects in the Ground Motion Models (GMMs);

b. Near fault ground motion recordings in large magnitude events are very rare; therefore, the motions recorded in these earthquakes are very valuable and should be used in dynamic analyses, updating ground motion models, and possible revisions of the seismic hazard map of Türkiye;

c. The response spectra of several of the recorded motions considerably exceeded the MCE levels for certain period ranges. Reliability studies have shown that there is a 10% collapse risk of risk category 2 buildings designed for the DBE-levels of modern codes. The seismic performance of modern-code-designed buildings subjected to ground motions of various intensities should be explored with realistic shaking table or hybrid simulation tests.

6. **Instrumentation of Structures:** There are many ground motion recording stations in the earthquake-impacted region; however, equally important is recorded response from instrumented structures, which is unfortunately lacking in these events. In a given block or neighborhood, variable performance was observed (collapses interspersed with non-collapsed buildings with a variety of damage levels). Recorded structural response would

have been very helpful in quantifying and understanding the behavior of these structures. Furthermore, such instrumentation would be helpful for characterizing the damage level and condition of the structures and for making predictions about the performance in aftershocks. Consideration should be given to instrumenting structures in this region and other seismically-active locations in Türkiye.

7. **Code Enforcement**: One of the reasons for the collapse of relatively new buildings might be insufficient compliance with the TBSC. Enforcing seismic codes and inspecting buildings for vulnerabilities is critical for ensuring the safety of buildings and their occupants during earthquakes. Several technical and non-technical aspects relating to these issues are:
    a. Strict enforcement of the seismic code: Building officials should enforce the seismic code strictly, both during the design and construction phases. They should ensure that all new construction and major renovations comply with the code and that any deviations are approved through the proper channels;
    b. Regular inspections: Existing buildings should be inspected regularly, particularly those in areas with high seismic hazards, to ensure that they comply with the seismic code and are safe for occupancy;
    c. Incentives for seismic retrofit: Governments can provide incentives, such as tax credits or grants, to encourage building owners to retrofit their buildings to meet the seismic code. Meanwhile the research community can continue to develop more cost-effective retrofit strategies;
    d. Public education and outreach: Building officials, earthquake engineers, and seismic experts can provide public education and outreach to raise awareness about the importance of seismic safety and the need for proper enforcement of the seismic code.

8. **Rebuilding and Protective Systems**: Reconstruction in several provinces, such as Hatay, Kahramanmaras, Adiyaman, Malatya, and others, should consider the feasibility of using cost effective protective systems (base-isolation, supplemental damping, etc.), which may have significant benefits in the medium to long term. In earthquake engineering literature, such lifecycle comparisons have been conducted by several researchers for buildings designed according to seismic codes and with enhanced performance using base-isolation (e.g., Terzic et al. 2012). The operational performance of the base-isolated hospitals in the region is in itself an impactful validation of the benefits of the use of such technologies.

9. **Infrastructure Performance**: Compared to the response of buildings, other infrastructure performance was generally successful, e.g., despite a few collapses, most highway bridges remained open. Performance of bridges should further be studied in detail.

Finally, after a major disaster like this, it is natural to focus on the problems, collapses, and significant losses, but it is also important to highlight recent successes in a proper context. The November 2022 Düzce earthquake was a "close to" design-level earthquake where a building stock properly designed and constructed according to TBSC, enforcing key regulations such as limiting the number of stories, resulted in performance as expected with generally minor to moderate damage (Sezen et al., 2023). This affirms that Türkiye has the capacity to achieve seismic resilience and can thus use the success of this November 2022 earthquake, along with the important lessons from the February 2023 earthquake sequence, to continue its progress in enhancing the safety of its building inventory for seismic hazards nationwide.

Joint PVRR: 2023 Türkiye Earthquake Sequence
PRJ-3824 | Released: 3/29/2023
Building Resilience through Reconnaissance

133

Based on the satisfaction of the majority (87.5%) of the escalation criteria (see Table 7.1) as informed by the preliminary observations outlined in this report, StEER's response to this event has escalated to Level 2. StEER and its partners have launched the **2023 Türkiye Earthquake Sequence Imagining Campaign** to support the local documentation of the performance of the built environment following this earthquake sequence. The campaign makes street-level panoramic imagery collected by the locally-based Makro 360 Google Maps Agency and served by US-based Site Tour 360 available through a custom web-based viewer. Due to the sensitive nature of the imagery, local authorities have placed terms of use on the viewer and prohibited its dissemination on publicly accessible websites or social media. However, StEER has made the viewer available to its members and partners through the secure DesignSafe Slack channel for this event. To support the recovery efforts, credentials have been provided to governmental and non-governmental agencies/organizations supporting the recovery effort. The viewer presents the acquired imagery alongside pre-event Google streetview imagery and aerial imagery. StEER will promote the use of this viewer for virtual assessment activities as part of the Level 2 response.

As part of its Level 2 response, StEER has also released an updated earthquake performance assessment mobile application in Fulcrum, with guidance documents, to support its partners who are already documenting building performance on-site. StEER will continue to coordinate with other organizations responding to this event to encourage the use of these platforms and to determine how best to cooperate in any future escalation to a Level 3 response deploying Field Assessment Structural Teams (FASTs) from the US.

Finally, due to State Department restrictions on travel to Syria and the border regions under Level 4 Travel Advisory, all field data collection at Level 2 or a future Level 3 response unfortunately will not document these areas.

EERI is responding to this event by several reconnaissance teams to Türkiye. First, an Advance team went to the field soon after the earthquake sequence. More recently, three additional EERI teams visited the field focusing on conducting post-earthquake reconnaissance of buildings, hospitals, and lifelines.
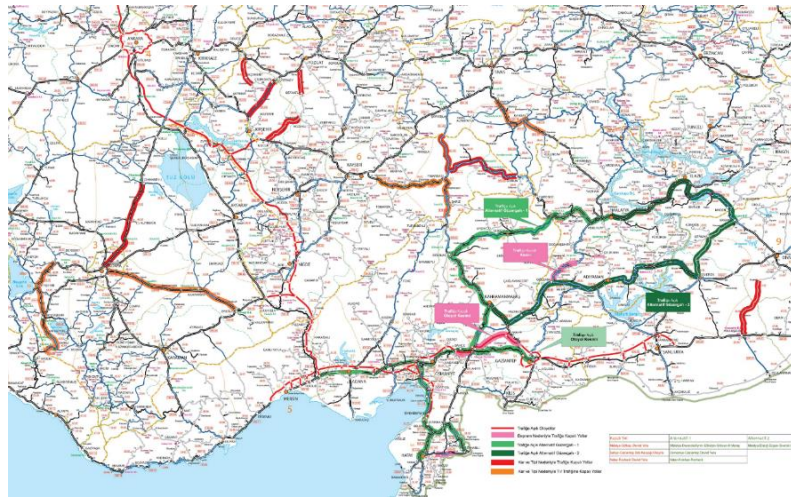
Joint PVRR: 2023 Türkiye Earthquake Sequence
PRJ-3824 | Released: 3/29/2023
Building Resilience through Reconnaissance

134

Table 7.1. Summary of escalation criteria satisfied by Feb. 2023 Türkiye earthquake sequence.

Hazard	Exposure	Feasibility
● Hazard intensity exceeds MCE levels in several locations. ● Unusual ground motion characteristics	● Highly vulnerable structures with severe damage or collapse ● Highly engineered structures with lower damage ● Cases of old buildings with lower damage & new ones with more damage ● Significant fatalities ● Potential for prolonged downtime and recovery ● Potential lessons to be learned from ground motion records and building performance	● Availability/interest of members in the impacted region ● Availability of sufficient support from regional nodes (imaging teams) ● EERI, GEER, EEFIT and others deployed

Joint PVRR: 2023 Türkiye Earthquake Sequence
PRJ-3824 | Released: 3/29/2023
Building Resilience through Reconnaissance

135

Appendix A. Road Closure Chronology

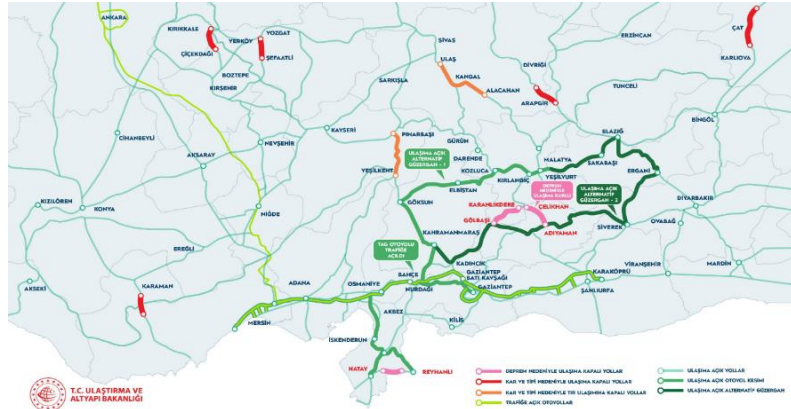|	Tweets from Karayolları Genel Müdürlüğü (Türkiye General Directorate of Highways) on road closures in the aftermath of the earthquake sequence *Original Tweet linked in first column for access to full image* <u>Legend</u>: pink is closure due to the earthquake sequence & red is due to inclement weather
February 6, 2023 at 10:29 pm	
February 7, 2023 at 9:25 am	
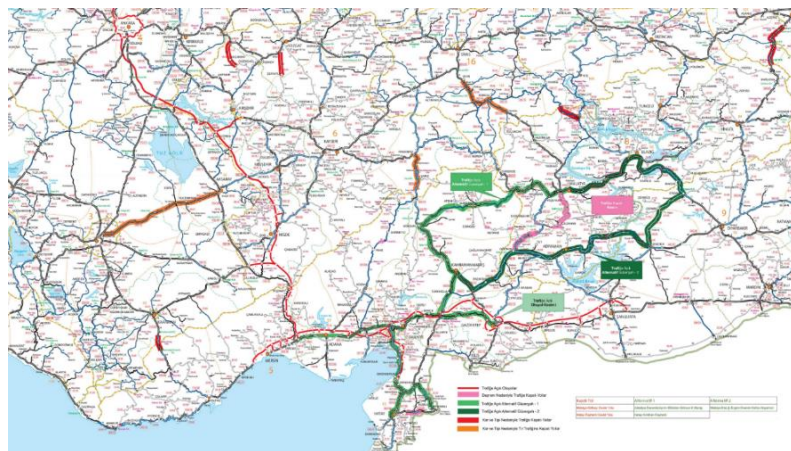
Joint PVRR: 2023 Türkiye Earthquake Sequence
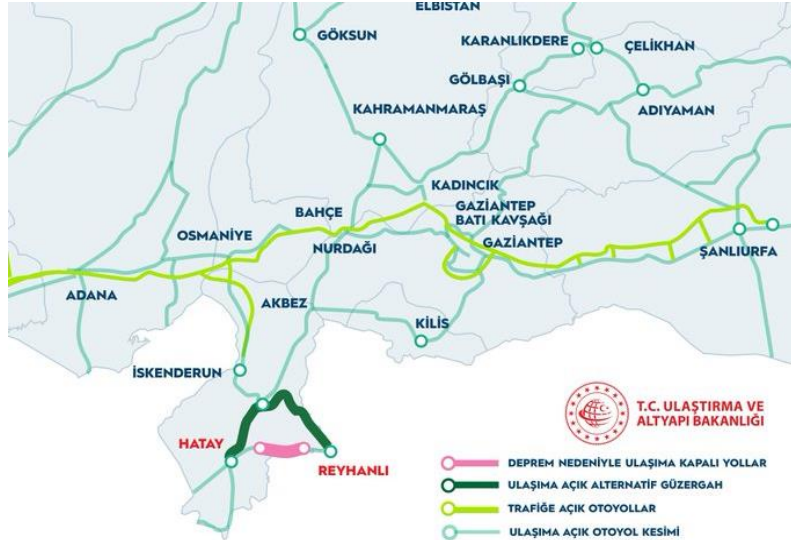PRJ-3824 | Released: 3/29/2023
Building Resilience through Reconnaissance

136
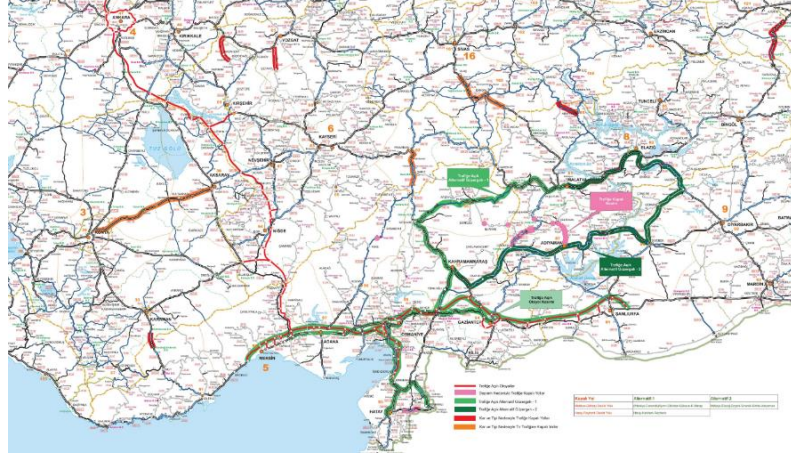
February 7, 2023 at 6:10 pm	
February 7, 2023 at 9:23 pm	
February 8, 2023 at 12:30 pm	

References

Abraham, L., Chang, A., Leatherby, L., Reinhard, S., Robles, P., Wu, A. and Walton Shaver, J. (2023) "What the Earthquake Destroyed in the Heart of One Turkish City," *The New York Times,* Feb. 10 https://www.nytimes.com/interactive/2023/02/10/world/middleeast/kahramanmaras-turkey-earthquake-damage.html

AFAD (2023a). "BASIN BULTENI" https://www.afad.gov.tr/kahramanmarasta-meydana-gelen-depremler-hk-36 & https://www.afad.gov.tr/kahramanmaras-merkezli-yurutulen-calismalar-hakkinda--basin-bulteni--37 Date accessed: March 10, 2023]

AFAD (2023b). "Earthquake Catalog." https://tadas.afad.gov.tr/event-detail/15499 & https://tadas.afad.gov.tr/event-detail/15512 [Date accessed: Feb 06, 2023]

AFAD (2023c). "Feb. 6th, 2023 Pazarcık (Kahramanmaras MW 7.7) and Elbistan (Kahramanmaras MW 7.6) Earthquakes Preliminary Report". Feb. 9th, 2023. https://deprem.afad.gov.tr/assets/pdf/Kahramanmaras%20%20Depremleri_%20On%20Degerlendirme%20Raporu.pdf [Date accessed: February 10, 2023]

AFAD (2023d). https://www.jmo.org.tr/genel/jeoloji_harita.php?kod=9004

AFAD (2023e). "AFAD - TADAS" https://tadas.afad.gov.tr/

Akkar, S., Azak, T., Can, T., Ceken, U., Tumsa, M. B. D., Duman, T. Y., Erdik, M., Ergintav, S., Kadirioglu, F. T., Kalafat, D., Kale, O., Kartal, R. F., Kekovali, K., Kilic, T., Ozalp, S., Poyraz, S. A., Sesetyan, K., Tekin, S., Yakut, A., Yilmaz, M. T., Yucemen, M. S., & Zulfikar, O. (2018). Evolution of seismic hazard maps in Turkey. Bulletin of Earthquake Engineering, 16(8), 3197-3228. doi:10.1007/s10518-018-0349-1

Adejumo, Q. (2023) "Turkey: Schools In Malatya Host 250,000 Earthquake Victims," *All News* https://allnews.ng/news/turkey-schools-in-malatya-host-250000-earthquake-victims [Date accessed: Feb 08,2023]

ANHA (2023). ¨(in Arabic) The majority of educational facilities in Sheik Maqsoud and Ashrafieh neighborhoods were damaged by the earthquake¨: https://hawarnews.com/ar/haber/tdhrr-ghalbyh-almnshaat-altalymyh-fy-hyy-alshykh-mqswd-walashrfyh-jraa-alzlzal-h76606.html [Date accessed: Feb 10,2023]

Armenpress (2023) "UPDATED: 2 Turkish-Armenians confirmed dead in earthquake, church in Iskenderun destroyed". https://armenpress.am/eng/news/1103383/ [Date accessed: Feb 08, 2023]

Boore, D. M., Thompson, E. M., & Cadet, H. (2011). Regional correlations of VS 30 and velocities averaged over depths less than and greater than 30 meters. *Bulletin of the Seismological Society of America*, *101*(6), 3046-3059.

Joint PVRR: 2023 Türkiye Earthquake Sequence
PRJ-3824 | Released: 3/29/2023
Building Resilience through Reconnaissance

138

Braga, F., Manfredi, V., Masi, A., Salvatori, A. and Vona, M (2011). "Performance of non-structural elements in RC buildings during the L'Aquila, 2009 earthquake." Bulletin of Earthquake Engineering, 9(1): 307-324.

Bull, D.K., (2011). Stair and access ramps between floors in mutli-storey buildings. A report at the Canterbury Earthquake Royal Commission, Christchurch, New Zealand.

Cabalar, A. F., Canbolat, A., Akbulut, N., Tercan, S. H., & Isik, H. (2019). Soil liquefaction potential in Kahramanmaras, Turkey. *Geomatics, Natural Hazards and Risk*, *10*(1), 1822-1838.

Daily Sabah (2023a). "Fire extinguished at Türkiye's quake-hit Iskenderun port," https://www.dailysabah.com/business/transportation/fire-extinguished-at-turkiyes-quake-hit-iskenderun-port

Daily Sabah (2023b) "Turkish Airlines helps in evacuation, transporting volunteers after quake," *Daily Sabah*, Feb 7, https://www.dailysabah.com/business/transportation/turkish-airlines-helps-in-evacuation-transporting-volunteers-after-quake

Demirci, G. (2023) "TAG Highway Divided In Two!" *Expat Guide Turkey* Feb. 6 https://expatguideturkey.com/tag-highway-divided-in-two/

ECHO (2023). *European Commission Civil Protection and Humanitarian Aid Operations, Civil Protection Message N°8* – Türkiye Earthquakes March 2023

El Ssayed, H. M., Zaineh, H. E., Dojcinovski, D., Mihailov, V. (2012) "Re-Evaluations of Seismic Hazard of Syria," *International Journal of Geosciences*, Sept. 3, 847-855.

Enab Baladi News (2023) https://www.enabbaladi.net/archives/627685, accessed Feb 7.

EN SON HABER (2023). "(in Turkish) Malatya's 200 adobe houses became unusable in the earthquake," https://www.ensonhaber.com/gundem/malatyanin-200-kerpic-evi-de-depremde-kullanilamaz-hale-geldi [Date accessed: Feb 15, 2023]

Federal Emergency Management Agency, FEMA (2012). Rapid Visual Screening of Buildings for Potential Seismic Hazards: A Handbook, FEMA-P154

Fitch (2023) "Fitch Ratings Comments on Insurance Losses from Turkiye-Syria Earthquake," *Fitch Ratings*, Feb. 9, https://www.fitchratings.com/research/insurance/fitch-ratings-comments-on-insurance-losses-from-turkiye-syria-earthquake-09-02-2023

ForeignPolicy (2023) https://foreignpolicy.com/2023/02/15/un-assad-syria-earthquake-aid-victims/

Francis, E. and Nadhir, A. (2023) "WHO warns of 'huge long-term' impact on health care in Turkey and Syria," Washington Post, https://www.washingtonpost.com/world/2023/02/08/turkey-syria-earthquake-death-toll-live-updates/#link-SQOOWS4SCJDPXBBM3XOFP6BW64

Getty Images (2023) https://www.gettyimages.com/detail/news-photo/man-looks-on-at-search-and-rescue-operations-conducted-in-news-photo/1246846649?adppopup=true

Getty Images (2023b) https://www.gettyimages.com/detail/news-photo/residents-walk-along-a-collapsed-building-following-an-news-photo/1246842869?adppopup=true

Getty Images (2023c) https://www.gettyimages.com/detail/news-photo/resident-stands-in-front-of-a-collapsed-building-following-news-photo/1246842558?adppopup=true

Gül, M., Darbaş, G., & Gürbüz, K. (2005). Alacık Formasyonunun (En Geç Orta Eosen-Erken Miyosen) Kahramanmaraş Havzası İçindeki Tektono-Stratigrafik Konumu. İstanbul Yerbilimleri Dergisi, 18(2), 183-197.

Haber7 (2023) https://ekonomi.haber7.com/ekonomi/haber/3300665-yatirim-ve-emeklilik-fonlari-islemleri-durduruldu

Holmes, W.T., 2000. Risk assessment and retrofit of existing buildings. Bulletin of the New Zealand Society for Earthquake Engineering, 33(3), pp.222-247.

Hurriyet Daily News, (2023) https://www.hurriyetdailynews.com/seismic-isolation-devices-prevent-damage-in-four-hospitals-180830

Hüsing, S. K., Zachariasse, W. J., Van Hinsbergen, D. J., Krijgsman, W., Inceöz, M., Harzhauser, M., ... & Kroh, A. (2009). Oligocene–Miocene basin evolution in SE Anatolia, Turkey: constraints on the closure of the eastern Tethys gateway. Geological Society, London, Special Publications, 311(1), 107-132.

Independent (2023) https://www.independent.ie/world-news/turkish-president-admits-shortcomings-in-earthquake-response-as-death-toll-reaches-12000-42332830.html

Kebab G. (2023, February 8). *Anatolian Plate moved 3-3,5 Meters after the Earthquake*. Reddit. Retrieved February 20, 2023, from https://old.reddit.com/r/europe/comments/10wss6o/anatolian_plate_moved_335_meters_after_the/

Li, B., Mosalam, K.M., (2013). Seismic performance of reinforced concrete stairways during 2008 Wenchuan earthquake. *ASCE Journal of Performance of Constructed Facilities*, 27 (*6*), 721-730.

Manfredi, G., Prota, A., Verderame, G.M., De Luca, F. and Ricci, P. (2014). "2012 Emilia earthquake, Italy: reinforced concrete buildings response." Bulletin of Earthquake Engineering, 12(5), 2275-2298

Marinković, M., Baballëku, M., Isufi, B., Blagojević, N., Milićević, I., & Brzev, S. (2022). Performance of RC cast-in-place buildings during the November 26, 2019 Albania earthquake. *Bulletin of Earthquake Engineering*, *20*(10), 5427-5480.

Joint PVRR: 2023 Türkiye Earthquake Sequence
PRJ-3824 | Released: 3/29/2023
Building Resilience through Reconnaissance

140

MaviKocaeli (2023) https://www.mavikocaeli.com.tr/adana-sehir-hastanesi-depremzedeler-icin-saglik-ussu-oldu/114861/

MassisPost (2023). ¨Cilician Armenian High School of Aleppo Damaged in Earthquake¨. https://massispost.com/2023/02/cilician-armenian-high-school-of-aleppo-damaged-in-earthquake/ [Date accessed: Feb 08,2023]

MEB (2023). Republic of Turkey Ministry of National Education: http://www.meb.gov.tr/education-has-been-suspended-until-march-1-in-10-provinces-affected-by-the-earthquake/haber/29029/en. [Date accessed: Feb 15, 2023]

Middle East Eye (2023) https://www.middleeasteye.net/discover/turkey-earthquake-iconic-mosques-destroyed

Ministry of Health (2023a). "(in Turkish) Health Minister Koca Made Inspections in Hatay Affected by the Earthquake" https://www.saglik.gov.tr/TR,94715/saglik-bakani-koca-depremden-etkilenen-hatayda-incelemelerde-bulundu.html [Date accessed: Feb 09, 2023]

Mosalam, K.M., Günay S., (2014) "Towards an Accurate Determination of Collapse Vulnerable Reinforced Concrete Buildings," in *ACI Special Publication: Seismic Assessment of Existing Reinforced Concrete Buildings*, 297(10), 14 pp.

Mosalam, K.M. and Günay, S., (2015) Progressive collapse analysis of reinforced concrete frames with unreinforced masonry infill walls considering in-plane/out-of-plane interaction. Earthquake Spectra, 31(2), pp.921-943.

Mroue, B. and Chehaeb, K. (2023) "Earthquake stuns Syria's Aleppo even after war's horrors," *ABC News*, Feb. 8, https://abcnews.go.com/International/wireStory/earthquake-stuns-syrias-aleppo-after-wars-horrors-96985917

Naddaf, M., (2023). Turkey-Syria earthquake: What scientists know. Nature. DOI: 10.1038/d41586-023-00364-y

Nadoor, M. (2016) "Past and present of Geology in Syria" (in Arabic), In M. Nadoor (EDS): *A trip Through Syrian Geologic Heritage*. Arab Geologist platform. Damascus.

Naji, D. M., Akin, M. K., & Cabalar, A. F. (2020). A comparative study on the VS30 and N30 based seismic site classification in Kahramanmaras, Turkey. *Advances in Civil Engineering*, *2020*, 1-15.

Naji, D. M., Akin, M. K., & Cabalar, A. F. (2021). Evaluation of seismic site classification for Kahramanmaras City, Turkey. *Environmental Earth Sciences*, 80(3), 97.

New Arab (2023) https://www.newarab.com/news/and-after-images-show-destruction-turkey-quakes

NTV (2023a) https://www.ntv.com.tr/turkiye/kahramanmaras-depremi-il-il-hasarli-yapi-sayisi-aciklandi,iiBJJMPG10a4Pw3Ww8DJHQ

Joint PVRR: 2023 Türkiye Earthquake Sequence
PRJ-3824 | Released: 3/29/2023
Building Resilience through Reconnaissance

141

NTV (2023b) https://www.ntv.com.tr/galeri/turkiye/adanada-13-katli-binanin-yarisi-yikildi-yarisi-ayakta-kaldi,MpvT0tCZuUyC_g-eeYFSDg/ytnl0FfjJkuC7aXyT7b3lQ

NTV (2023c) "Hatay'da yıkılan hastanenin 'deprem dayanıklılık testi olumsuz' geldiği ortaya çıktı," https://www.ntv.com.tr/galeri/turkiye/hatayda-yikilan-hastanenin-deprem-dayaniklilik-testi-olumsuz-geldigi-ortaya-cikti,cqWYUZcEiEanb5wTjv4hVA/6D7ASIbws0eHjEDDWQ7Asw

Oksijen (2023). "(in Turkish) Search and rescue work continues at Iskenderun State Hospital": https://gazeteoksijen.com/turkiye/iskenderun-devlet-hastanesinde-arama-kurtarma-calismasi-suruyor-169816 [Date accessed: Feb 07, 2023]

Only53.com news (2023) Kayseri'de Belediye Binası Da Depremden Etkilendi (olay53.com) [Data accessed: February 10, 2023]

Paköz, A. (2019). "Kahramanmaraş'ta Bir Erken Cumhuriyet Dönemi Evi: Çiftarslan Evi | A House From The Early Republican Period In Kahramanmaraş: Çiftarslan House," *Journal of Architecture and Life*, 5(1), 57-69. DOI: 10.26835/my.650076

Reddit (2023) https://old.reddit.com/r/europe/comments/10wss6o/anatolian_plate_moved_335_meters_after_the/

Reliefweb (2023c) "Delivering Urgently Needed Meds to Earthquake-Impacted Turkey, Syria," Feb. 7 https://reliefweb.int/report/turkiye/delivering-urgently-needed-meds-earthquake-impacted-turkey-syria

Reuters (2023a) https://www.reuters.com/world/middle-east/large-fire-plume-smoke-turkeys-iskenderun-port-witnesses-2023-02-06/

Reuters (2023b) https://www.reuters.com/world/middle-east/thirteen-killed-after-building-collapses-syrias-aleppo-state-media-2023-01-22/

RÖNESANS (2023) "Adana City Hospital," https://rsy.com.tr/proje/adana-city-hospital/?lang=en

Ros, M. (2023) "Turkish airports close after largest earthquake for a decade rocks Turkey, Syria," Aerotime Hub, Feb. 6 https://www.aerotime.aero/articles/turkish-airports-close-after-largest-earthquake-for-a-decade-rocks-turkey-syria

Ruetir (2023) https://www.ruetir.com/2023/02/terrible-turkish-earthquake-also-destroyed-the-historic-yeni-mosque/

SANA (2023). Syrian Arab News Agency. ¨248 schools affected by earthquake hit the country on Monday¨: https://www.sana.sy/en/?p=299566. [Date accessed: Feb 08, 2023]

Schildgen, T. F., Yıldırım, C., Cosentino, D., & Strecker, M. R. (2014). "Linking slab break-off, Hellenic trench retreat, and uplift of the Central and Eastern Anatolian plateaus," *Earth-Science Reviews*, 128, 147-168.

Joint PVRR: 2023 Türkiye Earthquake Sequence
PRJ-3824 | Released: 3/29/2023
Building Resilience through Reconnaissance

142

Selim, H. H., & Tüysüz, O. (2013). "The Bursa–Gönen Depression, NW Turkey: a complex basin developed on the North Anatolian Fault," *Geological Magazine*, 150(5), 801-821.

Sezen, H. Can Altunisik, A. Emin Arslan, M. Caglar, N. Demir, A. BEKTAS, N. Dilsiz, A. Gunay, S. Khalil, Z. Marinkovic, M. Safiey, A. Alam, M. Kijewski-Correa, T. Mosalam, K. (2023) "StEER 2022 Mw 6.1 Duzce, Turkey Earthquake Preliminary Virtual Reconnaissance Report (PVRR)", in *StEER - November 23 2022, Duzce, Turkey, Mw 6.1 Earthquake.* DesignSafe-CI. https://doi.org/10.17603/ds2-8710-ad45 v1

Perkins, R., Saadi, D., Coleman, N. and O'Byrne, D. (2023) "Crude loadings at Turkey's Ceyhan terminal suspended after earthquake cuts power", *SP Global,* Feb. 6 https://www.spglobal.com/commodityinsights/en/market-insights/latest-news/oil/020623-crude-loadings-at-turkeys-ceyhan-terminal-suspended-after-earthquake-cuts-power

Smithsonian (2023) https://www.smithsonianmag.com/smart-news/earthquakes-damage-turkeys-historic-gaziantep-castle-180981597/

Sözcü, (2023) https://www.sozcu.com.tr/2023/gunun-icinden/deprem-bolgesine-giden-akpli-vekil-devlet-hastanesi-girilemez-halde-7583416/

The Telegraph (2023) "Turkey earthquake: Rescuers race to find survivors as night falls and death toll passes 3,500," *The Telegraph,* February 7. https://www.telegraph.co.uk/world-news/2023/02/06/turkey-earthquake-live-updates-gaziantep-map-tremor-news-latest/

The Telegraph (2023b) "Europe must not abandon Syria", The Telegraph, March 24. https://www.telegraph.co.uk/opinion/2023/02/08/europe-must-not-abandon-syria/

The Syrian Ministry of Oil and Mineral Resources (2023) http://mopmr.gov.sy/index.php/en/

TGRT HABER (2023). "(in Turkish) How long are the schools off? School holidays until February 20?", https://www.tgrthaber.com.tr/aktuel/okullar-ne-zamana-kadar-tatil-20-subata-kadar-okullar-tatil-mi-2873935. [Date accessed: Feb 15, 2023]

TBSC: Turkish Building Seismic Code (2018) *Türkiye Bina Deprem Yönetmeliği,* Disaster and Emergency Management, Ankara, Turkey.

TRHaber TRHaber - Beş katlı bina depremde yıkıldı yangın merdiveni ayakta kaldı [Data accessed: February 10, 2023]

TÜIK (2023) https://data.tuik.gov.tr/Kategori/GetKategori?p=insaat-ve-konut-116&dil=1

Twitter (2023a) https://twitter.com/erenuslu38

Twitter (2023j) https://twitter.com/fatihaltayli/status/1623308543054020608

Twitter (2023n) https://twitter.com/bbcturkce/status/1622523281525059586

Twitter (2023p) https://twitter.com/ISMAIL_SARAC/status/1624366310518927361?s=20

Joint PVRR: 2023 Türkiye Earthquake Sequence
PRJ-3824 | Released: 3/29/2023
Building Resilience through Reconnaissance

143

Twitter (2023y) https://twitter.com/Darkwebhaber/status/1622432202192523264?t=41RSjknk_we6e0_aTKzhFg&s=08

Türkiye Ministry of Environment, Urbanization and Climate Change (2023) https://csb.gov.tr/en

USGS: US Geological Survey (2023a). "M 7.8 - Central Turkey" & "M 7.5 - 4 km SSE of Ekinözü, Turkey". Feb. 6th, 2023. https://earthquake.usgs.gov/earthquakes/eventpage/us6000jllz/executive & https://earthquake.usgs.gov/earthquakes/eventpage/us6000jlqa/executive

USGS: US Geological Survey (2023b). M 7.5 - 4 km SSE of Ekinözü, Turkey. Executive Summary. Retrieved February 20, 2023, https://earthquake.usgs.gov/earthquakes/eventpage/us6000jlqa/executive

US Geological Survey (USGS) (2023c). "M 7.8 - Central Turkey - PAGER". Feb. 6. https://earthquake.usgs.gov/earthquakes/eventpage/us6000jllz/pager

Verisk (2023) "Verisk Estimates Economic Losses from February 6 Earthquakes in Turkey Likely to Exceed USD 20 Billion," https://www.verisk.com/newsroom/verisk-estimates-economic-losses-from-february-6-earthquakes-in-turkey--likely-to-exceed-usd-20-billion/

Veryansin TV (2023) https://www.veryansintv.com/prof-dr-sozbilir-en-az-3-fay-segmenti-kirilmis-oldu/

World Health Organization (2023). "7.8 Earthquake - EMTCC in Turkïye: Situation Update": https://worldhealthorg.shinyapps.io/TurkiyeEarthquake/. [Date accessed: Feb 10, 2023]

Yilmaz, H., Over, S., & Ozden, S. (2006). "Kinematics of the east Anatolian Fault zone between turkoglu (Kahramanmaras) and celikhan (adiyaman), Eastern Turkey," *Earth, Planets and Space,* 58(11), 1463-1473.

Youd, T. L., & Idriss, I. M. (2001). Liquefaction resistance of soils: summary report from the 1996 NCEER and 1998 NCEER/NSF workshops on evaluation of liquefaction resistance of soils. Journal of geotechnical and geoenvironmental engineering, 127(4), 297-313.

Joint PVRR: 2023 Türkiye Earthquake Sequence
PRJ-3824 | Released: 3/29/2023
Building Resilience through Reconnaissance

144